University of Southampton

Faculty of Medicine

Human Development and Health

Personalising Device Therapy by Redefining the Sensing Mechanism of the Subcutaneous Implantable Cardioverter Defibrillator

by

Dr Benedict M Wiles MA MBBS MRCP

Thesis for the degree of Doctor of Philosophy

May 2019

Resubmitted after minor revision April 2020

University of Southampton

Abstract

Faculty of Medicine

Human Development and Health

Thesis for the degree of Doctor of Philosophy

Personalising Device Therapy by Redefining the Sensing Mechanism of the Subcutaneous Implantable Cardioverter Defibrillator

Dr Benedict M Wiles MA MBBS MRCP

Ventricular tachyarrhythmias (VTA) are rapid abnormal heart rhythms which can result in haemodynamic compromise, collapse and sudden cardiac death (SCD). The annual global mortality burden attributed to VTA is approximately 6 million. Fortunately, in populations at high risk of arrhythmic death, the implantable cardioverter defibrillator (ICD) significantly reduces mortality and is superior to medical therapy in both the primary and secondary prevention of SCD.

The subcutaneous ICD (S-ICD) represents a new approach in defibrillator therapy. Utilising an entirely avascular location, the S-ICD can diagnose and treat VTA, whilst avoiding the significant complications that have traditionally been associated with transvenous defibrillator leads. Accurate rhythm detection remains vital and increasingly sophisticated diagnostic algorithms are utilised. Life-saving therapy must never be incorrectly withheld, but inappropriate shocks, which are themselves associated with increased mortality and psychological morbidity, must also be minimised.

The S-ICD senses electrocardiogram (ECG) signals from a standardised subcutaneous location at which effective defibrillation has been consistently demonstrated. Three different sensing vectors are available of which one is selected for clinical use. Rhythm

detection requires certain morphological ECG characteristics to be present in the selected vector and pre-implant ECG screening is therefore a mandatory requirement.

The commonest cause for vector screening failure is the presence of a low R:T ratio, as this prevents the S-ICD from easily distinguishing R wave signal (ventricular depolarisation) from T wave signal (ventricular repolarisation). The overall axes of ventricular depolarisation and repolarisation are unique to an individual. R and T wave amplitudes are therefore determined, in part, by the angle from which they are observed.

Mathematical vector rotation is a novel strategy which can manipulate the angle of observation of an individual's ECG, using data recorded from the current S-ICD location. This can produce personalised vectors; unique individualised vectors with a recipient's maximal R:T ratio.

In this thesis, I will describe how personalised vector generation can be achieved, before applying the technique to a cohort of S-ICD ineligible patients. Significant improvements in R:T ratio and device eligibility will be demonstrated. I will then explore the broader impact of vector rotation on the current rhythm discrimination properties of the S-ICD system. I will demonstrate that both ventricular fibrillation detection and supraventricular tachycardia discrimination are not impaired by vector rotation. These are key principles of S-ICD sensing which must be maintained by any future sensing strategy.

Finally, I shall consider the phenomena of T wave over-sensing (TWOS), which despite the current screening process, remains the commonest cause of inappropriate shock therapy in the S-ICD population. I will describe a new concept, 'eligible vector time', and demonstrate experimentally that patients experience chronological fluctuations in their device eligibility. This preliminary work will redefine our current understanding of device eligibility and justify future research into the role of vector rotation in reducing inappropriate shock therapies.

In summary, I believe that clinicians and patients should not be restricted by the inherent limitations of standardised vector selection. Personalised vector generation can be achieved from the current S-ICD location, whilst maintaining the excellent rhythm detection qualities of the S-ICD system. Increased S-ICD eligibility can be achieved and the potential to reduce TWOS in the future cannot be ignored.

Table of Contents

Table of Tables

Table of Figures

Research Thesis: Declaration of Authorship

Print name:	**DOCTOR BENEDICT MARK WILES**

Title of thesis:	**Personalising Device Therapy by Redefining the Sensing Mechanism of the Subcutaneous Implantable Cardioverter Defibrillator**

I declare that this thesis and the work presented in it are my own and has been generated by me as the result of my own original research.

I confirm that:

1. This work was done wholly or mainly while in candidature for a research degree at this University.
2. Where any part of this thesis has previously been submitted for a degree or any other qualification at this University or any other institution, this has been clearly stated.
3. Where I have consulted the published work of others, this is always clearly attributed.
4. Where I have quoted from the work of others, the source is always given. With the exception of such quotations, this thesis is entirely my own work.
5. I have acknowledged all main sources of help.
6. Where the thesis is based on work done by myself jointly with others, I have made clear exactly what was done by others and what I have contributed myself.
7. Parts of this work have been published as:

    - Wiles BM, Roberts PR, Allavatum V, Maharatna K, Acharyya A, Chen H, et al. The future of S-ICD sensing: 'IMPROVE' significantly increases R:T ratio and generates universal device eligibility without impairing VF detection. EP Europace 2018:20(s4):iv1
    - Wiles BM, Roberts PR, Acharyya A, Allavatum V, Wilson DG, Vemishetty N, et al. Universal S-ICD eligibility: eliminating the need for pre-implant screening using mathematical vector rotation and a gradient filter. EP Europace 2018;20(s1):i175-176

- Wiles BM, Roberts PR, Acharyya A, Vemishetty N, Morgan JM. The end of pre-implant subcutaneous ICD screening? Using mathematical vector rotation to generate a personalised sensing vector resulting in universal device eligibility. EP Europace 2017;19(s1):i2
- Wiles BM, Wilson DG, Roberts PR, Allavatam V, Acharyya A, Vemishetty N, et al. Assessing the accuracy of surface ECG as a surrogate for the sensing vectors of the subcutaneous ICD. EP Europace 2017;19(s3):iii83
- Wiles BM, Wilson DG, Roberts PR, Allavatam V, Acharyya A, Vemishetty N, et al. Understanding the triangular relationship between subcutaneous ICD sensing vectors: can we accurately generate the secondary vector using just trigonometry? EP Europace 2017;19(s3):iii82
- Wiles BM, Roberts PR. Lead or be led: an update on leadless cardiac devices for general physicians. Clinical Medicine (London) 2017;17:33-36

Signature:		Date:	

Acknowledgements

I am extremely grateful to my supervisors Professor John Morgan and Dr Paul Roberts for their inspiration and guidance, but also for giving me the autonomy and freedom I needed to develop this project in my own way.

I would like to thank the entire Cardiac Rhythm Management Research Department and all the cardiac physiologists at University Hospital Southampton NHS Foundation Trust. In particular: Sarah Earles, Lisa Fletcher and Elizabeth Greenwood, who were a source of considerable support throughout the research process.

I wish to acknowledge the financial assistance that was provided by Boston Scientific and thank them tremendously for allowing me access to the technical expertise of Venugopal Allavatam, who was so instrumental in supporting my data analysis.

I would like to thank Professor Koushik Maharatna, Professor Amit Acharyya, and Dr Adam Kirk for agreeing to collaborate with me and for giving me access to their excellent teams.

I would also like to thank two of my cardiology colleagues from the Wessex deanery, Dr Mark Mariathas and Dr Ben Sieniewicz, with whom I shared the doctoral research journey. Thank you for listening and for always wanting a coffee.

Thank you to my predecessor Dr David Wilson for pointing me in the right direction from the outset.

Thank you also to the late Dr Borislav Dimitrov, Professor of Medical Statistics at the University of Southampton, who provided invaluable statistical support to the Cardiac Rhythm Management Research Department for a number of years. He will be missed tremendously.

These projects could not have been completed without the numerous patients who generously gave up their time to support my research. I am grateful to them all and hope that they were not too inconvenienced in the process.

Finally, I offer the most sincere and heartfelt thanks to my wife, Dr Lana Wiles, who offered me unwavering support throughout this process whilst juggling the needs of our three young children. I dedicate this work to her, Emma, Harry and Joshua.

Definitions and Abbreviations

A	alternate vector
ACE	angiotensin converting enzyme
ACHD	adult congenital heart disease
AIIRB	angiotensin II receptor blocker
ARVC	arrhythmogenic right ventricular cardiomyopathy
ASCII	American Standard Code for Information Interchange
AST	automated screening tool
ATP	anti-tachycardia pacing
AV	atrio-ventricular
AVID	Antiarrhythmic Versus Implantable Defibrillator (clinical trial)
AVNRT	atrio-ventricular nodal re-entrant tachycardia
AVRT	atrio-ventricular reciprocating tachycardia
BBB	bundle branch block
BCS	British Cardiovascular Society
BCT	broad complex tachycardia
BMI	body mass index
bpm	beats per minute
CABG	coronary artery bypass graft
CASH	Cardiac Arrest Study Hamburg (clinical trial)
CE	Conformité Européenne (European Conformity)
CIDS	Canadian Implantable Defibrillator Study (clinical trial)

CI	confidence interval
cm	centimetre
CRT	cardiac resynchronisation therapy
CRT-D	cardiac resynchronisation therapy defibrillator
CRT-P	cardiac resynchronisation therapy pacemaker
D	S-ICD distal sensing electrode
DA	stored data set from the S-ICD alternate vector (chapter 2)
DANISH	Defibrillator Implantation in Patients with Non-ischaemic Systolic Heart Failure (clinical trial)
DP	stored data set from the S-ICD primary vector (chapter 2)
DR-ICD	dual-chamber ICD
DS	stored data set from the S-ICD secondary vector (chapter 2)
ECG	electrocardiogram
EF	ejection fraction
eGFR	estimated glomerular filtration rate
EPS	electrophysiology study
ESC	European Society of Cardiology
ESRD	end stage renal disease
EVT	eligible vector time
FDA	United States Food and Drug Administration
HA	Holter data set that simulates the S-ICD alternate vector (see chapter 2)
HEART-TWO	Haemodialysis Associated Changes in R:T Ratio and T Wave Morphology (clinical trial)

HCM	hypertrophic cardiomyopathy
HP	Holter data set that simulates the S-ICD primary vector (see chapter 2)
HRA	Health Research Authority
HS	Holter data set that simulates the S-ICD secondary vector (see chapter 2)
Hz	Hertz
ICD	implantable cardioverter defibrillator
IDE	Investigational Device Exemption (clinical trial)
ISHNE	International Society for Holter and Non-invasive Electrocardiology
J	Joules
LA	left atrium or left atrial or left arm lead / electrode (ECG acquisition)
LBBB	left bundle branch block
LL	left leg lead / electrode (ECG acquisition)
LQTS	long QT syndrome
LV	left ventricle or left ventricular
MADIT	Multicentre Automatic Defibrillator Implantation Trial (clinical trial)
mm	millimetre
MRA	mineralocorticoid receptor antagonist
MRI	magnetic resonance imaging
ms	milliseconds
MS	mathetically generated secondary vector (see chapter 2)
MUST	Multicentre Unsustained Tachycardia Trial (clinical trial)
mV	millivolts
NCT	narrow complex tachycardia

NSVT	non-sustained ventricular tachycardia
NYHA	New York Heart Association
P	primary vector
Pr	proximal sensing electrode
pT	time from onset of QRS complex to peak of T wave
pTc	pT, corrected for heart rate
PTSD	post-traumatic stress disorder
QT	time from onset of QRS complex to end of T wave
QTc	QT, corrected for heart rate
RA	right atrium or right atrial or right arm lead / electrode (ECG acquisition)
RBBB	right bundle branch block
REC	Research and Ethics Committee
RL	right leg lead / electrode (ECG acquisition)
R:T	amplitude ratio of R wave to T wave
RV	right ventricle or right ventricular
s	seconds
S	secondary vector
SA	sinoatrial
SCD	sudden cardiac death
SCD-HeFT	Sudden Cardiac Death in Heart Failure Trial (clinical trial)
S-ICD	subcutaneous implantable cardioverter defibrillator
SVC	superior vena cava
SVT	supraventricular tachycardia

TV-ICD	transvenous implantable cardioverter defibrillator
TWOS	T wave over sensing
UHS	University Hospital Southampton NHS Foundation Trust
µV	microvolts
V	volts
VF	ventricular fibrillation
VR-ICD	single chamber ICD
VT	ventricular tachycardia
VTA	ventricular tachyarrhythmia

Chapter 1 Introduction

1.1 Prologue

The electrocardiogram (ECG) plays a vital role in the assessment of patients across a wide variety of different clinical environments. Surface ECG can be easily and rapidly obtained using simple non-invasive techniques and can provide health care professionals with a detailed and specific understanding of patient well-being.

In modern medicine, ECG analysis is used in the diagnosis of cardiovascular, respiratory and multisystem disorders. The ECG is also ubiquitously employed as a marker of physiological status, with disease severity and response to therapy frequently assessed using the ECG.

In recent years, the wide utility and importance of surface ECG analysis has been increasingly recognised by technology companies. Sophisticated diagnostic algorithms and miniaturised recording equipment have revolutionised the way in which surface ECG is both obtained and used. The modern patient can record their own ECG signal using a smart phone and remote physician interpretation is becoming increasingly common.

However, despite these technological advances, the basic principles of electrocardiography have remained largely unchanged since they were first described at the end of the 19th century. Electrocardiography employs standardised techniques for the detection and recording of myocardial electrical activity at a cellular level. Tiny fluctuations in the membrane potential of individual cardiac myocytes are detected and sequential wave fronts of depolarisation are recorded.

Wave fronts of depolarisation that move towards a recording electrode produce a positive ECG deflection, whilst depolarisation away from the same electrode produces a negative deflection. Consequently, the overall appearance of the ECG is determined, in part, by its angle of observation. This is an important concept which is frequently overlooked.

In this thesis I will examine how ECG signal can be manipulated by changing its angle of observation, before comprehensively describing a novel technique by which this can be achieved. The aim will be to produce a more personalised ECG and the work will focus on the potential impact that this could have on the capabilities of the subcutaneous

implantable cardioverter defibrillator (S-ICD), a novel device which uses ECG analysis to identify life-threatening ventricular arrhythmia. Focusing on one therapeutic device will allow a comprehensive assessment to be performed and ensure that a substantial body of interlinked experimental work can be presented.

The wider utility of ECG manipulation must not be disregarded. It is important to recognise that the principles explored in this thesis go beyond the relatively narrow world of S-ICD sensing. Although it is unfortunately beyond the scope of this work, I believe that the concepts of ECG manipulation that are described, could have wide-ranging future applications in clinical diagnostics, therapeutics and monitoring.

1.2 Sudden cardiac death and defibrillator therapy

Cardiovascular disease is a leading cause of global mortality. It accounts for 30% of all deaths, approximately 17 million each year.[1] 40-50% of cardiovascular deaths are defined as sudden cardiac deaths (SCD).[1] SCD is an event that is non-traumatic, non-violent, unexpected, and results from sudden cardiac arrest within six hours of previously witnessed normal health.[2] 80% of SCD are attributed to ventricular tachyarrhythmias (VTA).[1] These are rapid abnormal heart rhythms that originate in the ventricles and can result in haemodynamic compromise, collapse and death. The annual global mortality burden attributed to VTA is 6 million.[1]

SCD frequently affects individuals who are known to have cardiovascular disease, for example patients with coronary artery disease or cardiomyopathy. SCD can also impact seemingly healthy individuals. On average, every week in the United Kingdom, twelve apparently fit and healthy people aged 35 and under die from SCD.[3] In the non-atherosclerotic population 53% of SCD due to VTA occurs in patients with structurally normal hearts at post mortem.[4]

Patients who experience sudden cardiac arrest rarely survive. In the United Kingdom there are 60,000 cases of out of hospital cardiac arrest each year, with resuscitation attempts by emergency medical services made in around 30,000.[5] At the arrival of the emergency services 20% of these patients are in a heart rhythm which can be treated by defibrillation, but United Kingdom survival estimates range from just 2-12%.[6,7] The key to survival is high quality cardiopulmonary resuscitation and early defibrillation. Every minute without defibrillation reduces the chance of survival by 7-10%. Despite appropriate medical therapy arrhythmia recurrence rates are 40-50% at five years.[8-10]

The implantable cardioverter defibrillator (ICD) is a sophisticated cardiac implantable electronic device that is used in the treatment of VTA and therefore in the prevention of SCD. Designed for individuals at high risk of VTA, an ICD can diagnose and treat life-threatening rhythm disturbances, providing potentially lifesaving therapy within a few seconds of rhythm onset.

The ICD was first developed by Mirowksi and colleagues in the early 1970's but did not obtain FDA (United States Food and Drug Administration) approval for use until 1985.[11]

Early devices consisted of an epicardial patch that was sewn to the outer surface of the ventricle via a surgical thoracotomy, and an extremely large pulse generator that had to be sited in the abdomen. The pulse generator had poor battery life and almost no diagnostic or pacing capabilities.

Fortunately, the ICD has evolved tremendously over the last three decades. Modern devices are small enough to be implanted subcutaneously, often under local anaesthetic and increasingly as day-case procedures. Battery longevity is now greater than ten years and defibrillation technology has been successfully integrated with cardiac pacing, advanced rhythm detection algorithms and sophisticated clinical diagnostics.

1.3 Transvenous ICDs

Most modern defibrillator systems are transvenous ICDs (TV-ICD) comprised of two components; a pulse generator (or can), implanted in a pre-pectoral subcutaneous pocket, and a transvenous defibrillation lead. The lead is attached proximally to the pulse generator and fixated distally to the endocardial surface of the right ventricle (RV). The hallmark of an ICD lead is the presence of at least one shocking coil.

Defibrillation requires a high energy waveform to travel between the pulse generator and the shocking coil(s), passing through the entire myocardium in the process. Widespread cellular depolarisation effectively 'resets' the fibrillating heart and restores normal rhythm. An energy waveform of sufficient magnitude is created by a series of capacitors that are located within the pulse generator, attached to a lithium / silver vanadium oxide battery.

ICD leads can pace and sense the myocardium. Pacing requires extremely small amounts of electrical current to be transferred from the battery to the endocardial surface of the heart via the insulated transvenous lead. Depolarisation of cardiac myocytes around the lead tip creates a wavefront of depolarisation which propagates throughout the myocardium and produces muscle contraction. The lead can also sense intrinsic myocardial activity, identifying local fluctuations in current and relaying this information to the pulse generator.

Electrical activity within the heart chambers is continuously sensed by an ICD and capacitor charging is only instigated when a device diagnosis of VTA is reached. This relies upon increasingly sophisticated diagnostic algorithms. Rapid heart rhythms of suspected ventricular origin are also distinguished from the more benign disturbances that originate in the atria. Shock therapy is delivered for life-threatening rhythm disturbances where the calculated heart rate is above a pre-determined and programmable threshold.

TV-ICD systems can deliver anti-tachycardia pacing (ATP), a painless treatment for monomorphic ventricular tachycardia (VT). Arrhythmia termination is achieved through the delivery of rapid bursts of RV pacing, delivered at a faster rate than the cycle length of the tachycardia. ATP is intended to reduce the need for painful shock therapy, although there are no randomised controlled studies that directly compare ATP and non-ATP delivery systems.

1.3.1 Terminology

Numerous ICD systems are currently available with a variety of different lead configurations and several competing manufacturers. ICD terminology can be confusing, especially as TV-ICD systems are primarily differentiated by their pacing characteristics. The simplest TV-ICD system is a VR-ICD. A single transvenous ICD lead is implanted in the RV and the 'VR' notation relates to the system's ability to deliver rate responsive ventricular pacing.

A dual chamber, or DR-ICD, has an additional dedicated pacing lead that is sited in the right atrium (RA). Dual chamber rate responsive pacing can be delivered (DR) and atrio-ventricular (AV) synchrony can be maintained. The RA lead can also provide information regarding atrial activity during episodes of tachycardia. This can be integrated into rhythm detection algorithms, helping to distinguish between atrial and ventricular arrhythmia.

Cardiac Resynchronisation Therapy (CRT) is a well-established treatment for heart failure patients with left ventricular (LV) systolic dysfunction and asynchronous LV contraction.[12] It has been shown to both improve quality of life and reduce heart failure related hospitalisations and mortality.[13] The hallmark of CRT is the presence of an additional LV lead which is usually passed via the coronary sinus tributaries to the epicardial surface of the LV. This allows both ventricles to be paced together, eliminating the dyssynchronous LV contraction that is observed in both bundle branch block and RV only pacing.

CRT is often delivered in combination with ICD therapy, given the considerable overlap between the clinical indications for both therapies. A CRT-defibrillator (CRT-D) is therefore a device which combines a TV-ICD and an LV pacing lead. A CRT-pacemaker (CRT-P) is a permanent pacemaker with an additional LV lead that is unable to deliver high energy therapy. CRT devices usually incorporate a right atrial lead, although this is unnecessary in patients in permanent atrial fibrillation.

All TV-ICD leads contain a distal shocking coil that is sited within the RV. Dual coil leads, which contain an additional superior vena cava (SVC) coil are also available. Systems with dual coil leads have more available shocking vectors and are associated with lower defibrillation thresholds, although their leads are more challenging to extract in cases of infection or malfunction.

1.3.2 Landmark trials

Current indications for ICD therapy are based upon several landmark clinical trials, the overwhelming majority of which were conducted in TV-ICD recipients. ICD implantation was initially only recommended for patients who had already experienced a life-threatening VTA. This was the result of three landmark studies, published in the late 1990s.

Antiarrhythmic Versus Implantable Defibrillator (AVID) was a randomised controlled trial which compared ICD implantation to medical therapy (predominantly amiodarone) in patients with aborted cardiac arrest and poorly tolerated VT.[14] A significant reduction in mortality was observed in the ICD group with the greatest benefit seen in patients with left ventricular ejection fractions (EF) <35%.[14]

Canadian Implantable Defibrillator Study (CIDS) randomised patients with previous VT, ventricular fibrillation (VF), or syncope, to either amiodarone or ICD therapy.[15] This demonstrated a 20% reduction in mortality in the ICD group, although this did not reach statistical significance. Further analysis identified that patients over 70 and those with an EF <35% were most likely to benefit from ICD therapy.[16]

Cardiac Arrest Study Hamburg (CASH) randomised medical therapy (amiodarone or propafenone) to ICD implantation in patients with a history of cardiac arrest, demonstrating a 28% reduction in mortality in the ICD group.[17]

A meta-analysis of these three secondary prevention trials showed that implantation of an ICD was associated with an overall reduction in the relative risk of death of 28%, driven by a 50% reduction in arrhythmic death compared to optimal medical therapy.[18]

The first major primary prevention trials were the Multicentre Automatic Defibrillator Implantation Trial (MADIT) and the Multicentre Unsustained Tachycardia Trial (MUST).[19,20] These randomised controlled trials compared ICD therapy to medical therapy in patients with ischaemic cardiomyopathy, non-sustained VT (NSVT) and sustained monomorphic VT induced during an electrophysiology study (EPS). The trial designs differed but the results were very similar with ICD use decreasing mortality by 50%.[21]

The subsequent MADIT II study recruited patients with an ischaemic cardiomyopathy and an EF<30%, with no requirement for documented NSVT or an EPS. After a 20 month follow up the mortality rate in the ICD group was 14.2% compared to 19.8% in the control group.[22]

The Sudden Cardiac Death in Heart Failure Trial (SCD HeFT) was able to broaden the clinical indication for an ICD by eliminating the requirement of an ischaemic cardiomopathy. This large multicentre trial randomised over 2,500 patients with EF<35% and New York Heart Association (NYHA) class II or III symptoms to ICD implantation or amiodarone, regardless of the aetiology of their heart failure. ICD implantation was shown to reduce all-cause mortality, whilst amiodarone did not.[23]

In 2016, the results of the Defibrillator Implantation in Patients with Non-ischaemic Systolic Heart Failure (DANISH) trial questioned the value of ICD therapy in the primary prevention of mortality in non-ischaemic patients. The investigators randomised 1116 patients with symptomatic non-ischaemic systolic heart failure (EF ≤35%) to either ICD therapy or routine clinical care. After a mean follow up of 67.6 months the primary outcome of all-cause mortality had occurred in 120 patients (21.6%) in the ICD group and in 131 patients (23.4%) in the control group. ICD therapy was therapy associated with a non-significant reduction in mortality (hazard ratio, 0.87; 95% confidence interval [CI], 0.68 to 1.12; P=0.28).[24]

The DANISH trial resulted in significant debate within the ICD community. A subsequent meta-analysis of six trials of ICD therapy in non-ischaemic systolic heart failure, which included the results from DANISH, showed that ICD therapy was still associated with a statistically significant mortality reduction, odds ratio 0.76 (0.64 - 0.91).[25]

Much of the discussion focussed upon the study patients use of optimal pharmacological therapy; angiotensin converting enzyme (ACE) inhibitors, beta blockers and mineralocorticoid antagonists (MRA). In the DANISH group, compared to earlier studies, a higher percentage of patients received these medications and nearly 60% also received CRT pacing, perhaps better reflecting modern practice. The results of the DANISH study have not yet impacted upon the European guidelines for ICD implantation (discussed below), as these have not been updated since its publication.

1.3.3 Indications

In 2015 the Task Force for the Management of Patients with Ventricular Arrhythmias and the Prevention of Sudden Cardiac Death of the European Society of Cardiology (ESC) produced consensus guidelines outlining the clinical indications for ICD therapy across

Europe.[26] ICD implantation was strongly recommended for both the primary and secondary prevention of SCD.

In secondary prevention, ICD therapy has a class 1A recommendation in patients who have experienced haemodynamically compromising VTA, are expected to survive with a good functional status for more than one-year, and where no reversible cause for the dysrhythmia can be found.[26]

In primary prevention, patients with severe systolic heart failure, regardless of underlying aetiology, have a class 1 indication for ICD therapy. These patients must have symptomatic heart failure (New York Heart Association (NYHA) Class II or III) and an EF <35% after three months of optimal medical therapy. They are also expected to survive for at least one year with good functional status.

NYHA Class IV patients are excluded due to their significant risk of non-arrhythmic death, primarily due to pump failure. The level of evidence for primary prevention in patients with reduced EF is 'A' for ischaemic cardiomyopathies and 'B' for non-ischaemic cardiomyopathies, as the evidence of benefit is greater in the ischaemic population.[26]

The guidelines also cover rarer conditions which are associated with arrhythmic death such as hypertrophic cardiomyopathy (HCM), arrhythmogenic RV cardiomyopathy (ARVC), long QT syndrome (LQTS) and Brugada Syndrome. In these conditions ICD therapy is indicated for individuals with disease specific 'at risk' features that place them at sufficiently high risk of SCD.

1.3.4 Further considerations

In all potential ICD recipients, identifying the optimal balance of risk remains a significant ongoing challenge. One must balance the potential reduction in arrhythmic death with the financial and personal cost of device implantation. Consideration must be given to device related complications, both peri-implant and long-term, as well as an individual's relative risk of non-arrhythmic death. The psychological impact of both appropriate and inappropriate shock therapy also warrants consideration, as do the financial costs to society of implanting significantly expensive devices which may not prolong life expectancy.

Most ICD recipients do not experience life-prolonging therapy. Registry data from Israel suggests that 30 months post implantation only 2.6% of primary prevention patients and 7.4% of secondary prevention patients have received appropriate shock therapy. In the same period 4.8% have died, 65% from non-cardiac causes.[27] Determining what percentage of device recipients should receive life prolonging therapy is not straightforward, with equally valid but diverging economic and ethical arguments presented.

Further research is definitely required to better understand the 'at risk' concept, especially in cardiac conditions which can result in both arrhythmic and non-arrhythmic death. ICD indications are therefore likely to evolve, with the development of increasingly sophisticated risk stratification tools.

1.3.5 Complications

Cardiac device implantation is associated with high complication rates. Registry data from Denmark shows that 10% of patients undergoing any form of cardiac device implantation experience a complication, with a 6% chance of major complication.[28] TV-ICD implants are even higher risk than simple pacemakers, with in-hospital complication rates of 11-16%.[28]

Early complications relate to the implant procedure as it requires both the surgical formation of a subcutaneous pocket and central venous access. The subclavian, axillary and cephalic veins are frequently used to facilitate delivery of the transvenous lead. Complications include infection, haematoma, inadvertent arterial puncture, pneumothorax, haemothorax and cardiac tamponade. Late complications associated with TV-ICD systems include lead fracture, lead displacement, venous obstruction and infection.

Defibrillator lead longevity is also a significant issue and for many years the TV-ICD lead has been regarding as the 'weakest link' in the ICD system.[29] In one study the annual rate of ICD lead defects requiring intervention reached 20% in ten year old leads, with lead survival at 5 and 8 years just 85% and 60% respectively.[30] A recent study of >3000 ICD recipients also found a 12-year cumulative incidence of lead failure of 17% and a device related infection rate of 6%.[31]

One third of patients who experience lead failure present with inappropriate shock therapy.[30] Adequate treatment of both lead failure and device related infections may

require transvenous lead extraction; a highly specialist procedure with an in-hospital procedure-related major complication rate of 1.7% and a mortality rate of 0.5%.[32,33]

1.3.6 Living with an ICD

Clinicians must not underestimate the potential impact that defibrillator implantation can have on a patient's life. It is increasingly easy to overlook this important aspect of patient care, especially as ICD implantation has become an increasingly routine minor procedure. Most implants are performed as day case operations under local anaesthetic and post procedure the physical recovery time is extremely short. However, living with an ICD can result in profound psychological effects and mandates lifestyle limitations which may be of overwhelming significance to the recipient.

The negative psychological effects of an ICD are well documented. Some recipients are reassured by the presence of a device, but many are burdened by the constant reminder of their illness and mortality. Negative psychological effects are frequently reported. 87% of patients report anxiety post ICD implantation, with clinically diagnosed anxiety disorders occurring in 13-38% and depression occurring in 30% of ICD recipients.[34,35]

Shock therapies are associated with depression persistence, further increases in anxiety levels and a greater incidence of psychological distress.[36-38] Post-traumatic stress disorder (PTSD) is identified in 30% of cardiac arrest survivors. Concerningly, 20% of ICD recipients also develop this disorder, 2-5 years after device implantation, with ≥5 ICD shocks identified as a PTSD risk factor.[39,40]

Lifestyle limitations associated with ICD implantation include important restrictions on driving. ICD recipients cannot hold a Class 2 licence. Restrictions on a Class 1 licence also occur immediately after implantation and after any subsequent therapies, regardless of whether they were appropriate.[41] Patients who drive commercially or who rely on their driving licence, may find this limitation unacceptable and should be forewarned. Likewise, patients who hold licenses for other modes of transportation (flying, boating, motor sports) should contact the relevant licensing bodies for information prior to an implantation decision being made.

Strong electromagnetic fields can damage, deactivate or induce shock therapy from an ICD. Device recipients may therefore have to desist from certain leisure activities or even seek

alternative employment. Common household devices can be problematic, for example induction hobs and transcutaneous electrical nerve stimulation (TENS) machines. ICD recipients are generally discouraged from contact sports and high-risk activities, especially where individuals are isolated (such as mountain climbing or open water swimming).

Prior to implantation patients should be counselled regarding device follow up. Most ICD systems are compatible with remote monitoring, facilitated by small monitors which are provided to patients. Remote monitors regularly interrogate the implanted ICD, often during sleeping hours. Information on device function and clinical diagnostics are relayed to the centre conducting device follow up via a secure online server. Remote systems using both mobile phone signal and broadband internet are available. Remote follow up reduces the frequency of on-site device assessments, although some patients find it intrusive and express concerns about the security of the system.

Patients should be aware that their device may have an audible or vibration alarm and be instructed how to respond to its signal, especially out of normal working hours. Patients instinctively believe that an alarming device, in the middle of the night, means that shock therapy may be imminent. A non-significant increase in lead impedance, to marginally above the threshold value, is a more likely explanation.

Patients must be counselled regarding shock therapies and be aware that shock therapies can occur whilst conscious. Inappropriate shock therapies, those that are delivered in the absence of life-threatening arrhythmia, are particularly concerning to patients. Shocks delivered, without warning, to asymptomatic individuals, can significantly impact psychological wellbeing. It is not uncommon for patients, especially those in the primary prevention cohort, to request ICD deactivation after receiving high volumes of inappropriate shocks.

ICD recipients and their families should be aware of the potentially challenging decisions which they may face in the future. Examples include end of life care and the timing of ICD deactivation, re-withdrawal of therapy in the event of LV recovery, and the significant challenges presented by system infection or failure. These difficult and emotive decisions may not become relevant in every patient but are worthy of consideration.

1.4 Subcutaneous implantable cardioverter defibrillators

The subcutaneous ICD (S-ICD) represents an entirely new strategy in defibrillator therapy. Unlike TV-ICD systems the S-ICD does not enter the heart or the vascular system. S-ICD development has been primarily driven by the high complication rates associated with TV-ICD therapy, especially the significant concerns regarding defibrillator lead longevity.

The S-ICD compromises a subcutaneous can, implanted in a left axillary position, and a tunnelled subcutaneous lead. [*Figure 1*] The lead contains a single shocking coil and two sensing electrodes. Defibrillation is achieved in a similar fashion to TV-ICD systems. A biphasic high energy waveform is passed between the capacitor (located within the can) and the shocking coil, capturing the body of myocardial tissue in the process. By virtue of its subcutaneous location the S-ICD requires greater defibrillation energy than a TV-ICD, operating at 80 Joules (J) rather than 35J. These higher energy requirements result in longer charge times and necessitate a larger and heavier can.

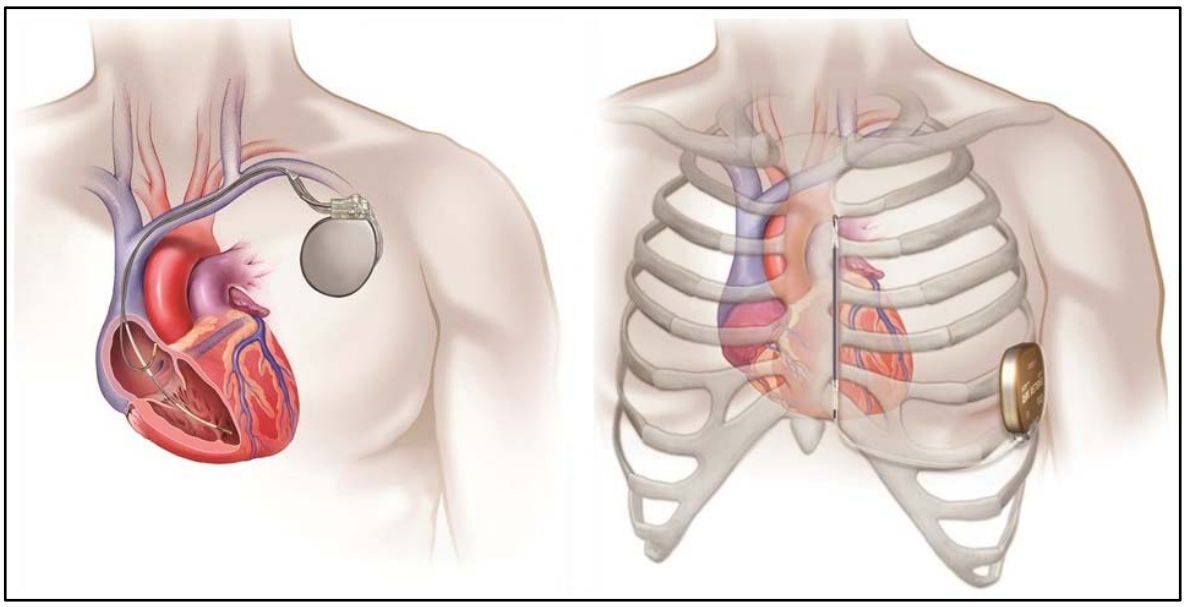

Figure 1: Transvenous versus subcutaneous ICDs

Left: a dual chamber transvenous ICD (DR-ICD). Right: a subcutaneous ICD (S-ICD).

The subcutaneous lead is not exposed to the repetitive contractions of the cardiac cycle or the hostile environment of the vasculature, it is therefore expected to have greater longevity than a transvenous lead. The central venous circulation is also preserved during S-ICD implantation making future vascular occlusion and systemic infection extremely

unlikely. Implant complications are reduced as no venous puncture is required. In the event of infection or lead failure, S-ICD extraction is an extremely low risk procedure compared to transvenous lead extraction.

The S-ICD has extremely limited pacing capabilities. Subcutaneous pacing can be delivered but is similar to external transcutaneous pacing. Repeated mechanical capture of skeletal muscle is uncomfortable for the conscious patient and the S-ICD will therefore only deliver transient pacing, if it is required, immediately after shock therapy. The S-ICD is therefore not suitable for patients with a permanent pacing indication, including those who require resynchronisation pacing for heart failure. The S-ICD cannot deliver ATP making it unsuitable in patients with a history of monomorphic VT that might be successfully treated by ATP.

1.4.1 Landmark trials

Developed by Cameron Health (CA, USA) but later acquired by Boston Scientific (MA, USA), the S-ICD obtained a CE (Conformité Européenne) mark in 2009. FDA approval was achieved in 2012, after the Investigational Device Exemption (IDE) Study met its primary end points for both safety and efficacy.[42]

The IDE study was a non-randomised, prospective, multicentre trial in which 321 patients with standard TV-ICD indications were implanted with an S-ICD. At 180 days 99% were free from complication (primary safety endpoint target 79%) and successful conversion of induced VF was observed in >90% (primary efficacy target of 88%).[42]

The EFFORTLESS S-ICD Registry, a non-randomised, standard of care, multicentre registry was subsequently formed to provide long-term S-ICD system related, clinical and patient reported outcome data.[43,44] A pooled analysis of the IDE study and EFFORTLESS registry at two years post implantation showed that in 882 S-ICD patients there were no episodes of endocarditis, cardiac injury, or electrode failure. Acute major complication rates for implant were also reduced in comparison to TV-ICD implants (haematoma, lead malposition or displacement and pneumothorax).[45]

Midterm outcomes from EFFORTLESS have also been published, with data from 985 patients analysed at a mean follow up of 3.1 ± 1.5 years.[46] Predefined endpoints for safety and efficacy continue to be fulfilled, whilst complication rates (4.1% at 30 days and 8.4% at

360 days), inappropriate shock rates (8% at one year) and VF conversion efficacy (97.4%) are similar to those observed in TV-ICD populations.[46,47]

1.4.2 Indications

The 2015 ESC Guidelines state that physicians should consider the S-ICD as an alternative strategy in all patients with an indication for a TV-ICD, providing there is no requirement for permanent pacing, cardiac resynchronisation or ATP (class IIa recommendation, level of evidence C).[26] The S-ICD should also be considered a useful alternative to a TV-ICD system when venous access is difficult, after the removal of an infected TV-ICD system or in younger patients with a long-term need for ICD therapy (class IIb recommendation, level of evidence C).[26]

A large cohort of patients exist in whom the guidelines support implantation of either a TV-ICD or an S-ICD system. In the absence of a comparative study, physician and patient preference are fundamental factors and a wide variation in clinical practice is seen throughout the United Kingdom, Europe and the United States of America. A prospective randomised controlled trial in which patients are randomised to receive either an S-ICD or a TV-ICD is currently in progress but will not report results until 2020.[48]

1.4.3 Implantation

S-ICD implantation can be performed using either conscious sedation or general anaesthesia. Correct positioning of the device is achieved using a combination of anatomical surface landmarks and real time x-ray fluoroscopy. To ensure an adequate defibrillation threshold the shocking coil and the lead must be sited with the cardiac muscle mass between them. This necessitates a posterior axillary position for the can, given the extremely anterior position of the shocking coil.

The can is being increasingly placed in an intermuscular location, between the anterior surface of serratus anterior and the posterior surface of latissimus dorsi, rather than in a subcutaneous pocket. A better cosmetic appearance is achieved in slim device recipients, whilst in larger individuals the reduction in sub-generator fat produces lower defibrillation thresholds.[49-51]

From the generator pocket the lead is tunnelled subcutaneously using a dedicated implantation tool. The lead travels medially across the chest to a surface landmark that is 1cm inferolateral to the xiphisternum. A small incision is made at this location and the lead is fixated to the underlying muscle using sutures. A further subcutaneous tunnel is created travelling superiorly, parallel to the sternum. The distal lead is inserted into this tunnel producing a ninety-degree lead angle. Conventionally the lead is placed on the left side of the sternum, but right sided lead placement may be required in some device recipients.

1.5 S-ICD sensing

1.5.1 Sensing vectors

The S-ICD lead contains two specialist sensing electrodes that are located at either end of the shocking coil. During implantation, the proximal electrode (Pr) is sited 1cm inferolateral to the xiphisternum, fixated to the underlying muscle. The distal electrode (D) is tunnelled to its final location, lying 14cm superior to the proximal electrode. The pulse generator (can) is electrically active and creates a third sensing point in the S-ICD system.

From their subcutaneous location, the small changes in current that are associated with intrinsic electrical conduction through the myocardium can be sensed. Electrocardiogram (ECG) signals can be recorded between any two of the three sensing points, creating three available signals. These are called 'vectors' and are named as follows; primary (proximal to can), secondary (distal to can) and alternate (distal to proximal). [

Figure 2]

From a strictly mathematical perspective they are not actually vectors, but scalars, in that they have an amplitude (voltage) which varies against time, but no given directional component. However, for consistency, they will be referred to as vectors throughout this manuscript.

The vectors strongly resemble a surface ECG and the individual ECG components (R wave, T wave) can be easily visually identified. This is different from the 'near field' electrograms which are recorded in a TV-ICD system, where the sensing electrode is sited within the RV itself. [*Figure 3*] As a consequence the S-ICD vectors are more susceptible to over-sensing of skeletal muscle contractions and to electrical noise.

After implantation, the most favourable vector from a morphological perspective, is selected for clinical use. At routine follow up appointments the morphologies of all three available vectors are routinely reassessed. The clinical vector can subsequently be changed if problems are identified, for example as a result of baseline ECG changes in the device recipient, or where inappropriate sensing has been detected.

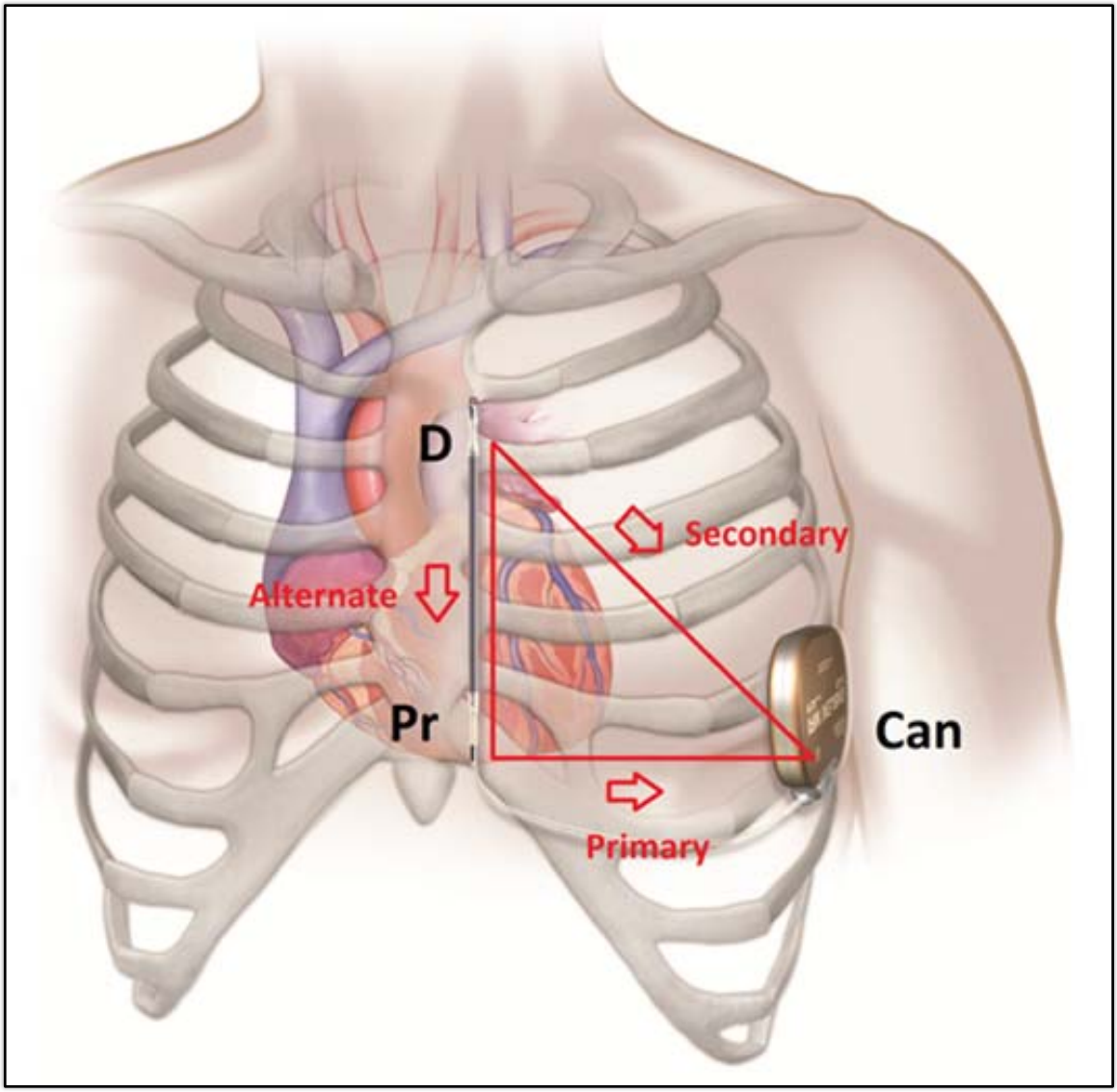

Figure 2: S-ICD sensing electrodes and vectors

An implanted S-ICD with underlying anatomical features showing the location of the can (pulse generator), the proximal (Pr) and distal (D) sensing electrodes and the shocking coil (located between the electrodes) Image (prior to annotation) © Boston Scientific Corporation or its affiliates. Reproduced with permission.

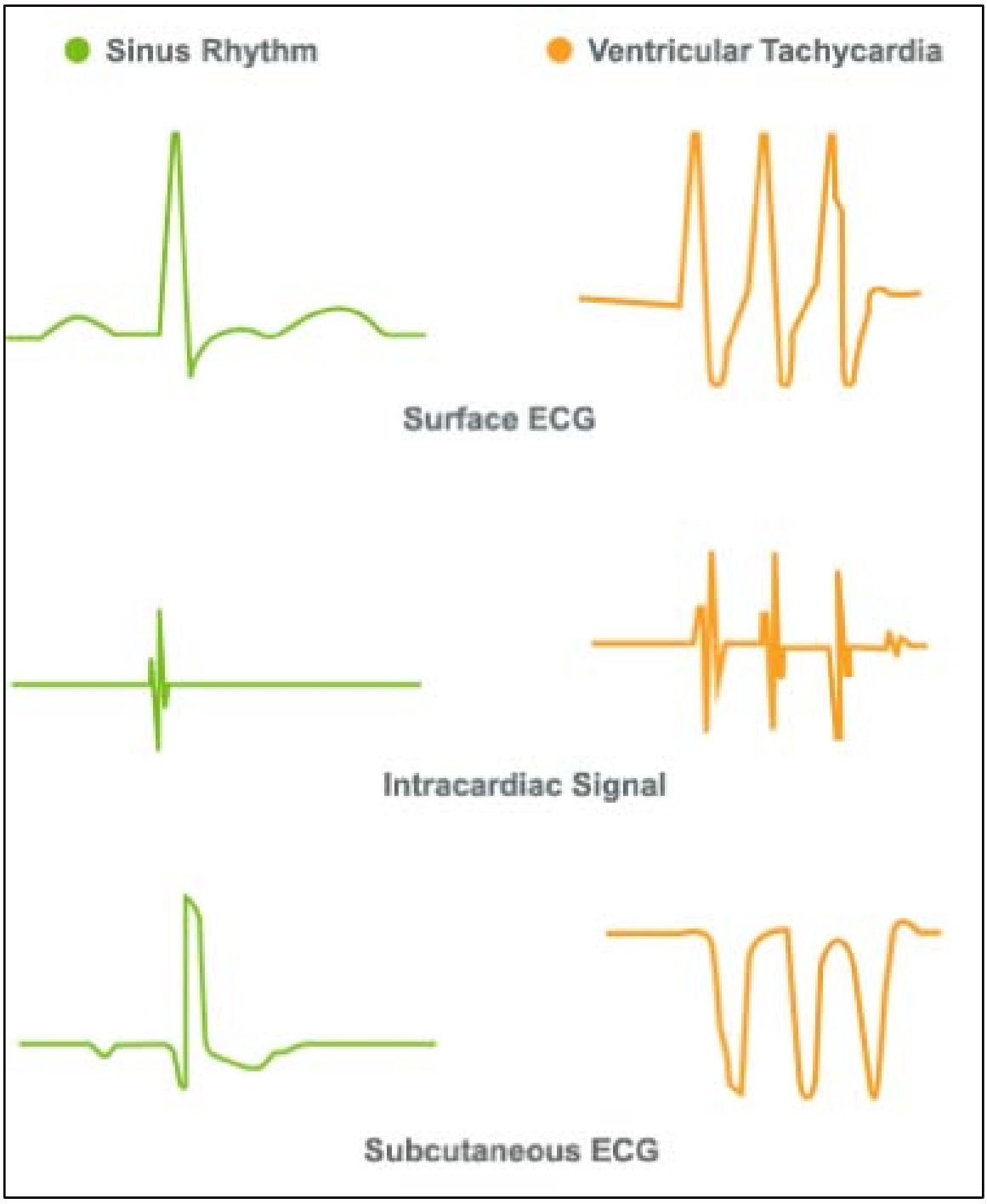

Figure 3: Surface ECG, intracardiac signal and S-ICD sensing vectors

The S-ICD vectors have a similar morphological appearance to the surface ECG, whilst the intracardiac signals (from a TV-ICD) are markedly different. There is no identifiable 'T wave' deflection in these intracardiac signals.

1.5.2 Tachycardia detection

Life-threatening VTA is characterised by rapid ventricular activity. During VF, the heart rate is invariably greater than 300 beats per minute (bpm), whilst haemodynamically compromising VT rarely occurs at less than 160bpm. S-ICD treatment strategies can therefore be primarily determined by heart rate. Shock therapies are only ever delivered if the heart rate exceeds a pre-determined threshold. Heart rate ranges can also be used to program different treatment zones, with variable algorithms and treatments attributed to different degrees of tachycardia.

In an S-ICD, the patient's heart rate is calculated by a continuous assessment of their vector amplitude using a programmed sensitivity level. Amplitudes above the sensitivity level are identified as R waves (ventricular depolarisation) whilst amplitudes below this level are effectively ignored. The heart rate is calculated using the average of four consecutive RR intervals.

The sensitivity level must be high enough to prevent over-sensing. This occurs when components of the ECG signal, for example atrial activity (P waves) or ventricular repolarisation (T waves) are incorrectly counted as R waves. Over-sensing can also be secondary to interference from background noise or myopotentials from skeletal muscle.

The sensitivity level must also be low enough to prevent the inadvertent under-sensing of R waves, which can vary slightly in amplitude from beat and beat, and can change significantly with alterations in posture, autonomic tone or electrolyte balance.

Cardiac pacemakers have traditionally been programmed to use a fixed sensitivity level, requiring an adequate safety margin between the mean R wave amplitude and the amplitude of any signal components which must not be over-sensed (i.e. T waves, far-field R waves or pacing artefacts in a dual chamber system).[52]

Fixed sensitivity is inappropriate for an ICD. VF is characterised by complexes of rapidly fluctuating amplitudes, which can be very low in amplitude. Fixed sensitivity could therefore lead to under-sensing of VF, inhibiting VF detection. [*Figure 4*]

The widely utilised solution to this problem is 'auto adjusting sensitivity', whereby the sensitivity level of the device falls gradually after the detection of a R wave, before being rapidly increased to a percentage value of the next sensed R wave.[52] This adjustment of

sensitivity is designed to prevent under-sensing of low amplitude VF. A simplified schematic diagram which displays the principles of auto adjusting sensitivity is provided below. [*Figure 5*]

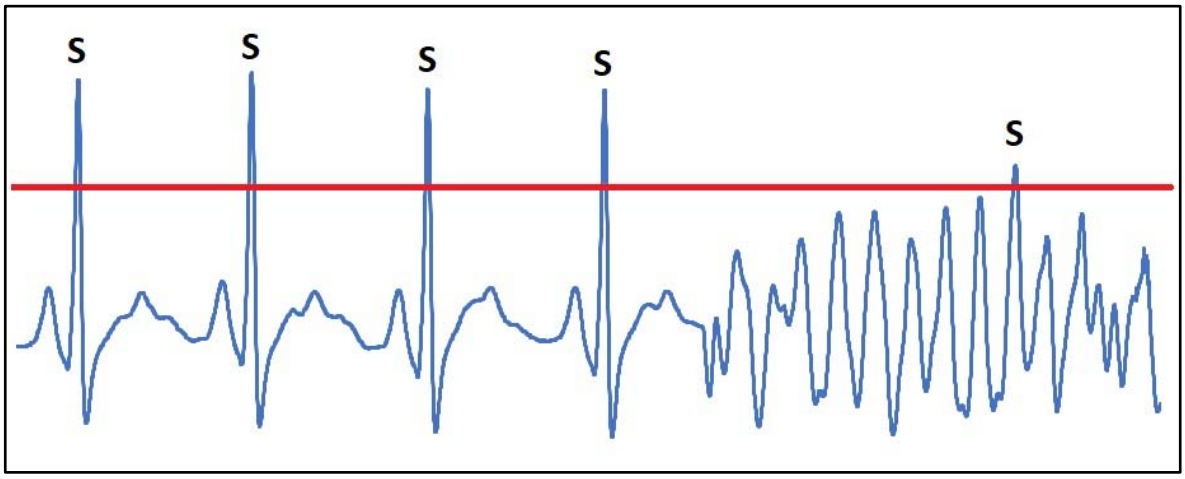

Figure 4: S-ICD sensing with fixed sensitivity

S-ICD vector signal is displayed chronologically from left to right. The hypothetical fixed sensitivity value is shown by the red line. 'S' is a sensed event (i.e. the S-ICD has identified an R wave with an RR interval that is too long to meet the criteria for tachycardia which would be denoted as 'T'). At the start of the recording the patient is in normal sinus rhythm, but onset of VF occurs after four normal beats. During VF there is significant under-sensing of the fibrillation waves and tachycardia is never detected. Shock therapy would not have been delivered and the patient may not have survived this episode. Image created for this thesis by the author.

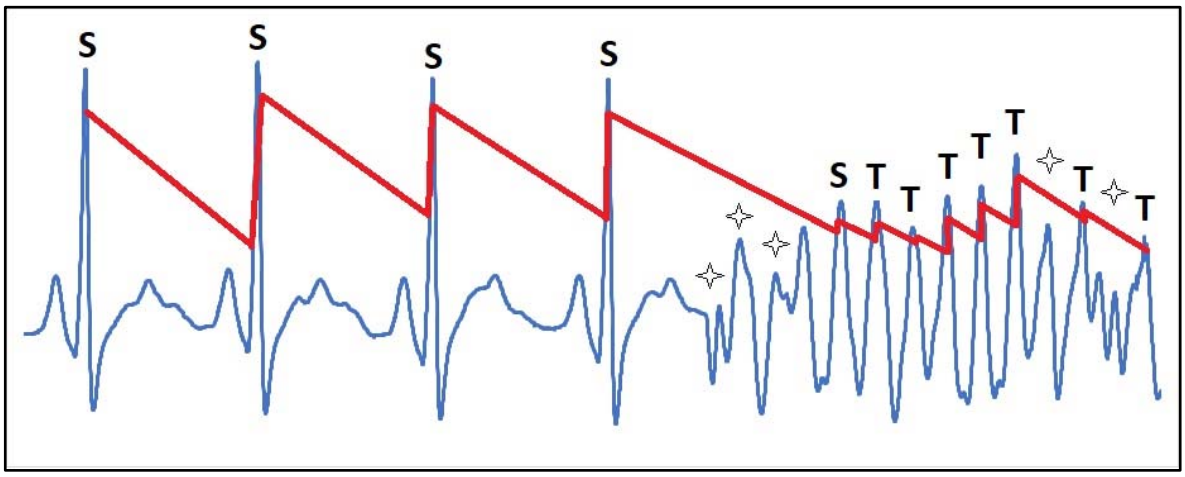

Figure 5: Auto adjusting sensitivity

The S-ICD vector signal from Figure 4 is displayed once again. In this example the auto adjusting sensitivity (red line) falls after detection of a sensed event ('S'), before increasingly rapidly to a fixed percentage of the amplitude of the next sensed event. Where a short RR interval is identified the event is marked 'T' for tachycardia. During VF, the increase in heart rate is correctly identified with several consecutive T markers displayed. Note that there is still some under-sensing during VF (*). Image created for this thesis by the author.

S-ICD sensing is more complicated than the schematic provided. After each event detection, the S-ICD actually employs a short blanking period, during which no sensing occurs. This is to prevent double counting of an R wave with more than one peak, a pattern that is often seen in the presence of ventricular conduction disease. The length of the blanking period varies from 160ms-200ms depending on the preceding detection interval, with shorter blanking periods at faster heart rates and immediately post shock therapy.

The S-ICD does not employ uniform sensing parameters, but rather a finite series of sensing profiles. Between sensed events, profiles employ different rates of decline in their sensitivity level and rise to variable percentage values on detection of a further event. The application of a given sensing profile is dependent on the preceding detection interval, such that more aggressive sensing is performed at faster heart rates and during tachycardia events.[53,54]

The S-ICD also alters the way in which heart rate is determined during an episode of tachycardia. During sensed events (i.e. during normal rhythm) the heart rate is calculated as the mean of the four preceding RR intervals. However, once this calculation places the heart rate above the pre-determined tachycardia zone, the device will switch to tachycardia detection using a rolling 'X out of Y' counter. This probabilistic counter is a safety mechanism that is used in all modern ICD systems. It is designed to prevent intermittent under-sensing of low amplitude VF from inhibiting, or delaying, the delivery of life-saving therapy.

In the S-ICD 'X' is number of detection intervals which fall in the tachycardia zone, whilst 'Y' is the total number of intervals in the rolling window of interest. Shock therapy is only delivered when 18 out of 24 intervals fall in the tachycardia detection zone. Once the decision to deliver shock therapy is taken, capacitor charging is initiated. As this can take several seconds 'persistence analysis' is employed immediately prior to shock delivery to ensure that spontaneous termination of the tachycardia has not occurred. This requires the 'X out of Y' condition to be maintained or exceeding in the last two certified intervals.[55]

The sensing mechanism of the S-ICD has been shown to be extremely effective. In an experimental study, where VTA episodes were deliberately induced to test the sensitivity of S-ICD detection, 100% (n=44) of VTA episodes were correctly detected by the S-ICD. In the same study TV-ICD systems were found to be equally effective.[56]

1.5.3 Rhythm discrimination

An S-ICD can be programmed with a single tachycardia zone. In this configuration a single heart rate boundary is identified above which all rhythm disturbances are treated as VTA (i.e. >220bpm). Single zone programming is simple and effective. Capacitor charging is instigated once the '18 out of 24' criteria is met, and shock therapy is delivered if persistence analysis reveals ongoing tachycardia.

If the shock is not successful, redetection of tachycardia occurs allowing further shocks to be delivered. A maximum of 5 shocks are delivered for each single tachycardia episode. If the shock is successful normal sensing function will resume, after a short period in which post shock pacing may be delivered for bradycardia. Successful shocks, which are immediately followed by further rhythm disturbance, can result in this cycle being indefinitely repeated. Patients who experience recurrent tachycardia, for example during electrical storm, can experience high numbers of shocks, far outweighing the maximum number that is programmed for a single tachycardia event.

The S-ICD can also provide dual zone programming, where two separate tachycardia zones are identified. The two zones have different heart rate boundaries and different rhythm detection algorithms are applied in each zone. In the 'shock zone' detection and treatment are identical to those described for single zone programming.

In the 'conditional zone', slower rhythm disturbances (i.e. 170-220bpm), have discriminators applied to assess their probable origin prior to treatment. Shock therapy is withheld if the rhythm disturbance is felt to be a supraventricular tachycardia (SVT) and not ventricular in origin. Dual zone programming is more complicated than single zone programming but is designed to reduce the incidence of inappropriate shock therapies.

Rhythm discrimination in the conditional zone is based upon the morphological appearance of the QRS complex during tachycardia. This is achieved by comparing vector morphology during tachycardia with a vector template. The template is originally recorded around the time of device implant but can be updated at subsequent follow up appointments.

Conditional zone rhythms are treated by shock therapy if they have a combination of a poor QRS morphology match to the stored template and either a variable beat to beat

morphology, or an increased QRS width compared to the template. The conditional zone treatment algorithm is summarised below. [*Figure 6*]

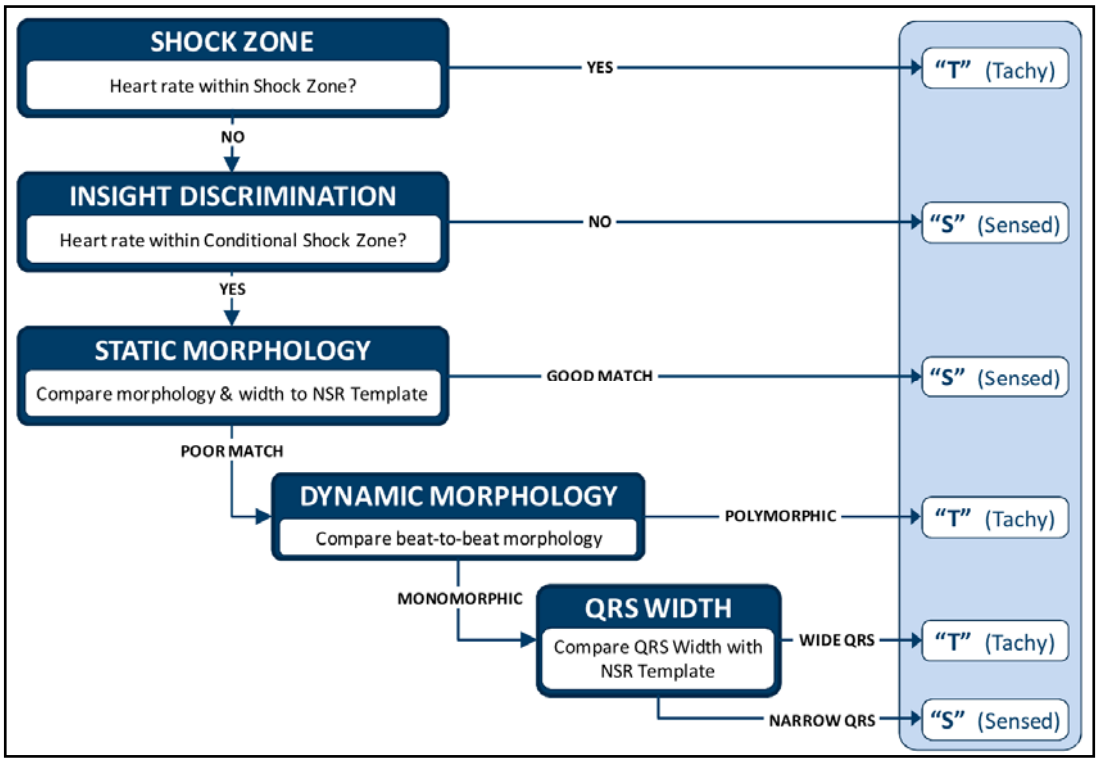

Figure 6: S-ICD rhythm discrimination algorithm

QRS morphology is determined by the pattern of depolarisation of the ventricles, this should be unchanged during SVT episodes as ventricular depolarisation is still initiated through the His-Purkinje system. Onset of SVT may alter the activation of the atria, but this is not expected to result in significant changes to the QRS complex. Conversely during VTA, the activation pattern of the ventricle should be significantly altered as the ventricle mass will not be depolarised through the His-Purkinje system, resulting in a morphological change.

These principles are not absolute. An SVT that utilises an anterograde accessory pathway, (an abnormal electrical connection that allows electrical signals to travel from the atria to the ventricle) would result in a change in QRS morphology as the His-Purkinje system would be bypassed. Rhythms like this include pre-excited atrial fibrillation and antidromic AVRT, both of which are rare in the ICD population.

Furthermore, heart rate related bundle branch block (BBB), where ventricular activation is altered due to failure of rapid conduction down one of the main branches of the His-

Purkinje system, is also a well-recognised condition. The prevalence of rate related BBB occurring during SVT is not well documented in the literature.

Rate related changes in QRS morphology are also not restricted to the development of a new BBB pattern. In patients with a pre-existing BBB major changes in QRS morphology have been demonstrated to occur in 39% of patients during SVT with minor morphological changes seen in a further 37%.[57] Ventricular tachycardia with a similar QRS morphology to that observed in sinus rhythm has also been described in the literature.[58]

Tachycardias of supraventricular origin include atrial fibrillation, atrial flutter and a group of abnormal rhythms which are commonly described using the umbrella term SVT. These include focal atrial tachycardia, atrio-ventricular reciprocating tachycardia (AVRT), AV nodal re-entrant tachycardia (AVNRT) and junctional tachycardia. These rhythms can result in extremely rapid heart rates, with episodes in excess of 200bpm frequently seen.

Younger patients, who are capable of rapid conduction through the AV node, can also significantly increase their sinus rate during exercise. In sinus rhythm a patient's estimated peak heart rate is calculated as '220 minus their age' placing younger fitter individuals at risk of shock therapy, even in the absence of a rhythm abnormality.

Supraventricular rhythm disturbances can cause palpitations, shortness of breath, pre-syncope and chest pain. They are very rarely associated with haemodynamic collapse or SCD. ICD treatment is not required for these rhythm disturbances and any shock therapies that are delivered during SVT are inappropriate.

VTA episodes, which are life-threatening, can occur over a wide range of different heart rates. VF is inevitably extremely rapid (>300bpm) but the cycle lengths of monomorphic VT vary tremendously. In large studies, patients with structural heart disease and either a primary or secondary prevention ICD, up to 50% of clinical arrhythmias have been found to have a heart rate <200bpm.[59]

Despite these theoretical challenges, the S-ICD displays excellent supraventricular discrimination when tested experimentally. In one study, appropriate detection of SVT episodes occurred in 98% of induced events (n=50) and the S-ICD outperformed a composite group of three TV-ICDs, whose overall sensitivity was 68% ($p<0.001$).[56]

1.6 S-ICD screening

Reliable determination of heart rate is critical to S-ICD function and requires the R wave to be accurately differentiated from other ECG components contained within the vector signal. Consequently, to be eligible for an S-ICD, a patient must have at least one sensing vector with QRST morphology that can be accommodated by the device sensing mechanism.

The main morphological determinant of eligibility is the relative amplitudes of the R wave and the T wave, with small R:T ratios being unacceptable. This is because after R wave detection the system's sensitivity level is required to gradually fall to prevent inadvertent under-sensing of VF.

In vectors with small R:T ratios, this results in double counting, as the T wave sits above the sensitivity level. The consequence is that a second sensed event is registered, a phenomenon called T wave over-sensing (TWOS). In these circumstances the S-ICD may be unable to differentiate normal rhythm at 120bpm, from a monomorphic VT at 240bpm.

An optimal balance must be achieved. After R wave detection the S-ICD must be sufficiently sensitive to ensure tachycardia detection, but sufficiently insensitive to prevent TWOS. Avoidance of VF under-sensing must also remain the clinical priority as this is likely to be associated with a high risk of death.

The suitability of an individual's vector morphology is identified during a mandatory pre-implant screening process that is undertaken in all potential S-ICD recipients using guidelines provided by the device manufacturer.[55] Patients with no suitable vector are currently deemed to be ineligible for an S-ICD.

1.6.1 Overlay technique

Pre-implant S-ICD screening can be undertaken using an overlay technique. This requires an individual's surface ECG to be compared to a series of acceptable templates provided on a transparent ruler. The printed ECG is used as a non-invasive surrogate of future vector morphology and is obtained by accurate positioning of surface ECG electrodes.

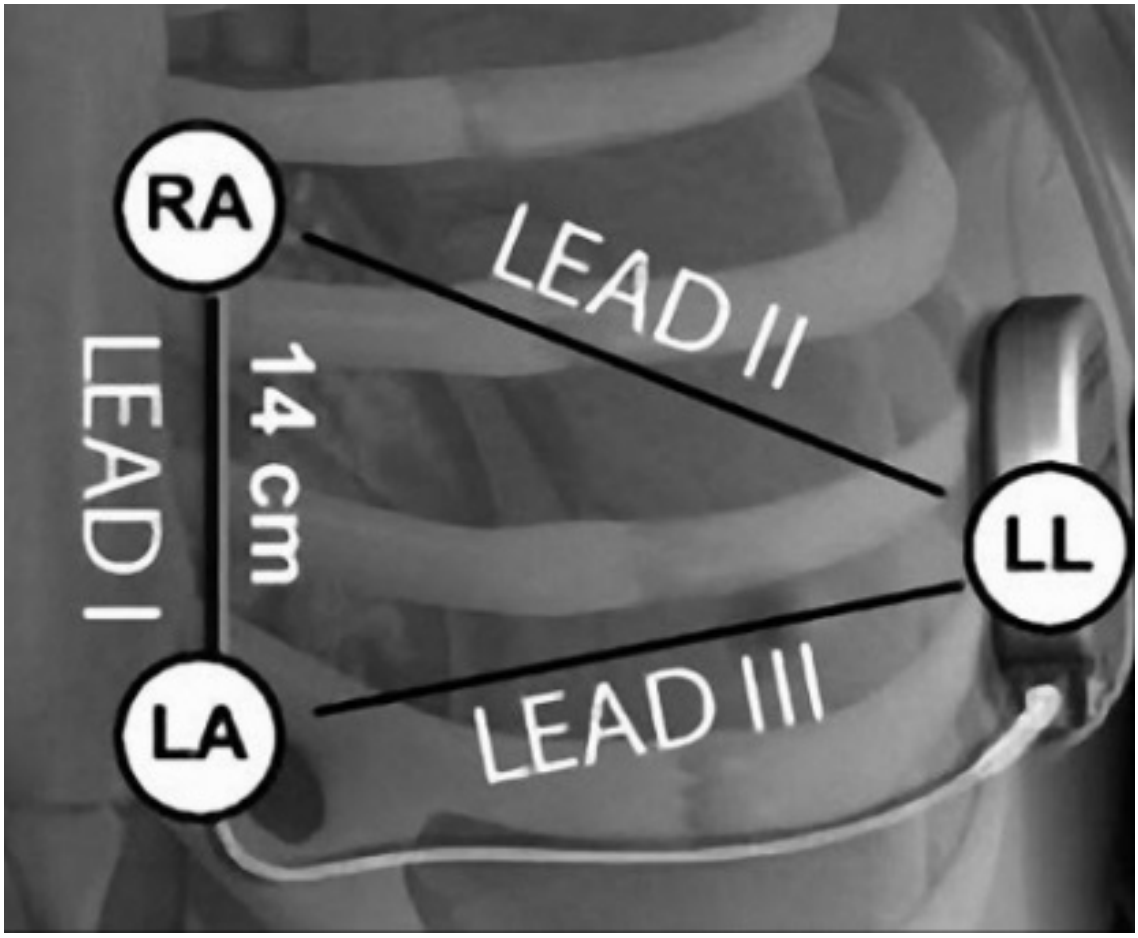

Figure 7: Surface ECG placement for S-ICD screening

LL: left leg lead, placed at the 5th intercostal space along the mid-axillary line to represent the intended location of the implanted pulse generator. LA: left arm lead, placed 1 cm inferolateral to the xiphisternum to represent the intended location of the proximal sensing electrode. RA: right arm lead, should be placed 14 cm superior to the ECG Electrode LA, to represent the intended position of the distal sensing electrode. The left leg lead (LL) is a neutral lead which is not shown, it is usually placed on the right side of the chest wall. © Boston Scientific Corporation or its affiliates. Reproduced with permission.

The electrodes are placed on the chest wall using the same anatomical landmarks that will guide future S-ICD implantation. In this configuration the limb leads, from a standard 12 lead ECG machine, display the three S-ICD vectors as leads I, II and III on a printed ECG rhythm strip. All three vectors are captured in at least two postures (i.e. standing and sitting) using standard ECG paper speed (25mm/s) and ECG amplitudes of 5 millimetre/millivolt (mm/mV), 10mm/mV and 20mm/mV.

The recorded QRST morphology in every vector is then compared to the acceptable templates. The template is aligned to the isoelectric line of the ECG, and the QRST complexes are viewed through the appropriately sized template. The R wave peak of the

ECG must be placed within either hashed box (positive or negative) of any template. A vector passes screening if the remainder of the QRST complex sits entirely within the boundary of the template. To be eligible for an S-ICD a patient requires a single vector to pass screening in both postural positions at the same amplitude.

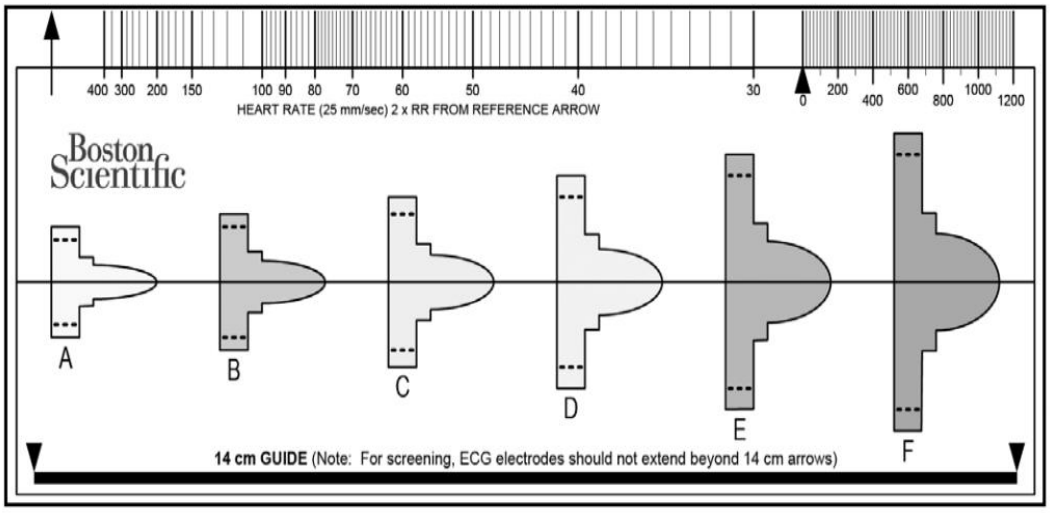

Figure 8: S-ICD screening tool

© Boston Scientific Corporation or its affiliates. Reproduced with permission.

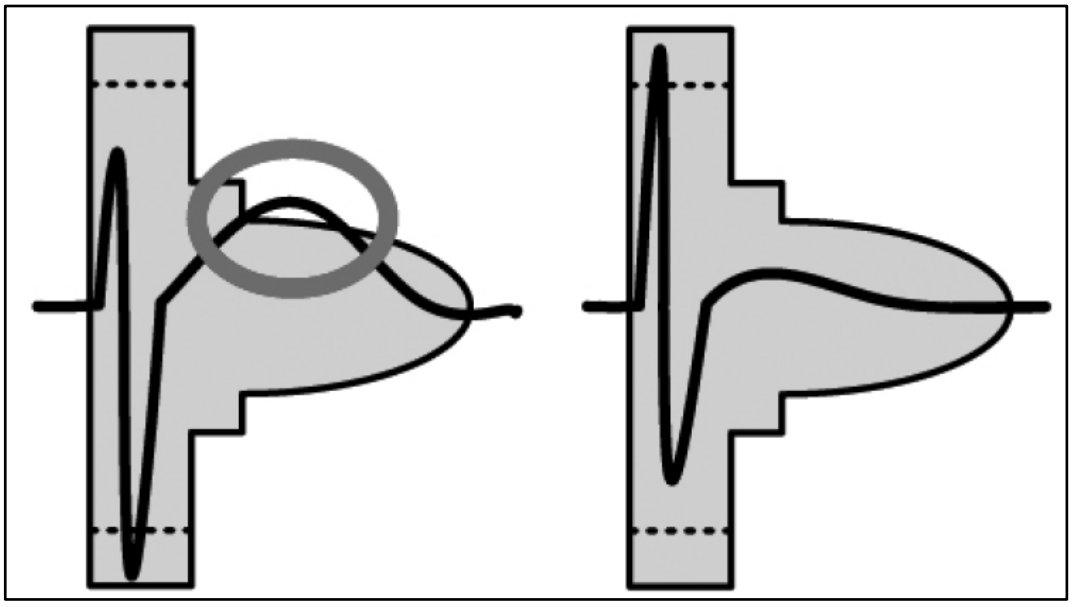

Figure 9: Screening success and failure

Left: the vector fails screening as the T wave does not remain within the template. Right: The peak of the R wave is appropriately sited within the hashed box and the T wave is entirely contained within the template. This vector passes screening. © Boston Scientific Corporation or its affiliates. Reproduced with permission.

1.6.2 Automated screening tool

The overlay screening technique has now been largely replaced by the introduction of an automated screening tool (AST). This is a software program that is integrated into the S-ICD programmer. The AST can perform surface ECG analysis allowing vector eligibility to be automatically determined. The process of manual ECG assessment is therefore eliminated.

The S-ICD programmer is a specialised device that can communicate wirelessly with the S-ICD. It is utilised in device interrogation, programming and during implantation. The programmer has external ECG cables which can acquire ECG signal via the application of skin electrodes.

Despite the transition from overlay screening to AST, the underlying principles of screening have remained unchanged. Surface ECG is still used as a surrogate of vector morphology, the same recording positions are utilised, and multiple postures are assessed.

Screening is only performed during baseline rhythm. This is confirmed by the operator, who also inputs information regarding the patient's posture prior to each recording. As with overlay screening the vector outcomes are binary; a given vector can either pass or fail.

During automated screening both R wave and T wave amplitudes are calculated. The R wave amplitudes are relatively easy to determine as they are the highest amplitude components of the entire vector signal. T wave amplitude is the highest amplitude signal observed during the detection window that follows each R wave, allowing of course for auto-adjusting sensitivity and blanking periods.

Whilst this signal is likely to represent the T wave, the device is in fact calculating a signal amplitude (R wave) and a noise amplitude (all other signal components). The signal to noise or R:T ratio is combined with an overall assessment of signal amplitude to generate a numerical 'vector score'. High signal amplitudes and high R:T ratios are desirable and result in high vector scores. The threshold at which a vector is deemed to be eligible is 100, with scores of <100 denoting an ineligible vector.

The vector score that is calculated during screening is not reported to the operator. In fact, vector scores have only ever been used during internal product development, and most S-ICD implanters would be unaware of their existence. To a clinician a vector that passes is safe for clinical use, whilst a vector that fails cannot be used in clinical practice.

Consequently, clinical and experimental assessments of S-ICD sensing have never differentiated between passing vectors, despite the wide range of passing vector scores that must exist. It is tempting to assume that a vector score of 1200 would be preferable to a vector score of 120, in that this might convey protection against tachycardia under sensing or signal over sensing. Unfortunately, there is currently no data to support or refute this hypothesis.

1.6.3 Surface ECG versus subcutaneous ECG

Surface ECG is used as a surrogate of future S-ICD vector morphology as this allows screening to be performed cheaply and non-invasively, using equipment that is widely available. During the screening process surface electrodes are placed relatively close to the proposed final position of the subcutaneous lead electrodes, as the same anatomical landmarks are used in screening and implantation. Of course, some variability must exist, especially as the pulse generator is increasingly implanted in a submuscular location.

In a large individual the final position of the pulse generator might be several centimetres nearer to the myocardium than the surrogate surface marker used during screening. The overall degree of correlation between S-ICD signals and surface ECG recordings has never been assessed.

A comparison study has been undertaken which compared ECG recordings from the surface and the subcutaneous

s tissue, but this did not relate directly to the S-ICD system. The study was performed using a Reveal Plus (Medtronic Inc., MN, USA). This is a small implantable diagnostic device that is sited on the anterior chest wall. It is designed to provide symptom to rhythm correlation in patients with intermittent cardiac symptoms.

The Reveal Plus device differs from the S-ICD in that it has a single chest wall location with two adjacent sensing points located a few centimetres apart. Whereas the S-ICD records ECG vectors between two subcutaneous sensing electrodes over a far greater distance. The Reveal Plus is also more superficial that an S-ICD pulse generator would be, and the signal undergoes different processing.

Despite these differences, the study remains informative from an S-ICD perspective. At rest the subcutaneous and surface ECGS were found to be highly correlated (96.0%, n=48) with similar R wave amplitudes (487 ± 40 versus 507 ± 49 μV) and signal to noise ratios (13.4 ± 0.8 versus 13.5 ± 0.7).[60] Subcutaneous ECGs were also found to be less susceptible to artefact inducing manoeuvres than surface ECGs.

1.6.4 S-ICD ineligibility

Approximately 5.7% of all ICD recipients have no suitable S-ICD sensing vector and are therefore ineligible for an S-ICD by virtue of their vector morphology. I have derived this value from two separate studies in which S-ICD screening was performed on consecutive ICD patients with no pacing indication.[61,62] In both studies patients were screened using the overlay technique, with passing vectors demonstrating suitability in two different postures. [*Figure 10*]

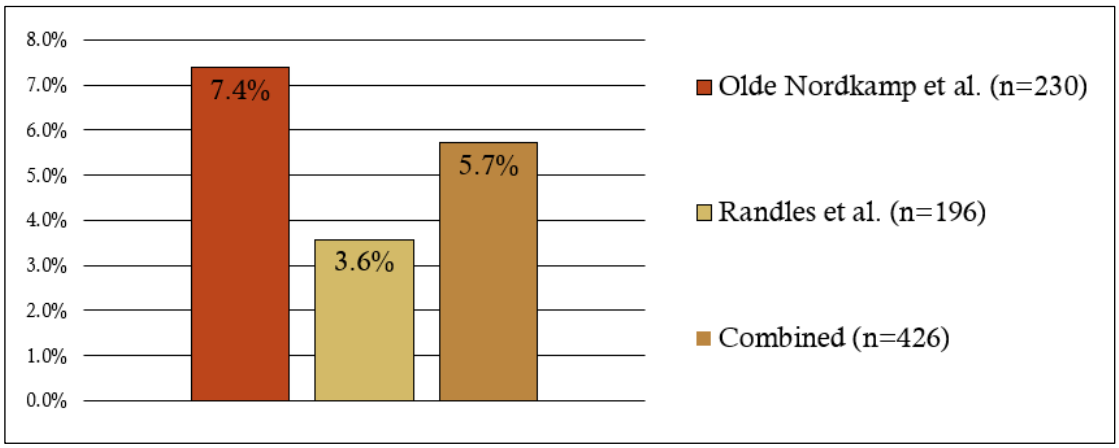

Figure 10: S-ICD ineligibility

S-ICD ineligibility (i.e. those with no suitable vector) in consecutive ICD patients with no pacing indication. Left and middle: results as reported in the literature.[61,62] Right: the combined results for these two studies.

In certain population groups even higher rates of ineligibility have been detected. For example, in patients with adult congenital heart disease (ACHD), screening failure rates have ranged from 13% (n=30) to 24.6% (n=102).[63,64] These substantial screening failure rates are driven by the high prevalence of left and right bundle branch block in the ACHD cohort, with altered repolarisation and abnormal T wave morphology frequently observed.[65]

Increasing numbers of ACHD patients are surviving to adulthood and many will require an ICD at some stage. High failure rates are particularly concerning in this population as many ACHD patients have undergone complex surgical repairs which leave them with challenging venous access (i.e. Fontan circulation, atrial switch operations). Additionally, for those with residual intracardiac shunts, an extravascular device would eliminate the risk of stroke associated with transvenous lead thrombosis or vegetation.[65]

Patients with HCM are another group in whom high rates of screening failure have been observed. HCM is characterised by left ventricular hypertrophy which results in both high amplitude signal and abnormal repolarisation. In one study ineligibility due to vector morphology was calculated to be 16% (n=165).[66] Concerningly, this rose to 36% (n=22) in patients with HCM and a high risk of SCD.[66] This patient cohort are particularly important as they have a 5-year risk of SCD >6%, the threshold at which a primary prevention ICD is indicated in HCM.[67]

Most potential ICD recipients who fail S-ICD screening will, as an alternative, have a TV-ICD system implanted. In patients for whom S-ICD therapy offers the greatest potential benefit, S-ICD ineligibility is a significant limitation to their care. Examples include patients with difficult venous access, individuals at high risk of systemic infection, and younger patients who may require decades of defibrillator therapy.

1.7 Inappropriate shock therapy

Inappropriate shocks, those delivered in the absence of ongoing VTA, are reported to occur in between 3 and 21% of ICD patients in large meta-analyses.[68] Inappropriate shocks adversely affect quality of life and psychological health. They can also be responsible for the induction of ventricular arrhythmias and are associated with increased mortality.[69-72]

A single inappropriate shock has been shown to increase all-cause mortality (hazard ratio 1.6, p=0.01). Every subsequent shock further increases mortality risk, up to a hazard ratio of 3.7 after 5 inappropriate therapies (n=1544, follow up 41 ± 18 months).[72] Fortunately, in the TV-ICD population, the introduction of increased VTA detection times and higher heart rate treatment zones has reduced inappropriate therapy rates to around 5%.[73-75]

In the S-ICD population, the rate of inappropriate shock therapy is reported at 8.3%, with 73% of these episodes the result of cardiac over-sensing (follow up 21 ± 13 months, n=581).[47] Cardiac over-sensing occurs where any part of the QRST signal is misinterpreted as a sensed event, resulting in an over-estimation of heart rate.

Total inappropriate shock episodes	**101**
Cardiac over-sensing	**74 (73%)**
- Low amplitude signal / T wave over-sensing (TWOS)	61 (82%)
- P wave over-sensing	1 (1%)
- QRS over-sensing	7 (10%)
- Other / combined types	5 (7%)
SVT	**18 (18%)**
Non cardiac over-sensing	**9 (9%)**

Table 1: Causes of inappropriate S-ICD shocks

Results from the EFFORTLESS registry with data from 581 patients after mean follow up 21 months.[47] Non cardiac over-sensing includes the incorrect sensing of noise and myopotentials.

1.7.1 T wave over-sensing

In the S-ICD population the commonest cause of cardiac over-sensing is TWOS. This occurs when the T wave is of greater amplitude than the sensitivity level of the S-ICD at that moment in time. The T wave is counted as a second event and a single QRST complex is misinterpreted as two separate R waves with a short R:R interval.

TWOS can be caused by large amplitude T waves or low amplitude R waves, as the sensed R wave amplitude determines the starting point from which the post R wave sensitivity level degrades.[76] TWOS occurs despite pre-implant screening, which is of course designed to preventing individuals with unsuitable vectors (low R:T wave ratio, low R wave amplitude) from ever receiving S-ICD therapy.

TWOS can only ever be diagnosed retrospectively using stored episodes of tachycardia downloaded from the S-ICD using a programmer. Downloaded episodes provide a visual representation of vector morphology and the S-ICD's interpretation of events, displayed in the marker channel. This allows the clinician or physiologist to determine if tachycardia was correctly diagnosed, whether treatments received were appropriate or inappropriate, and to identify evidence of under or over-sensing.

An example of a TWOS episode that has been retrospectively downloaded from a patient's S-ICD is provided below. Visually there is no obvious change in T wave morphology or size, but the device can be seen to start double counting after around 5.5 seconds. At this time 'T' in the marker channel denotes sensed intervals which fall within the tachycardia zone. Every QRST complex is denoted with two corresponding 'T' markers. In this example capacitor charging is initiated ('C') but therapy is not delivered as the TWOS does not persist. The patient is fortunate to have avoided inappropriate shock therapy. [*Figure 11*]

1.7.2 Subclinical T wave over sensing

The S-ICD is only programmed to store episodes of tachycardia that result in capacitor charging. If the '18 out of 24' criteria are not met; no record of the event is made. This preserves battery life and limits the internal memory requirements of the system. Given that within six months of ICD implantation 60% of patients will have experienced at least one episode of non-sustained VT (NSVT), this is an understandable approach.[77]

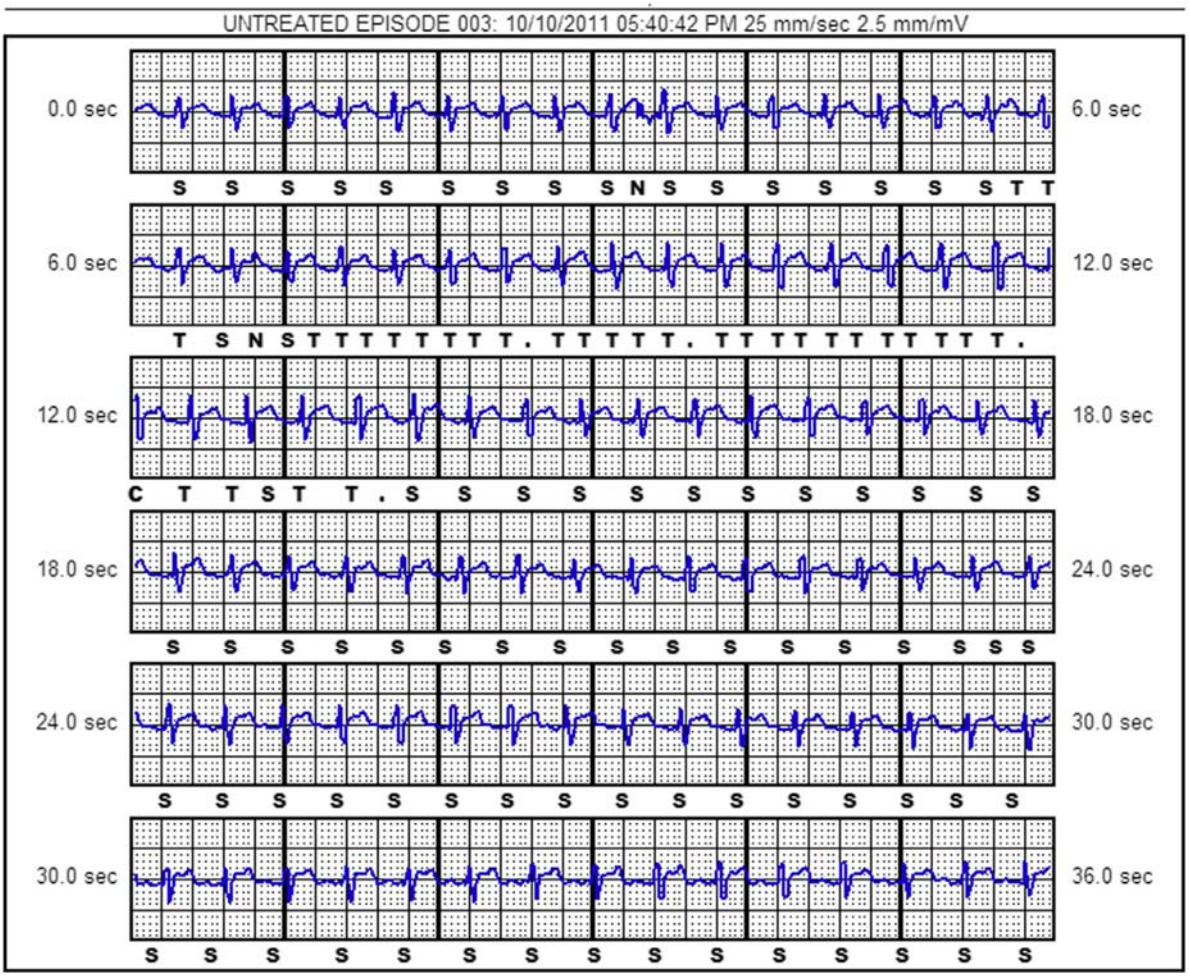

Figure 11: An example of T wave over-sensing

The device, which labels normal sensed beats with an 'S', has incorrectly labelled a period of normal rhythm as a tachycardia ('T'). This has occurred as the device is counting both the QRS complex and the T waves as ventricular beats during this period. This is easy to diagnose as there are clearly twice as many event markers as QRS complexes. Fortunately, this episode did not result in therapy being delivered as the issue spontaneously resolved itself, but capacitor charging was initiated ('C') and the episode was therefore stored for analysis.

Unfortunately, TWOS can therefore only ever be diagnosed if it results in capacitor charging. For the purposes of this manuscript episodes of TWOS which do not result in capacitor charging shall be described as 'subclinical TWOS'. I feel this is an important concept as subclinical TWOS is likely to be a risk factor for the development of both clinical TWOS events and inappropriate S-ICD shocks. The incidence of TWOS in the S-ICD population is unknown and cannot currently be calculated.

Wilson et al. described the case of a man who experienced five inappropriate shocks due to over-sensing by his S-ICD. The patient received shock therapy due to a cascade of over-sensing which started from a single over-sensed T wave. Incorrect detection of a short R:R

interval resulted in the S-ICD adopting a more aggressive sensing profile, with a more rapidly declining post R wave sensitivity. The consequence was further TWOS and the instigation of an even more aggressive sensing. The cycle continued and ultimately led to inappropriate shock therapy.[54]

The importance of this case is that it demonstrated how subclinical TWOS can rapidly escalate into shock therapy, underlying the potential importance of subclinical TWOS as a concept. Of course, one must be cautious when extrapolating from a single case report. It is however possible that the uniqueness of this case is not the mechanism of inappropriate shock therapy described, but that enough event data was available for the over-sensing to be explained in such detail.

At present most episodes of inappropriate shock therapy due to TWOS appear to be random probabilistic events. There is usually a background of normal sensing and no ongoing evidence of TWOS at review. I believe that subclinical TWOS may be an important and potentially identifiable pre-cursor to inappropriate shocks therapies.

1.7.3 Risk factors for T wave over sensing

The high prevalence of inappropriate shock therapy due to TWOS is a significant concern for S-ICD recipients and their physicians. Independent researchers have considered whether TWOS events can be predicted in advance, and their research has focussed upon the identification of clinical and electrocardiographic criteria which might confer an increased risk.

A recent multi-centre observational study of S-ICD recipients identified ECG parameters that predict inappropriate shock therapy due to TWOS.[78] In this study the pre-implant ECG of six S-ICD recipients who had received inappropriate shock therapy due to TWOS were compared to a control group of 95 S-ICD recipients who had not experienced this phenomena.

In the TWOS cohort the following parameters were found to be significantly prolonged: QRS duration (140.7 ± 28.7 versus 105.9 ± 24.6ms, p = 0.007) time to peak T wave amplitude (pT) (369.9 ± 52.2 vs. 322.7 ± 41.0, p = 0.014), time to peak T wave amplitude corrected for heart rate (pTc) (403.9 ± 22.6 vs. 347.8 ± 41.4, p = 0.006), QT interval (462.5 ± 58.4 vs. 417.6

± 51.9 p = 0.021), QT interval corrected for heart rate (QTc) (500.4 ± 41.2 vs. 446.8 ± 49.7, p = 0.021) and R:T ratio (3.5 ± 1.1 vs. 9.5 ± 13.2, p = 0.034).

By multivariate analysis pTc was shown to be the ECG parameter that was most predictive of inappropriate shock therapies due to TWOS. A pTc >390ms predicts inappropriate shocks due to TWOS with a specificity of 98.9%, sensitivity of 38.5%, positive predictive value of 83.3%, and negative predictive value of 91.6%.[78]

A further observational study of 96 S-ICD recipients, of whom 6 had experienced TWOS, did not completely support these findings.[79] In this study 21 different ECG parameters were compared between the two patient cohorts and no significant difference was identified in QRS duration, QT interval, QTc or R:T ratio. The only ECG parameter with a significant difference between the groups was the R wave amplitude in lead I, (3.7 ± 1.6mV versus 7.4 ± 3.7mV, p=0.002). R wave amplitudes in other ECG leads showed no difference.[79] Unlike the previous study the authors used 12 lead ECG recordings instead of vector screening ECGs and pTc, the most predictive ECG parameter in the previous study, was not assessed.[79]

The small sample size of these two studies and their divergent findings, significantly limit the conclusions which can be drawn. Inappropriate shocks remain difficult to predict and continue to occur in individuals with suitable vector morphologies, normal S-ICD function and no record of previous TWOS events.

1.7.4 Smart Pass

The device manufacturers have developed a system modification which is designed to reduce the incidence of TWOS. 'Smart Pass' is a programmable high pass filter which has been designed to reduced TWOS and has been incorporated into the newest models of S-ICD (A219 and A209).[80] It is designed to modify the vector signal such that the R:T ratio is optimised during tachycardia detection. Smart Pass does not fundamentally alter the sensing mechanism that has been described previously but represents an additional filter that can be applied during rhythm determination.

Smart Pass operates by reducing the amplitude of lower frequency signal (<10Hz), whilst allowing high frequency signal (>10Hz) to pass through without modification. This optimises vector morphology as R waves, VT and VF are all high frequency signal, whilst T

waves are lower frequency. Application of the filter reduces the T wave amplitude, resulting in an increase in R:T ratio. Smart Pass automatically disables in the presence of low amplitude (<0.5mV) signal.

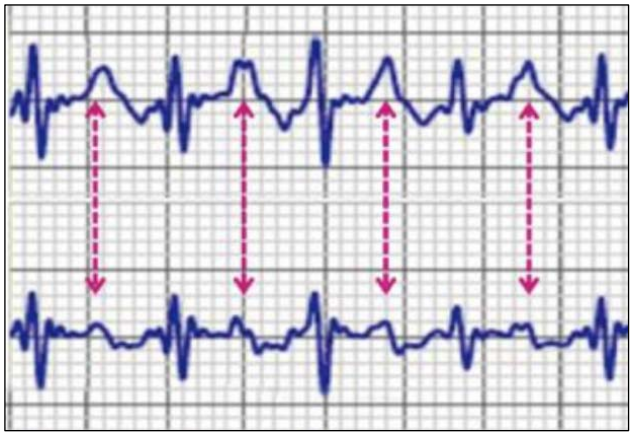

Figure 12: Smart Pass

Top: original vector signal. Bottom: vector signal after application of the Smart Pass Filter. The T wave amplitude is significantly reduced by Smart Pass whilst the QRS complexes are relatively unchanged. © Boston Scientific Corporation or its affiliates. Reproduced with permission.

Smart Pass has been retrospectively tested using episode data obtained from the Latitude remote patient monitoring system.[81] One year follow up data from 1984 patients implanted with an S-ICD between 2015 and 2016 was analysed, with episode data from 880 shocks presented to a blinded adjudication panel. In 655 of the patients (33%) Smart Pass had been enabled at implant, whilst in the remaining 1329 patients (67%) Smart Pass has been disabled.

Smart Pass was found to reduce the risk of first inappropriate shock by 50% ($p<0.001$), reduce the risk of all inappropriate shocks by 68% ($p<0.001$) and reduced the overall incidence of inappropriate shocks to 4.3%.[81] This inappropriate shock rate is significantly lower than that described in the EFFORTLESS registry and is comparable to the inappropriate shock rates achieved by TV-ICD systems employing modern programming techniques.[47,73-75]

T wave amplitude reduction by Smart Pass filtering did not lead to an increase in under-sensing of dysrhythmia. When the Smart Pass enabled and disable cohorts were compared, statistically significant differences were not detected in appropriate shock rates (5.2% versus 6.6%, $p=0.18$) or in the time taken to correctly diagnose and treat the patient's first VTA episode (17.4s versus 16.7s, $p=0.92$).[81]

1.8 Personalised vector sensing

The personalised vector is a hypothetical, individualised vector, which has optimal morphology for S-ICD sensing. In this section, I will describe how personalised vectors can be produced, thereby presenting a novel solution to the inherent limitations of a three-vector system. To understand the method by which personalised vectors are generated, it is first necessary to review some key principles of electrocardiography.

Electrocardiography is the science of detecting and recording myocardial electrical activity, as such a review of the underlying principles of cardiac conduction is also required.

1.8.1 Cardiac conduction system

The heart is a complex multicellular organ comprised of electrically active cardiac myocytes with unique and varied electrophysiological properties. The myocytes, which are built around an electrically inert fibrous 'skeleton', generate and propagate electrical impulses. At a cellular level this controls the movement of calcium ions across the cell membrane and produces myocyte contraction. At a structural level, the timing and co-ordination of electrical impulses determine both the heart rate and rhythm, as well as the cardiac output.[82]

Cardiac myocytes have a negative resting membrane potential of around -90mV, the result of negative ions present within the cell. When appropriately stimulated, ion channels in the cell membrane open and close facilitating the co-ordinated movement of ions across the membrane. The resulting changes in membrane potential, plotted against time, is called an action potential. The cardiac action potential has three distinct periods; depolarisation (phase 0), repolarisation (phase 1-3) and a resting phase (phase 4).

Depolarisation is predominantly driven by the rapid influx of sodium ions. The change in membrane potential associated with depolarisation of a single cell is sufficient to stimulate the opening of sodium channels on adjacent cell membranes. From a single stimulus a wave of depolarisation can therefore be established, travelling from cell to cell throughout the myocardium.

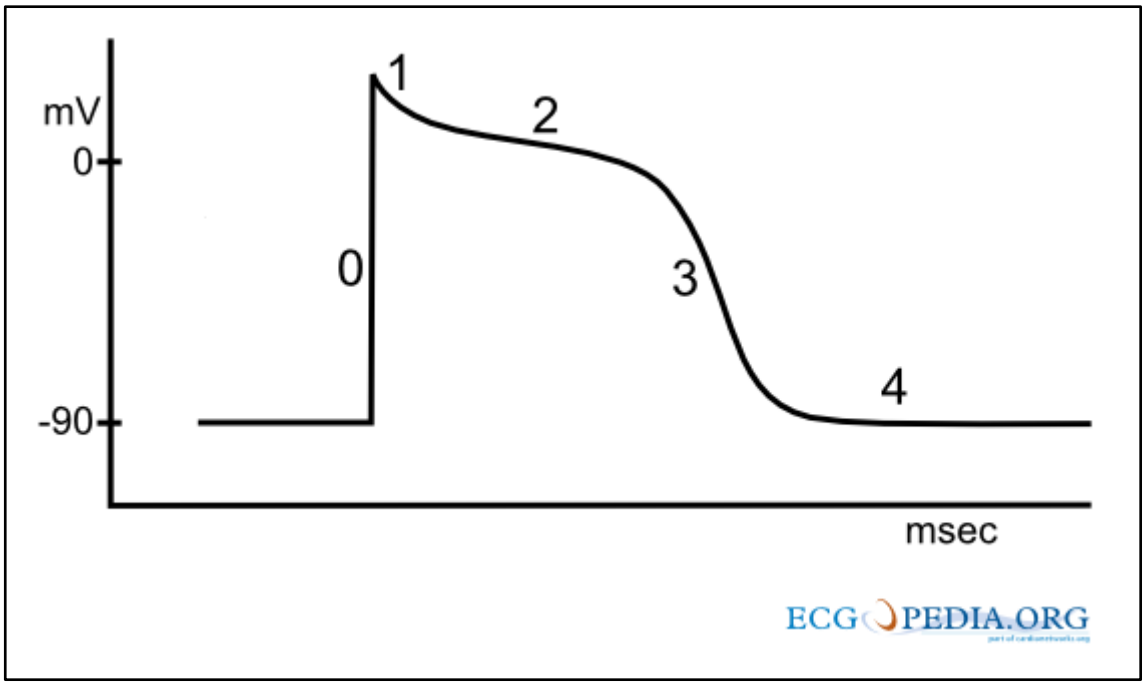

Figure 13: The cardiac action potential

The action potential of a ventricular cardiac myocyte. Stage 0 represents depolarisation. Stages 1-3 represent repolarisation. Stage 4 is the resting stage where the membrane potential approximates -90mV. Image modified to remove additional annotations. © ECGpedia.org. Original image available online at https://www.textbookofcardiology.org/wiki/File:AP.png

An individual cell cannot be stimulated again until the movement of ions associated with depolarisation has been reversed. This return to resting membrane potential is called repolarisation and the period of time during which the cell cannot be stimulated is the refractory period. Repolarisation is much slower than depolarisation and is predominantly driven by the efflux of potassium and calcium ions. In most myocytes the resting phase is not associated with a net movement of ions across the membrane.

Electrical activation (excitation) is converted into mechanical force (contraction) by a chemical process named excitation-contraction coupling. This requires the further coordinated movement of calcium ions within the cardiac myocyte.[83,84]

1.8.2 Specialised conduction tissue

The shape and duration of the cardiac action potential is not consistent across the myocardium. Instead, a network of specialised conduction tissue exists. These cells have unique properties and action potentials. [*Figure 14*]

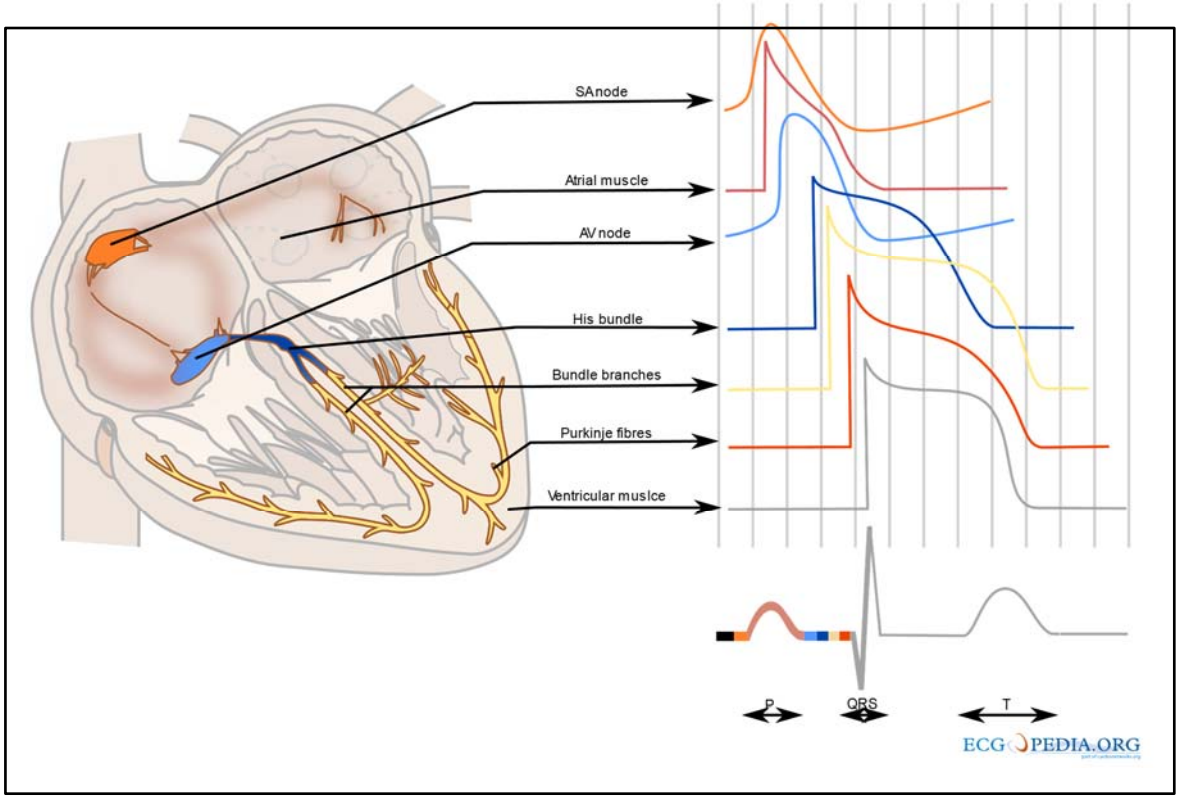

Figure 14: Variations in cardiac action potential

Schematic diagram showing the anatomical location of key components of the cardiac conduction system and their different associated action potentials. The resting membrane potential in the SA and AV node does not remain constant during the resting phase but gradually drifts back towards threshold voltage. The recorded ECG is a summation of the action potentials throughout the myocardium. Available online at https://www.textbookofcardiology.org/wiki/File:Conductionsystem.svg, ©ECGpedia.org

The cardiac myocytes within the sinoatrial (SA) node and the AV node display automaticity; the ability to spontaneously generate an electrical impulse, without stimulation from an adjacent cell. In cells that demonstrate automaticity the resting stage of the action potential is not static. Instead, a gradual drift in membrane potential occurs, governed by the presence of slow sodium channels.

Spontaneously generated cardiac impulses are the hallmark of the intrinsic cardiac pacemaker. In normal rhythm this is located within the SA node, as the cells in this area possess the fastest rates of automaticity. From the SA node a wave of depolarisation spreads throughout both atria, moving consecutively from cell to cell.

The fibrous rings of the atrio-ventricular valves are electrically inert. Normally the only electrical connection between the atria and the ventricles is the AV node; a region of specialised tissue that connects the atria to the rapidly conducting Purkinje system of the ventricles. The AV node depolarises slowly due to the absence of rapid sodium channels in

the cell membrane. Depolarisation in this region is entirely dependent on slow calcium channels and the action potential has a prolonged depolarisation phase.

Slow conduction through the AV node is advantageous as it protects the ventricle from conducting atrial arrhythmias at fast heart rates. The short delay that precedes ventricular activation also ensures the prior completion of atrial contraction, optimising LV filling and improving cardiac output.

Once an electrical impulse has travelled through the AV node, ventricular activation via the His-Purkinje system is rapid as the specialised conduction fibres have a greater conduction velocity than the surrounding myocardium. Electrical impulses follow the pathways of the left and right bundle branches, travelling down the interventricular septum, before simultaneously depolarising the RV free wall and the LV lateral wall. This results in co-ordinated contraction of the LV which optimises systolic function.

The autonomic nervous system has an important role in modulating the cardiac conduction system. The sympathetic nervous system innervates the majority of the heart's electrical system with significant innervation seen in the SA and AV nodes. Increased sympathetic tone causes enhanced automaticity, increased conduction velocity and decreased refractory periods. The parasympathetic nervous system primarily innervates the SA and AV nodes where increased tone has the exact opposite effects; decreased automaticity, reduced conduction velocity and increased refractory periods.[82]

1.8.3 Electrocardiography

Electrocardiography is the process of recording and displaying the changes in membrane potential described above. The overall graph of voltage against time that is generated is called an electrocardiogram (ECG). While the action potential represents the electrical activity of an individual cell, the ECG reflects the electrical activity of the entire heart, effectively the sum of all the individual action potentials.

Depolarisation is effectively instantaneous, as it only takes a single cell 1-3ms.[82] The wave of depolarisation can therefore be followed across the heart by studying the pattern of activation on the ECG. Atrial depolarisation is represented by P waves and ventricular depolarisation by the QRS complex (usually called an R wave in S-ICD sensing). The mean direction of travel of a depolarisation wavefront is called its axis.

The time taken for ventricular depolarisation to occur is represented by the duration of the QRS complex. If electrical impulses cannot be transmitted down one of the bundle branches, due to BBB, then a section of myocardium must be activated via slow conduction through the adjacent tissue. Consequently, ventricular depolarisation takes longer and the QRS duration is prolonged (>120ms).

On a standard 12 lead ECG, the change in activation sequence can also be identified. In left BBB for example the depolarisation pattern of the septum is altered producing a typical appearance in the precordial leads. The same is true of full thickness myocardial infarcts, where a regional territory of myocardium effectively becomes electrically inert. The infarcted area is bypassed by the depolarisation wavefront and a recognisable pattern of QRS complexes is produced.

A change in activation sequence is also observed during anterograde conduction through an accessory pathway. The majority of the myocardium is depolarised via the His-Purkinje system, but slow conduction through the AV node makes this delayed compared to pathway conduction, and early activation can be observed in the region of the pathway. On the ECG the PR interval is shortened and the initial deflection of the QRS is 'slurred' as the pathway usually enters the ventricular muscle mass, rather than the rapidly conducting fibres of the His-Purkinje system. This change in direction of travel of the depolarisation wavefront can be easily identified from a twelve lead ECG.

The wave of repolarisation that follows depolarisation is represented by T waves. The QT interval, the time duration from the start of the QRS complex to the end of the T wave, is the average action potential duration of the ventricular muscle.[82]

Unlike depolarisation, the repolarisation of individual cells is not instantaneous, but associated with a significant time duration. Repolarisation is therefore occurring in many different cells at any one time. The mean direction of travel of the repolarisation wavefront, or T wave axis, can be calculated, but subtle changes in repolarisation sequence are harder to characterise from the surface ECG.

During depolarisation, the endocardial surface of the ventricle is normally activated before the epicardial surface. Repolarisation occurs in the opposite direction and with an opposite change in voltage. Positive QRS deflections are therefore usually followed by positive T waves and negative QRS complexes are usually followed by negative T waves.

Numerous different disease processes can influence the appearances of an individual's ECG by disrupting these normal patterns of depolarisation and repolarisation. Disruption can occur at any point in the pathway.

At a cellular level, inherited channelopathies might affect the cardiac action potential by critically altering the interplay between ion channels on the myocyte cell membrane. Likewise, from a macroscopic perspective, significant muscle hypertrophy can lead to abnormal depolarisation and repolarisation patterns.

Different physiological factors also influence the ECG. These include, but are not limited to: posture, heart rate, autonomic activity, electrolyte concentration, ischaemia, medications, body habitus and heart failure status.[85-91] The ECG is therefore dynamic and highly individualised.

1.8.4 Frontal plane axis

A standard twelve lead ECG displays six limb leads. Three are bipolar leads (I, II and III) and three are augmented unipolar leads (aV_L, aV_R, and aV_F). In combination they record the electrical activity of the heart in the frontal plane.

Leads I, II and III are bipolar recordings created from surface electrodes placed on the four limbs. In lead I the potential difference between the two arms is measured (using a positive electrode on the left arm and a negative electrode on the right arm). Similarly, in lead II the potential difference between the left leg (+) and the right arm (-) is measured, whilst in lead III the potential difference between the left leg (+) and the left arm (-) is measured.

The augmented limb leads are generated using the same four electrodes. They are termed unipolar as they utilise a single negative electrode, the Wilson Central Terminal, which is the average of the three limb lead voltages (with reference to the neutral lead placed on the right leg).

The augmented leads are in fact derived mathematically, using combinations of the bipolar lead voltages. The result is six limb leads with a standardised axial relationship. In the frontal plane, lead I is considered to be at 0° with respect to the heart, lead II is at 60°, aV_F 90°, lead III 120°, aV_R -150° and aV_L -30°. [*Figure 15*]

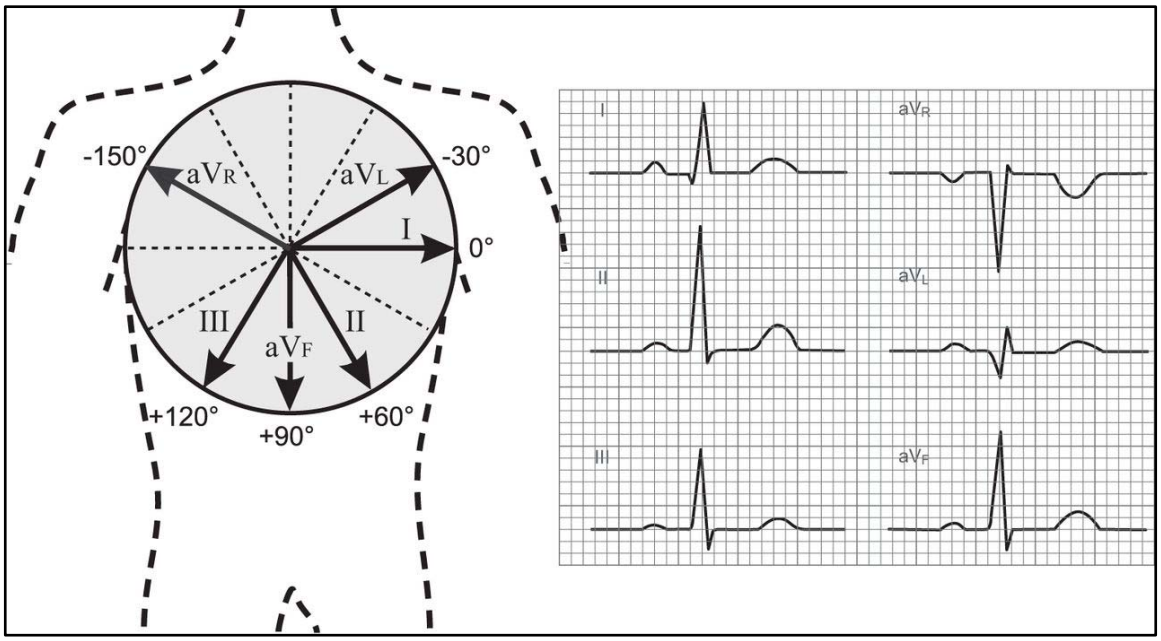

Figure 15: Standard ECG limb leads

Left: the standardised axial relationship of the six limb leads with lead I at zero degrees. Right: ECG recordings from a single time period, corresponding to one PQRST complex, are displayed simultaneously in all six limb leads. Note that the absolute R:T ratio in lead III is approximately seven (as the positive R wave is seven times the amplitude of the T wave). In aV_L the larger R wave deflection, which happens to be negative, is only twice the size of the T wave in that lead. Image available online at http://www.cvphysiology.com, ©Klabunde RE, 2016

A wave of depolarisation that travels towards a positive electrode always results in a positive deflection on the ECG. Conversely, a wave of depolarisation that travels away from a positive electrode always produces a negative deflection. Consequently, a limb lead that is parallel to a wave front, produces a signal with a large absolute amplitude (for example, lead II in the image above). A limb lead that is perpendicular to a wave front, produces a biphasic signal with a small absolute amplitude, as it has equal positive and negative components (for example, lead aV_L in the image above).

The same principles of electrocardiography also apply to the repolarisation wavefront. R and T wave amplitudes are therefore determined, in part, by the angle from which they are observed. For example, a lead that is parallel to the R wave axis, but perpendicular to the T wave axis, will have an R wave with large absolute amplitude and a biphasic T wave with small absolute amplitude. From this angle of observation, an ECG with a large R:T ratio is observed.

In normal hearts, the intrinsic R and T wave axis are often very similar and changes in angle of observation might not be expected to alter the R:T ratio significantly. In the ICD population, where myocardial scar, muscle hypertrophy, channelopathies and conduction disease are highly prevalent, the R and T wave axis are often substantially different. In the ICD population a change in angle of observation can result in marked variations in R:T ratio.

1.8.5 S-ICD vector rotation

The three standard S-ICD vectors also observe the heart from different angles and have different R:T ratios. The recipient's QRST morphology and intrinsic axes of depolarisation and repolarisation determine which vector has the best morphology for sensing, with the most favourable chosen for sensing.

Changing the angle of observation would create a new sensing vector and alter the amplitudes of R and T to different degrees. The new vector would have a unique R:T ratio. Hypothetically, an optimal angle of observation could be identified in any S-ICD recipient. The vector recorded from this angle would be a truly personalised vector as the angle of observation would have been determined by the patient's unique conduction axes and not by the standard location of the S-ICD.

Vector rotation could be achieved by placing the S-ICD in a different location in every recipient. This approach would be fraught with challenges. Firstly, the S-ICD has proven defibrillation efficacy from its current location and has achieved FDA approval for clinical use in this configuration. Implantation using consistent anatomical landmarks also allows implanters to develop a reproducible and safe technique, and for dedicated tools to be designed for tunnelling. The current location of the lead also allows for easy suturing at the proximal electrode and an appropriate axillary location for the large generator.

1.8.6 Mathematical vector rotation

Vector rotation that is achieved purely through mathematics is a novel potential solution that would allow alternative angles of observation to be explored from the pre-existing S-ICD location. This can be achieved as mathematical rotation of two-dimensional vectors is, in all scenarios, governed by simple Euclidian trigonometry.

The mathematics are described below. A graphical representation and a discussion of the limitations of this approach follow.

1. *All vectors can be described by two dimensional co-ordinates (x,y)*

2. *Clockwise rotation of vector (x,y) by z degrees, generates a new vector (x_z, y_z)*

3. *The location of x_z and y_z are given by the following formulae:*
   - *x_z = [x.cosz] + [y.sinz]*
   - *y_z = [x.sinz] - [y.cosz]*

4. *In the two-dimensional frontal plane the S-ICD vectors approximate a right-angled triangle, whereby the secondary vector (S) forms a hypotenuse between the horizontal primary vector (P) and the vertical alternate vector (A).*

5. *At any given point in time, the (x,y) coordinates of the secondary vector (S), can therefore be described using the amplitudes of the primary (P) and alternate (A) vectors at that time. Therefore S = (P,A).*

6. *If vector (P,A) is rotated in a clockwise direction by z degrees, a new vector (P_z,A_z) is created.*

7. *The mathematical relationship between the co-ordinates of the original vector and those of the rotated vector is described as follows:*
   - *P_z = [P.cosz] + [A.sinz]*
   - *A_z = [P.sinz] - [A.cosz]*

Figure 16: Mathematical principles of S-ICD vector rotation

Points 1-3 are accepted mathematical facts which can be derived from simple trigonometry. Points 4-7 describe my application of this theory to the current S-ICD vectors.

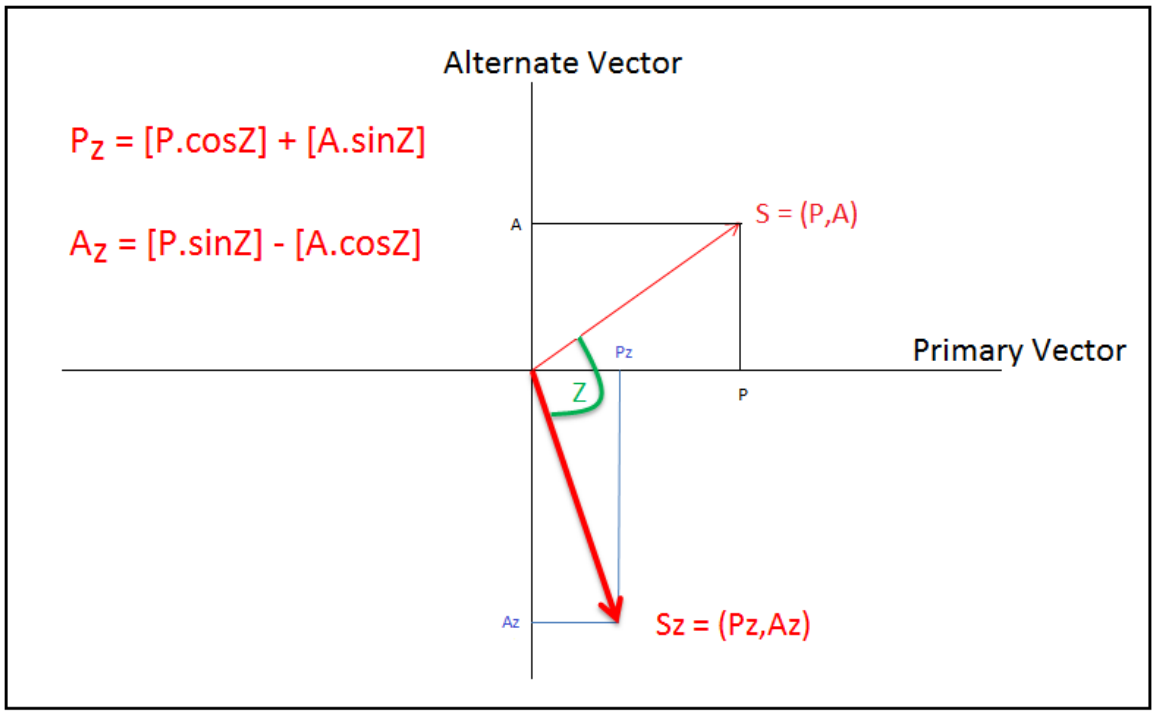

Figure 17: Graphical representation of mathematical vector rotation

Thin red arrow (top right quadrant): the secondary vector (S), at a given point in time, plotted graphically using the primary (P) and alternate (A) values as its (x,y) co-ordinates. Fat red arrow (bottom right quadrant): vector S_z, (vector S rotated in a clockwise direction by z degrees). Mathematical rotation from S to S_z alters the relative P and A co-ordinates (P_z,A_z). The location of the new co-ordinates is provided by the mathematical formulae in the top left quadrant.

1.8.7 Limitations

In applying this mathematical theory, I have modelled the S-ICD vectors as a right-angled triangle in the two-dimensional frontal plane. This make two assumptions, firstly that the primary and alternate vectors have a perpendicular relationship, and secondly that they exist only in two-dimensions. Whilst a 90 angle is deliberately introduced during lead implantation, some variability in the exact angle formed between the primary and alternate vectors must exist, as patients of different shapes and body sizes receive S-ICDs. The S-ICD pulse generator is also always located posteriorly with respect to the sensing electrodes and the S-ICD vectors must therefore have a three-dimensional component.

The significance of these two assumptions is not currently known. This will be addressed in Chapter 2, where experimental work justifying the use of mathematically modelling and quantifying the effect of these assumptions will be presented.

Significant caution must also be given to the impact which vector rotation might have upon the fundamental rhythm determination properties of the S-ICD system. If a rotated vector were ever to be selected for clinical use, due to its beneficial R:T ratio, would VF at that angle of observation still be detected as VF? Would shock therapy be prolonged or inappropriately withheld? Likewise, would the rhythm determination algorithms that decide whether arrhythmias are ventricular or supraventricular be affected? A significant alteration to the sensing mechanism of the S-ICD system mandates that these questions are explored by experimental testing, this will be conducted in later chapters.

A further important consideration is whether rotation of vectors could offer any clinical benefit to patients who already have a suitable vector. Whist one might expect a vector with greater R:T ratio to be associated with less TWOS than a vector with a smaller R:T ratio, but there is currently no evidence to support this assertion. Assessing this experimentally might help our understanding of the wider clinical applications of vector rotation. This is an additional priority which will also be subjected to further research.

1.9 Special patient groups

The ICD population is a heterogenous group encompassing a broad range of ages and a wide variety of cardiac pathologies. Whilst considering S-ICD sensing and the potential role of mathematical vector rotation, certain patient cohorts are worthy of specific consideration. These groups currently challenge the S-ICD sensing mechanism, by virtue of their changing ECG morphologies. They therefore represent individuals who might also benefit in the future from vector modification by mathematical rotation.

1.9.1 Athletes

Athletic individuals, especially those partaking in high intensity exercise, are at greater risk of TWOS and inappropriate shock therapy when implanted with an S-ICD. This is due to their baseline ECG characteristics, exercise-induced ECG changes and the more aggressive sensing profiles employed by the S-ICD at faster heart rates.

Long-term cardiovascular training is associated with ventricular hypertrophy. As discussed earlier this can disrupt the normal patterns of ventricular depolarisation and repolarisation. High amplitude R waves are common, whilst T wave amplitudes can also be greater in athletes as they have been linked to an individual's physical fitness.[92]

Exercise induced ECG changes have been observed in R and T wave amplitudes, R and T wave axes, QRS duration and QT interval. T wave amplitudes have also been shown to increase significantly during exercise recovery.[93] The important of QT interval cannot be understated. Variations in the timing of a T wave, with no associated change in amplitude, can result in TWOS if the T wave occurs when the S-ICD has a lower sensitivity level. At higher heart rates double counting is also more likely to result in S-ICD therapy, as the incorrectly calculated heart rate is more likely to fall above the treatment threshold.

No clear solution has been identified for these challenges. Vector morphology screening during exercise, for example using a treadmill test, is a potential strategy for S-ICD recipients in whom high intensity exercise is anticipated. However, experimental studies in which exercise testing has been performed on small cohorts of unselected potential S-ICD recipients have found little evidence to support this strategy.

A study of 87 patients showed that vector discrimination was not improved by performing an exercise test.[94] In another study, 14 patients were exercised and an associated change in vector eligibility was only observed in one patient.[95] Despite the lack of clear evidence, many implanting physicians routinely perform exercise ECG screening in any S-ICD recipient who intends to return to high intensity exercise.

1.9.2 Brugada syndrome

Brugada syndrome is a channelopathy that is associated with increased risk of SCD due to VTA. Patients with Brugada are generally younger than patients with ischaemic cardiomyopathies and rarely have a permanent pacing indication. S-ICD therapy is therefore a potentially attractive option in high-risk individuals with Brugada syndrome.

Patients with Brugada syndrome also present a unique morphological challenge to the S-ICD due to the dynamic and marked ECG changes which characterise the condition. In up to a third of cases an abnormality can be identified in a gene that encodes voltage gated sodium channels (SCN5A), resulting in abnormalities of the transmembrane ion currents that determine phase 0 and phase 1 of the cardiac action potential.

On the surface ECG Brugada syndrome is characterised by coved ST elevation and changes in both T wave axis and T wave amplitude. Approximately 18% of patients with Brugada Syndrome are ineligible for an S-ICD due to ECG morphology (n=61), predominantly due to high amplitude T waves.[96]

The typical Brugada syndrome ECG may be intermittent or only occur in response to sodium channel blocking agents. In Brugada patients who do not consistently display the pathological ECG, administration of Ajamline has been shown to unmask screening failure in 14.8% of patients who would otherwise have appeared eligible.[96] A study of exercise testing in S-ICD eligible patients with Brugada syndrome (n=45) also revealed that 24% of this cohort became ineligible with exercise.[97]

1.9.3 Hypertrophic cardiomyopathy

HCM is a genetic disorder that is characterised by abnormal ventricular wall thickening in the absence of abnormal loading conditions. Familial HCM is inherited in an autosomal dominant manner, with around 50 causative gene defects identified. Penetrance and

phenotypic presentation are highly variable, as is the pattern of hypertrophy. Large amplitude R and T waves are frequently observed and HCM is associated with both a high S-ICD screening failure rate and increased rates of inappropriate shock therapy.[47,66] Ineligibility has been shown to further increase after treadmill testing, rising from 6.1% to 15.2%.[98]

1.9.4 Haemodialysis

Patients with end stage renal disease (ESRD), especially those undergoing regular haemodialysis, also require special consideration. Approximately 1 in 4 (27%) of haemodialysis patients die from SCD,[99] although the percentage in whom the cause is VTA is less well established. Only around 6% of patients are currently treated with primary prevention ICDs.[100]

International guidelines from both Europe and the United States, have failed to recognise ESRD as a risk factor for SCD in its own right, despite registry data showing that haemodialysis patients obtain a survival benefit from ICD implantation.[26,101,102] In patients with chronic kidney disease, the rate of appropriate ICD therapy has been shown to increase with declining renal function, with the highest rates observed in haemodialysis patients.[103]

Historically, clinicians have been concerned regarding the possible complications of transvenous device implantation in patients with ESRD. Regular haemodialysis, for example, frequently exposes device recipients to bacteraemia and ESRD is associated with a significantly increased risk of device infection.

The United States Renal Data System (URSDS); a registry of 546,769 patients with renal disease, shows that cardiac implantable device implantation in ESRD is associated with an infection rate of 8.0%.[104] This is a considerably rate than that observed in a comparable US device registry (1.6%).[105] Device infections in patients with ESRD are associated with a very poor prognosis. Median time to death after device infection is just 9.2 months in those receiving medical therapy and 15.7 months after extraction, with the majority of infected systems managed medically in ESRD (71.6%).[104]

Haemodialysis often requires surgical formation of arteriovenous fistulae, resulting in high venous pressures within the upper limbs. The periprocedural bleeding risk from pacemaker

and TV-ICD implantation is significantly increased, from 0.2% in control populations to 12.5% in ESRD (p<0.001, n=82).[106]

Given the increased risks of bleeding and infection associated with TV-ICD implantation, haemodialysis patients who require defibrillator therapy, are expected to benefit from the entirely extra vascular S-ICD. Unfortunately, at present, there is limited data regarding concurrent haemodialysis and S-ICD therapy.

In the EFFORTLESS registry, only 8.2% of patients had renal disease, reflecting clinical practice during the infancy of S-ICD implantation.[46] The use of S-ICDs in haemodialysis patients is expected to increase. The S-ICD Post-Approval Study has shown that contemporary S-ICD patients in the United States have more comorbidities than previous S-ICD cohorts. They are also younger and have more ESRD than TV-ICD groups.[107]

The ATLAS study (Avoid Transvenous Leads in Appropriate Subjects) is a randomised multicentre study in which 500 patients with risk factors for TV-ICD therapy, including haemodialysis, will be randomised to either TV-ICD or S-ICD therapy. This study, if adequately powered with regards to haemodialysis, is expected to support the potential benefits of S-ICD therapy in ESRD. The results of this study are not expected until 2021.[108] The only published reports of S-ICD recipients undergoing haemodialysis have been limited to small patient numbers (n=18 and n=27). Procedural outcomes, which were comparable to control groups, were demonstrated in both studies.[109,110]

Haemodialysis is associated with rapid shifts in fluid volume and changes in electrolyte concentration. Given the critical importance that intracellular and extracellular electrolyte concentrations have on the myocyte action potential, haemodialysis results in morphological ECG changes. Small electrocardiographic studies of patients undergoing haemodialysis have shown significant changes in QTc, T wave amplitude, T wave duration and QRS/T axis.[111-115] Changes in fluid status have also been associated with variations in both QTc and QRS amplitude.[85]

Haemodialysis can also influence S-ICD vector eligibility. When S-ICD screening was undertaken on 51 patients before and after haemodialysis, variations in eligibility were observed in 10% of patients. In the remaining 90% S-ICD eligibility remained consistent across both assessments (84% eligible, 6% ineligible).[116]

1.10 Aims and objectives

Mathematical vector rotation is a novel idea that has not previously been applied to the sensing vectors of an S-ICD. In this thesis a series of experiments will be described that will comprehensively explore the concept.

The overall objectives are as follows:

- Apply mathematical vector rotation to a cohort of S-ICD ineligible patients to determine whether this technique can be used to increase device eligibility.
- Determine whether vector rotation reduces the VF detection efficacy of the S-ICD, assessing both detection accuracy and time to therapy.
- Determine whether vector rotation impacts upon the sensitivity or specificity of S-ICD rhythm determination, specifically with regards to discrimination of narrow complex tachycardia.
- Explore how vector rotation might be used to reduce T wave over-sensing in the future, by calculating how vector eligibility varies over time, in individuals who are at risk of TWOS.
- Assess how vector eligibility varies over time in a cohort of individuals in whom dynamic ECG changes might challenge the sensing mechanism of the S-ICD.

The overall aim, as alluded to in the prologue, is to demonstrate one possible use of ECG modification. Focus has deliberately been given to the sensing mechanism of the S-ICD system, but the wider applications of ECG modification in diagnostic, therapeutics and monitoring should not be overlooked.

1.11 Proposal

To achieve the aims described above the following experimental chapters will be presented.

1.11.1 Vector analysis from surface ECG

In Chapter 2, the suitability of surface ECG as a surrogate of S-ICD vector morphology will be assessed using comparative recordings from a cohort of patients. The accuracy of modelling the S-ICD vectors as a right-angled triangle will also be calculated by comparing secondary vector signal recorded by the S-ICD, with secondary vector signal generated using Pythagoras' theorem. This study will be used to verify the methods that are utilised in subsequent chapters.

1.11.2 Mathematical vector rotation

In Chapter 3, S-ICD screening will be performed on a cohort of ICD patients to identify those who are ineligible for an S-ICD by virtue of their vector morphology. Mathematical vector rotation will then be performed using simultanoues recordings of their primary and alternate vectors. This will allow identification of a personalised vector. The calculated R:T ratio in the personalised vectors will be compared to the recorded vectors and the personalised vectors screened for S-ICD eligibility.

1.11.3 VF detection

In Chapter 4, patients undergoing defibrillation threshold testing will have their induced VF episodes recorded using surface ECG as a surrogate of their S-ICD vectors. VF detection accuracy and time to VF detection in the current S-ICD vectors will be compared to a series of rotated vectors. This will determine whether vector rotation has a detrimental effect on VF detection.

1.11.4 SVT discrimination

In Chapter 5, patients undergoing EPS procedures will have their induced tachycardia episodes recorded using surface ECG as a surrogate of their S-ICD vectors. The sensitivity and specificity of SVT detection in the current S-ICD vectors will be compared to a series of

rotated vectors. This will determine whether vector rotation has a detrimental effect on SVT discrimination.

1.11.5 Alternating angle of observation

In Chapter 6, I shall consider the risk of inappropriate reduction in overall signal amplitude that could occur with rotation and describe two possible solutions. One will combine vector rotation with a morphological filter, and one will combine vector rotation with a gradient filter. The improved personalised vectors will then be retested using the data sets obtained in Chapter 3. An S-ICD simulator will be used to more accurately determine S-ICD eligibility.

1.11.6 Eligible vector time

In Chapter 7, I will assess how vector eligibility varies across a 24-hour period, using surface ECG recordings and an S-ICD simulator. ICD recipients who are at risk of TWOS, by virtue of their resting ECG characteristics, will be compared to a control group of ICD patients. By demonstrating that S-ICD eligibility is highly variable, I will take the first step towards determining whether improvements in R:T ratio, for example by vector rotation, could have a clinical benefit in S-ICD eligible patients.

1.11.7 Haemodialysis

In Chapter 8, I will revisit the concept of variable vector eligibility that was described in Chapter 7. The variability across a single session of haemodialysis will be assessed in a cohort of dialysis dependent patients. This study will aim to provide further evidence for the future role of vector modification, focussing on a specific group of patients in whom S-ICD therapy has significant potential benefits, but who currently challenge the sensing capabilities of an S-ICD system.

Chapter 2 Vector analysis from surface ECG

2.1 Introduction

The S-ICD comprises an electrically active can and a single subcutaneous lead containing two sensing electrodes; primary and distal. By measuring the voltage differences between these sensing points, the system creates three different sensing vectors; primary (P) - proximal electrode to can, secondary (S) – distal electrode to can, and alternate (A) – distal to proximal electrode.

2.1.1 Surface ECG as a vector surrogate

Prior to S-ICD implantation surface ECG recordings are used as a surrogate marker of future S-ICD vectors. Using this technique clinicians are able to non-invasively assess vector morphology and determine S-ICD eligibility.

The use of surface ECG as a vector surrogate is also important in clinical research and will, by necessity, be used throughout this thesis. For example, in chapter 3, where the morphology of S-ICD ineligible patients will be assessed. Or in chapter 7, where a 24-hour assessment of vector morphology will be undertaken. In both of these scenarios the prerequisite data cannot be recorded from an S-ICD system, mandating the use of an appropriate surrogate.

In chapter one, I described the technique by which vector surrogate ECG is recorded using surface electrodes that overlie the intended anatomical locations of the S-ICD sensing points. The exact location of the implanted subcutaneous device is of course not recreated. At the site of the can, especially in individuals with a large body mass index, the surface ECG electrodes can be several centimetres further from the myocardium than the implanted S-ICD. The accuracy with which surface ECG can be used to recreate S-ICD vector morphology has not previously been assessed.

2.1.2 Modelling the vectors as a right-angled triangle

In chapter 1, I described how the S-ICD vectors approximate a right-angled triangle in the two-dimensional frontal plane, a consequence of the deliberate introduction of a ninety-

degree angle during lead implantation. Inevitably variation exists in the final position of implanted systems and in the angular relationship between the vectors. The can is also always posterior with respect to the lead and in the vectors have a three-dimensional relationship.

The accuracy of modelling the vectors as two-dimensional right-angled triangle has never been assessed. In this chapter I shall compare the morphologies of two secondary vectors; one recorded from an implanted S-ICD, the other generated by Pythagoras' theorem. Mathematical generation of a secondary vector using Pythogoras' theorem effectively assumes a perfect right-angled relationship. As such, the calculated degree of correlation between the mathematically generated secondary vector and the true secondary vector, will quantify the overall accuracy of this mathematical modelling technique.

2.2 Objectives

- To quantify the degree of accuracy with which surface ECG can be used as a surrogate marker of S-ICD vector morphology.
- To quantify the degree of accuracy of mathematical modelling of the S-ICD vectors as a right-angled triangle in the two-dimensional frontal plane.

2.3 Method

This was a prospective observational study performed between January 2016 and March 2016. Ethical approval (reference 14/EE/0197) was obtained from both the East of England Research and Ethics Committee (REC) and the Health Research Authority (HRA). The study was sponsored by the Department of Research and Development at University Hospital Southampton NHS Foundation Trust (UHS). All study participants gave informed written consent prior to study enrolment.

All participants were adult patients with implanted S-ICDs undergoing a clinically indicated follow up appointment with a cardiac physiologist at UHS. Recruited patients underwent a device interrogation, with electronic recordings of their three sensing vectors captured using an S-ICD programmer.

At the same time as the S-ICD interrogation, participants also underwent a 60 second surface ECG recording using a five-lead two channel digital Holter recorder (Model AFT-1000, Holter Supplies, Paris). Surface electrodes were placed using anatomical landmarks such that the two recording channels generated surrogate primary and secondary sensing vectors. [*Figure 18*]

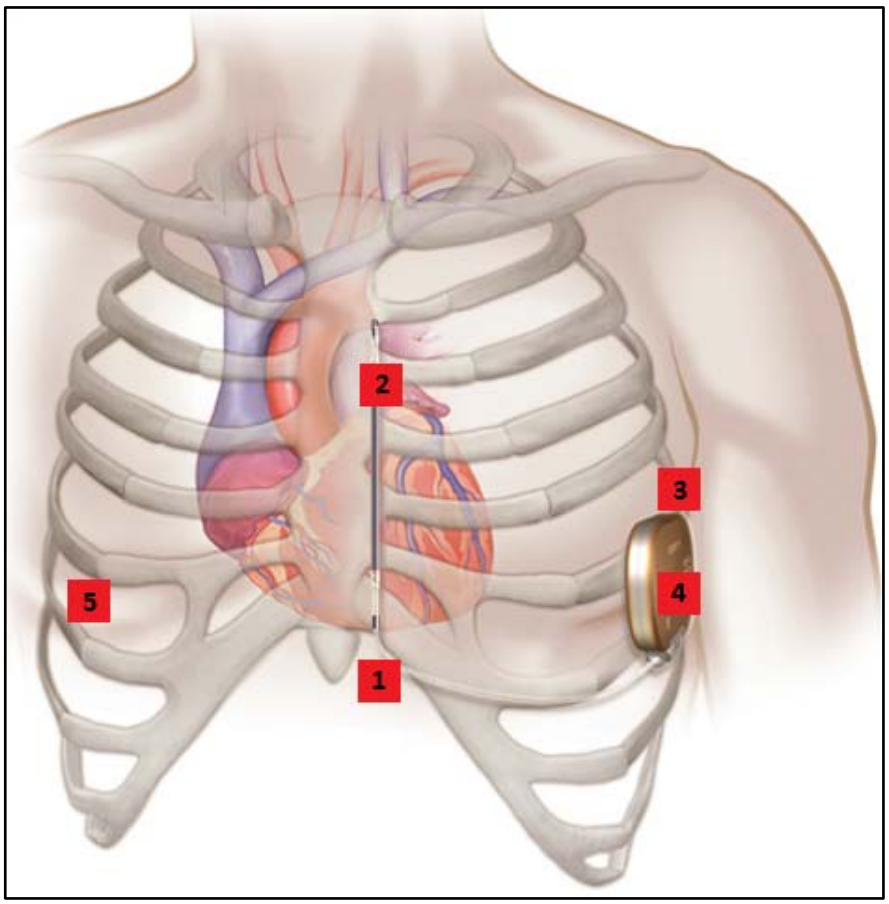

Figure 18: Surface ECG to record primary and secondary S-ICD vectors

1 = 1cm infero-lateral to the xiphisternum *2 = 14 cm superior to position 1*

3 = 5th intercostal space left mid axillary line *4 = 6th intercostal space left mid axillary line*

Holter Channel A records between points 1 and 4 *= surrogate of S-ICD primary vector*

Holter Channel B records between points 2 and 3 *= surrogate of S-ICD secondary vector*

5 = 5th intercostal space right mid clavicular line *= neutral electrode*

The vector signals were downloaded in ASCII (American Standard Code for Information Interchange) format and a single QRST complex was identified from each data set. The data sets were denoted; DP (device primary), DS (device secondary) and DA (device alternate). An additional secondary vector (denoted MS) was mathematically generated using the formula $MS^2 = DP^2 + DA^2$.

ECG data from the Holter recorders were downloaded in ASCII format at a frequency of 250Hz (to match the recording frequency of the S-ICD system). For each Holter recording a single QRST complex was isolated and the data sets were denoted; HP (Holter primary) and HS (Holter secondary). The Holter signals were visually aligned to the isoelectric line and manual alignment of the H and D data sets was performed using the time of peak R wave amplitude.

Hospital records were used to record patient and device demographics including body mass index (BMI). If LV function had been quantified using echocardiography or cardiac magnetic resonance imaging (MRI) in the preceding three years, then LVEF was also recorded.

2.3.1 Surface ECG as a vector surrogate

The primary and secondary vector recordings from the S-ICD (DP and DS) were compared to their equivalent Holter recordings (HP and HS) using the correlation coefficient function (*corrcoef*) within the MATLAB platform (Mathworks Inc., MA, USA). This analysis was undertaken in collaboration with the University of Southampton Department of Electronics and Computer Science.

The *corrcoef* function reports a value between -1.0 and 1.0 and is an appropriate and commonly used correlation function for comparing complex signals, for example ECG data. A correlation of 1.0 denotes perfect positive correlation, this mean that if one signal increases or decreases, the other follows suite. Two signals with no correlation receive a value of 0. A perfect negative correlation is indicated by a value of -1.0, which means when one signal increases or decreases, the other signal does the exact opposite. It is generally accepted that signals with correlation values >0.90 have very high correlation, 0.70-0.89 high correlation, 0.50-0.69 moderate correlation and 0.30-0.59 low correlation.[117]

Where discrete T waves could be visually identified R:T ratios in both the Holter and S-ICD data sets were calculated. These ratios were compared using a paired t-test. A paired (or dependent) test was chosen as each individual patient had their R:T ratio measured twice, using different techniques, and the intent was to determine if the difference between them was significant. The values were also expected to be normally distributed, although the small sample size prevented this from being accurately assessed.

The correlation values for each patient were plotted against their BMI. A Pearson correlation was performed to assess the relationship between signal correlation and BMI, given the continuous nature of these two variables.

2.3.2 Modelling the vectors as a right-angled triangle

The absolute amplitude signals of MS and DS were compared using the *corrcoef* function described above. Absolute amplitude signals were required as the use of Pythagoras' theorem converted MS into a vector with entirely positive amplitudes (as the product of two negative integers is always a positive integer). This was deemed to be acceptable given that, as described in chapter 1, polarity is irrelevant in S-ICD sensing.

2.4 Results

Ten consecutive patients undergoing routine S-ICD interrogations were recruited. Their mean age was 44.5 ± 8.2 years, 70% were male and the mean time from S-ICD implant to recruitment was 24.0 ± 12.5 months. [*Table 2*]

Total Number of Participants		10	
Patient:	Mean age [years ± 95% confidence interval (CI)]	44.5 [± 8.2]	
	Mean time since S-ICD implant [months ± 95% CI]	24.0 [± 12.5]	
	Male	7	70%
	EF<0.35	2	20%
	Previous transvenous system	3	30%
	Transvenous pacemaker in situ (atrial lead only)	1	10%
Device:	Primary prevention (all Brugada syndrome)	3	30%
	Secondary prevention	7	70%
	Programmed vector: Primary	4	40%
	Programmed vector: Secondary	6	60%

Table 2: Vector analysis from surface ECG – patient demographics

2.4.1 Surface ECG as a vector surrogate

The S-ICD and Holter signals were found to be highly correlated. The mean correlation value for the primary vector was 0.84 (95% CI 0.72-0.96), whilst mean correlation for the secondary vector was 0.83 (95% CI 0.80-0.87). The correlation values for each patient are detailed below. [*Table 3*]

Patient ID	BMI	HP vs DS	HS vs Ds	Overall H v D
001	27.2	0.79	0.83	0.81
002	37.8	0.85	0.91	0.88
003	26.2	0.94	0.73	0.83
004	35.7	0.78	0.82	0.80
005	33.4	0.90	0.88	0.89
006	49.7	0.75	0.80	0.77
007	26.9	0.91	0.90	0.90
008	26.1	0.82	0.85	0.83
009	26.3	0.84	0.83	0.84
010	35.8	0.84	0.81	0.83
Mean [± 95% CI]	32.5 [±4.7]	0.84 [±0.04]	0.83 [±0.03]	0.84 [±0.04]

Table 3: Holter and S-ICD Correlation Values

Despite the high overall correlation values a visual assessment of the signals did reveal some subtly differences in morphology between the signals. For example, in *Figure 19*, the S-ICD signal has a small S wave (negative deflection after the positive R wave) and the Holter signal does not.

Minor morphological variations were common, with the ST segment and T wave the commonest region for abnormalities to be noted. Increased BMI was associated with a tendency towards lower correlation values, but this did not reach statistical significance (Pearson correlation -0.41, p=0.24).

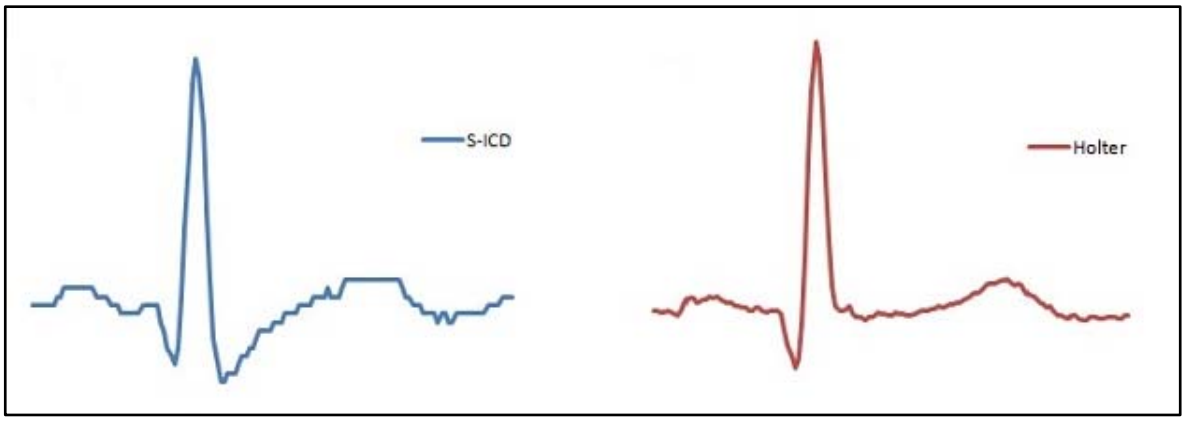

Figure 19: S-ICD versus Holter

Left: S-ICD signal from a single vector in one of the study patients. Right: Signal from the corresponding Holter recording. The correlation in this example was calculated at 0.83 which is equal to the calculated mean correlation.

T wave amplitudes could only be measured in 9 out 10 patients as, due to the presence of coarse atrial fibrillation, T waves could not be clearly visualised in one patient. The R:T ratio results are provided below. [*Table 4*]

Patient ID	HP	DP	Difference	HS	DS	Difference
001	1.81	3.60	1.79	2.63	5.43	2.80
002	8.00	6.33	-1.67	8.54	9.67	1.13
003	10.83	12.40	1.58	8.01	7.25	-0.76
004	5.56	6.50	0.94	4.13	14.67	10.54
005	14.44	18.00	3.56	7.34	18.50	11.16
006	6.54	6.75	0.21	8.83	5.17	-3.66
008	4.87	8.00	3.13	3.49	5.83	2.34
009	5.31	9.64	4.63	4.66	7.92	3.25
010	8.35	16.33	7.98	21.38	8.86	-12.52

Table 4: R:T ratio - Holter versus S-ICD

The R:T ratio was increased when recorded by the S-ICD, compared to the Holter, by a value of 2.01 (95% CI -0.62 - 4.63, n=18) although this was not found to be statistically significant (p=0.165). When the vectors were analysed separately, the S-ICD R:T ratio was greater than the Holter R:T ratio in both vectors. In the primary vector the difference was 2.42 (95% CI

0.30 - 4.55, n=9, p=0.03) and in the secondary vector it was 1.59 (95% CI -3.91 – 7.08, n=9, p=0.524).

2.4.2 Modelling the vectors as a right-angled triangle

The mathematically generated secondary vectors (MS) were found to be very highly correlated with the secondary vectors recorded via the S-ICD (DS). The mean correlation value was 0.95 (95% CI 0.91-0.98, n=10). The correlation result for each patient and a single pictorial representation are displayed below. [*Table 5*, *Figure 20*]

Patient	001	002	003	004	005	006	007	008	009	010	Mean
MS vs DS	0.89	0.98	0.92	0.99	0.99	0.92	0.92	0.92	0.99	0.96	0.95

Table 5: Mathematical versus recorded secondary vectors – correlation results

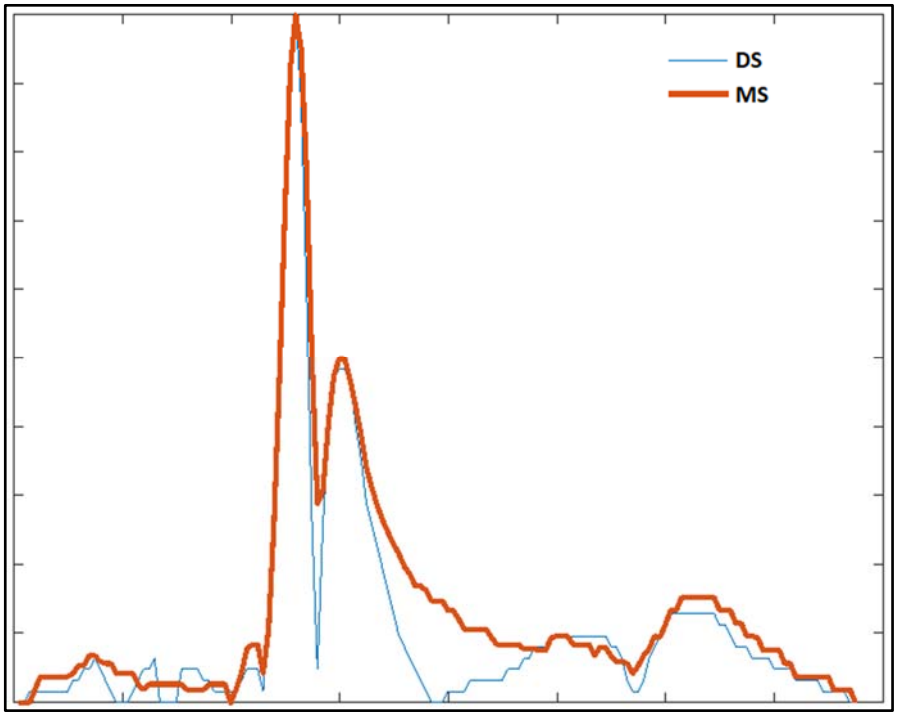

Figure 20: A graphical representation of correlation

The MS and DS data from patient 010 have been plotted against time on the x axis. The signals are highly correlated overall with a correlation value of 0.96. This image was chosen as the mean correlation for the cohort was 0.95. The y axis denotes absolute amplitude which gives the signal an unusual appearance for observers who are used to looking at ECGs. The 'S wave' appears as a second positive deflection immediately after the 'R wave', whilst the T wave appears bifid rather than biphasic.

2.5 Discussion

This study has quantified the accuracy of using surface ECG as a surrogate of vector morphology and of modelling the S-ICD vectors as a right-angled triangle in the frontal plane. It has thereby successfully achieved its predefined objectives.

2.5.1 Surface ECG as a vector surrogate

A high degree of correlation (0.84 ±0.04) was demonstrated between the S-ICD vectors and their surface ECG surrogates, a finding which was consistent across both analysed vectors. The correlation between these two signals has not previously been calculated.

In chapter one, I discussed a study in which the overall correlation between surface ECG and subcutaneous recordings from an implantable loop recorder was found to be 0.96 (n=48).[60] S-ICD vectors are therefore less well correlated to surface ECG than loop recorder signal. This is likely due to the relative proximity of loop recorders to the skin surface, in comparison to the deeper, often submuscular location of the S-ICD pulse generator.

The alternate vector, which does not record from the pulse generator, but uses only the two superficial lead sensors may have demonstrated higher correlation than the tested vectors, which would have supported this theory. The alternate vector was however not studied as the high frequency research Holter could only simultaneously record two channels, and the alternate vector was omitted as it is the least commonly used vector clinically.

The main limitation of this study is the small cohort size. Similar findings, from a considerably larger cohort, would have provided more evidence of the correlation between the two signals. The aim however was not to provide adequate justification for the clinical use of surface ECG as a surrogate marker of vector morphology, but rather to provide an estimate of the accuracy of our experimental technique. This has been achieved.

In the experimental chapters that follow surface ECG will be used as surrogate of vector morphology. This will allow vector data to be recorded in patients without S-ICD systems, for example due to ineligibility. I considered implantation of subcutaneous recording systems in these individuals to be unethical, when surface ECG is already routinely accepted as an appropriate surrogate in clinical practice.

A larger cohort would also have provided a better understanding of the relationship between physical size and signal correlation. In this study patients with larger BMIs tended to have lower correlation values but this did not reach significance. This should perhaps be revisited in a larger study, with consideration also given to alternate measures of subcutaneous fat in the axillary location, which may not have been adequately reported by BMI. This may be clinically relevant in the future S-ICD screening of morbidly obese individuals.

The results of the R:T ratio analysis showed no significant difference overall between the S-ICD vectors and the surface ECG surrogates. This is consistent with the findings of the overall signal correlation. When the primary vectors were considered alone a greater R:T ratio was found in the S-ICD vectors, although this was from a data set of just nine individuals so must be interpreted with caution.

The morphological differences in the ECG signals and the difference in primary vector R:T values should also be interpreted from the perspective of an S-ICD. Implanted systems record only the peak R wave and then any subsequent signal above the post R wave sensitivity level. Consequently, morphological changes are only of significance if they disturb this sensing process. In this regard a more accurate technique would have been to use an S-ICD simulator to process the data. Consideration will be given to this technique in subsequent chapters.

A potential limitation which requires discussion is the use of a single representative PQRST morphology, which was spliced from each data set prior to correlation calculation. Given the intrinsic variation that can be observed in an individual's ECG complexes, it might be argued that a more appropriate method would have been to compare several complexes to their exact signal counterparts. However, exact signal counterparts could not be easily identified.

Although the Holter device was worn at the precise time the vector templates were downloaded, the S-ICD download provided a 'last stored vector' template rather than a snapshot image from that precise moment. This was confirmed by the slight variations in heart rate that were observed between the Holter data and the S-ICD data, which demonstrated that the signals were not simultaneously recorded. This also prevented larger data sections from being used for correlation analysis as the failure of alignment of

consecutive QRS complexes would have significantly reduced correlation. This is a commonly encountered challenge with this form of signal comparison. Indeed, in the Reveal study discussed above, manual identification of the QRS complex prior to the correlation analysis was performed.

2.5.2 Modelling the vectors as a right-angled triangle

The mathematically generated secondary vectors, calculated on the assumption that S-ICD vectors form a right-angled triangle, were found to be very highly correlated with the secondary vectors recorded via the S-ICD. The mean correlation was 0.95 ± 0.036, where a value of 1.00 would represent perfectly correlated signals. This strongly suggests that modelling the S-ICD vectors as a right-angled triangle in the frontal plane is an accurate technique.

The vectors obtained from implanted S-ICD systems will always have a three-dimensional component and some variation will exist in the final lead position in each recipient. These factors do not however appear to have a significant impact upon the recorded vector morphology.

The main limitation of this study is the small sample size, with just ten individual S-ICD recipients analysed. The intent however was not to adequately prove a perpendicular relationship between the primary and alternate vectors, as I know this not to be the case, but rather to estimate the degree of accuracy of the proposed technique. This has been achieved.

Higher correlation values were observed in the mathematical study that in the surface ECG versus S-ICD vector correlation study. The most likely explanation is that different filtering processes are built in to the S-ICD and the Holter respectively, and that this could have limited the correlation in the previous study. Conversely, in the mathematical study, all the data originated from an S-ICD, and this limitation was overcome.

Future consideration should be given to the effect of postural change on the angular relationship between the vectors. Clinical S-ICD screening mandates that the vector assessment is performed in at least two vectors as position of the can is known to alter, with respect to the heart, when a patient changes posture. This has not been assessed in this study and represents possible future work in this area.

2.6 Conclusion

ECG obtained from surface locations that overlie the anatomical position of the S-ICD sensing components is highly correlated to the corresponding vectors of an implanted S-ICD. Surface ECG is therefore an appropriate surrogate of vector morphology in research and device screening.

Modelling the S-ICD vectors as a right-angled triangle in the two-dimensional frontal plane is a reliable research technique as secondary vectors generated using this assumption are very highly correlated to recorded secondary vectors.

Chapter 3 Mathematical vector rotation

3.1 Introduction

Mathematical vector rotation is a novel technique whereby the angle of observation of an individual's S-ICD vector is manipulated mathematically. The principles of vector rotation and the underlying mathematics have already been described at length and will therefore not be repeated here. [*Section 1.8*]

In every patient, vector rotation generates a series of new vectors using data recorded from the current S-ICD location. Each vector is expected to have a unique R:T ratio, allowing the identification of a 'personalised vector'; one with optimal R:T ratio for that individual. Personalised vectors have the potential to reduce S-ICD ineligibility, which commonly results from low R:T ratios.

These fundamental principles have not previously been tested experimentally. In this chapter, I will perform vector rotation on a cohort of S-ICD ineligible patients to determine its effect on both R:T ratio and device eligibility. The experimental cohort will be identified through standardised S-ICD screening of current TV-ICD recipients who have no permanent pacing indication. These patients provide an accurate real-world representation of S-ICD recipients and are readily available due to their lifelong commitment to ICD follow up.

3.2 Objectives

- Apply mathematical vector rotation to electronic data recorded from a cohort of S-ICD ineligible patients.
- Describe the relationship that is subsequently observed between 'angle of mathematical vector rotation' and R:T.
- Calculate the angle(s) of rotation which result in an optimal R:T ratio and compare this angle with the patient's intrinsic R and T wave axes.
- Determine whether personalised vectors can increase R:T ratio.
- Determine whether personalised vectors can increase S-ICD eligibility.

3.3 Method

This was a prospective observational study performed between July 2016 and March 2017. Ethical approval (reference 16/LO/0534) was obtained from both the London (Brent) REC and the HRA. The study was sponsored by the Department of Research and Development at UHS. All study participants gave informed written consent prior to study enrolment. Adult patients with implanted TV-ICD systems were recruited at the time of a routine device follow up at UHS. Patients were excluded if device interrogation revealed a ventricular pacing percentage of >1%.

All study participants underwent standardised S-ICD screening in line with the pre-implant screening guidelines provided by the manufacturer.[55] ECG recordings were undertaken in both standing and supine positions at amplitudes of 5mm/mV, 10mm/mV and 20mm/mV. The resulting ECG morphologies were assessed against the manufacturer's screening tool by a cardiologist or cardiac physiologist trained in S-ICD template screening. Individual vectors were suitable if the vector passed screening in both postures and S-ICD ineligibility was declared when all three vectors failed.

Participants who failed S-ICD screening and were deemed to be S-ICD ineligible, were invited for a further assessment of their ECG morphology. A series of surface electrodes were positioned using anatomical landmarks and a five-lead two channel digital Holter recorder (Model AFT-1000, Holter Supplies, Paris) was used to simultaneously capture their primary and alternate vectors for one minute. [*Figure 21*]

For each patient, both channels of the Holter recording were downloaded in 1000Hz ASCII format and aligned visually so that the isoelectric lines in both vectors corresponded to an amplitude of zero. The time period corresponding to a single PQRST complex was isolated, providing simultaneous amplitude values of P (primary vector) and A (alternate vector).

Simulated vector rotation was performed at 5-degree intervals from 0 to 360 degrees, generating a rotated primary vector and a rotated alternate vector at every angle. These were denoted as 'P_z' and 'A_z' where z = angle of clockwise rotation.

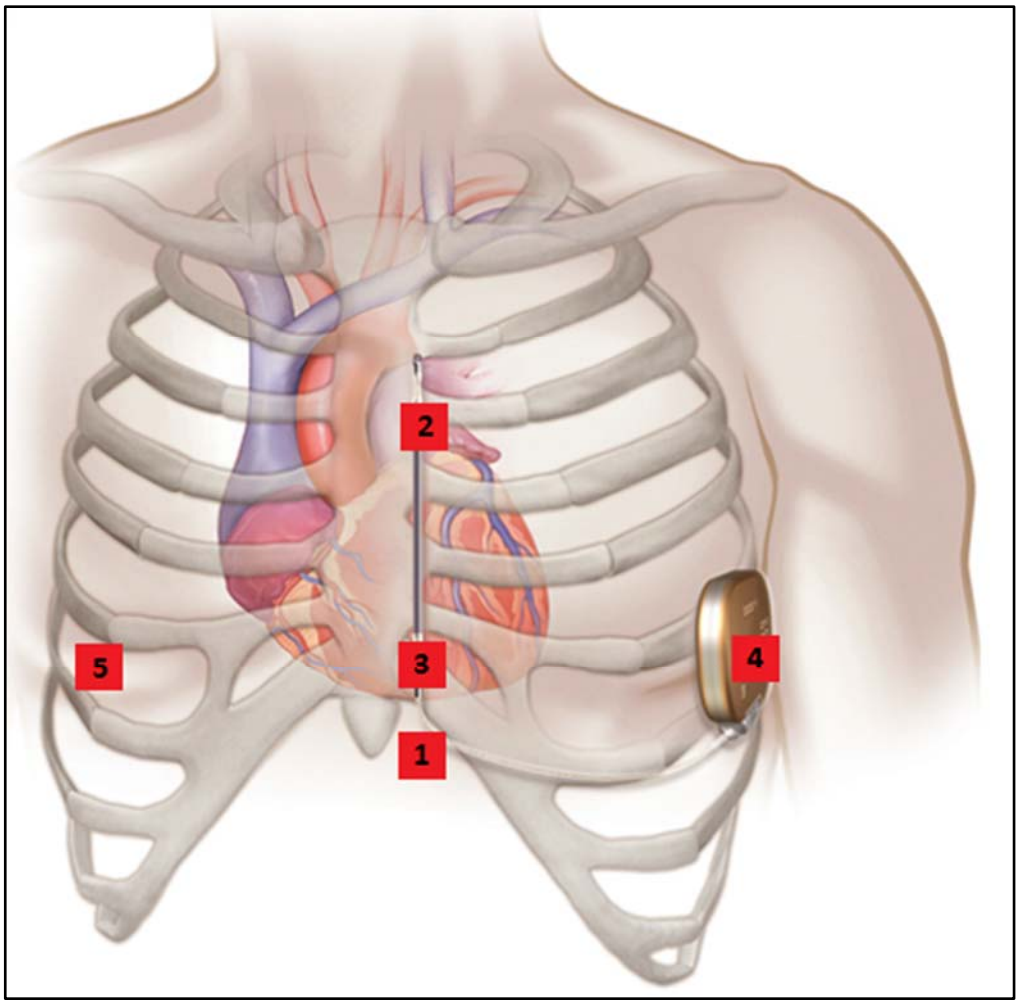

Figure 21: Surface ECG to record primary and alternate S-ICD vectors

1 = 1cm infero-lateral to the xiphisternum

2 = 14 cm superior to position 1

3 = immediately superior to position 1

4 = 6th intercostal space left mid axillary line

Holter Channel A records between points 3 and 4 = surrogate of S-ICD primary vector

Holter Channel B records between points 1 and 2 = surrogate of S-ICD alternate vector

5 = 5th intercostal space right mid clavicular line = neutral electrode

Image prior to annotation © Boston Scientific Corporation or its affiliates. Reproduced with permission.

R and T wave amplitudes were identified visually and recorded for every vector. The angle of rotation associated with the highest R:T ratio was denoted as the personalised vector angle. This was then compared to the intrinsic R and T wave axes of the individual. These axes were calculated using basic trigonometry, from the amplitude relationship of the R and T waves in the perpendicular primary and alternate vectors.

The vectors corresponding to the identified optimal degrees of rotation were denoted as personalised vectors. Mean R:T ratio in the personalised vectors was compared to the mean R:T ratio in the recorded vectors using an independent t-test. For each personalised

vector, a graph of amplitude against time was printed, with the time axes adjusted to match the sweep speed (25mm/s) of a standard ECG machine. Overlay screening could then be performed and the overall S-ICD eligibility recalculated.

All the participants were asked to provide some background medical information. With the patient's consent, hospital and device records were also used to record the device implant indication, the participant's EF (where this value has been assessed clinically in the preceding three years) and the haemoglobin and renal function (where this had been assessed clinically in the preceding twelve months).

3.4 Results

A total of 92 participants were recruited with a mean age of 64.9 (±2.7) years. 79.3% were male and 65.2% had a secondary prevention device. Common co-morbidities included ischaemic heart disease (48.9%), atrial dysrhythmia (38.0%), severe LV systolic dysfunction (33.0%) and hypertension (30.4%). Full patient demographics are given below. [*Table 6*]

Overlay S-ICD screening revealed that 94.6% of patients had at least one passing vector. The proportion of patients with three, two and one passing vector respectively were 18.5%, 62.0%, and 14.1%. The remaining 5.4% (n=5) had no passing vector and were therefore S-ICD ineligible by virtue of their vector morphology. The full results of the screening process are provided below. [*Table 7*]

The mean age of the ineligible cohort was 68.7 (±12.8) years. The ineligible patients were all male recipients of a secondary prevention device. In the S-ICD ineligible cohort mathematical vector rotation successfully produced a series of new vectors with different morphological appearances and R:T ratios. A pictorial representation of vector rotation from one patient is provided below. [*Figure 22*]

Vectors in the range P_0 – P_{180} were found to be inverted images of the vectors in the range P_{180} - P_{360}, giving them identical absolute R:T ratios. Given the perpendicular relationship of P and A, vector P_z was also found to be identical to vector $A_{z+90.}$ Therefore, a total of 35 vectors with unique R:T ratios were identified for each patient, with P_5 - P_{180} providing a complete data set for analysis. The relationship between angle of observation and the amplitudes of R and T is shown graphically below. [*Figure 23]*

The mean R:T ratio in the sensed vectors was 2.21 (95% CI 1.79-2.63, n=10). In the personalised vectors the mean R:T ratio was 7.21 (95% CI 4.54-9.88, n=5). The generation of a personalised vector was therefore associated with a statistically significant increase in R:T ratio ($p<0.001$).

The angle of rotation associated with each personalised vector is displayed on a bar chart below. [*Figure 24*] When the personalised vector angle is compared to the intrinsic T wave angle we see that in all five patients that the angle of observation is near perpendicular to the intrinsic T wave axis.

An example of a personalised vector is demonstrated below. [*Figure 25*] All the personalised vectors passed overlay screening, increasing the eligibility in this cohort from 0% to 100%, and the overall eligibility from 94.6% to 100% (n=92).

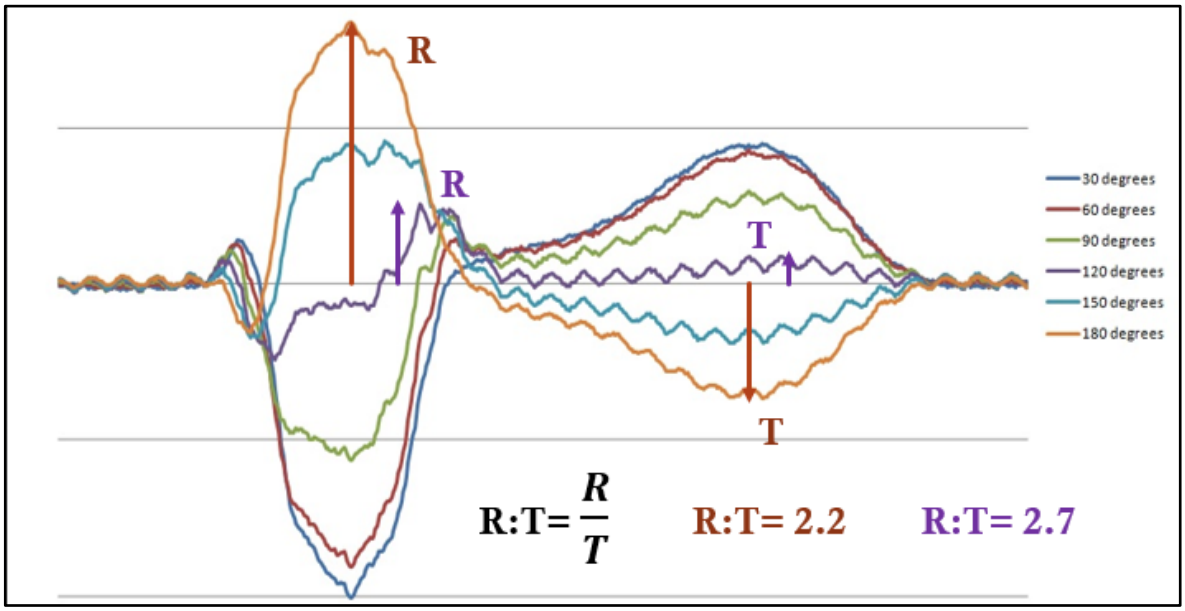

Figure 22: Changes in vector morphology with rotation

Graphical representation (x axis = time, y axis = signal amplitude) of a single PQRST complex which has been rotated by 30-degree intervals from 30-180 degrees. As rotation occurs both the R wave and the T wave can be seen to vary in absolute amplitude resulting in different R:T ratios at each angle of rotation. Note that the underlying rhythm in this patient is atrial fibrillation which results in artefact throughout.

Total Number of Participants (unless otherwise stated)		n = 92	
Demographics:	Mean age [years ± 95% CI]	64.9 [± 2.7]	
	Male	73	79.3%
Device:	Mean time since implant [months ± 95% CI]	77.3 [± 10.3]	
	Primary Prevention	32	34.8%
	Secondary Prevention	60	65.2%
	Dual chamber system (DR-ICD)	50	54.3%
	Single chamber system (VR-ICD)	42	45.7%
Co-morbidities:	Ischaemic heart disease	45	48.9%
	Previous atrial fibrillation or atrial flutter	35	38.0%
	Severe left ventricular (LV) systolic dysfunction (n=88)	29	33.0%
	Hypertension	28	30.4%
	eGFR < 60 ml/min/1.73m^2 (n=73)	19	26.0%
	Diabetes	13	14.1%
	Valve disease (>mild) or previous valve surgery (n=89)	13	14.6%
	Airways disease	12	13.0%
	Previous coronary artery bypass graft (CABG)	11	12.0%
	Peripheral vascular disease	6	6.5%
	Haemoglobin < 120 g/dL (n=79)	5	6.9%
	Cerebrovascular disease	5	5.4%
	eGFR < 30 ml/min/1.73m^2 (n=73)	3	4.1%

Table 6: Mathematical vector rotation - patient demographics

Not all participants had undergone investigation within the pre-determined time period for inclusion. Where these results were unavailable adjusted values of 'n' are provided.

Total Number of Participants (unless otherwise stated)		n = 92	
By vector	Primary vector pass	73	79.3%
	Secondary vector pass	74	80.4%
	Alternate vector pass	31	33.7%
By patient	3 passing vectors	17	18.5%
	2 passing vectors	57	62.0%
	1 passing vectors	13	14.1%
	0 passing vectors (S-ICD ineligible)	5	5.4%

Table 7: Mathematical vector rotation - S-ICD screening results

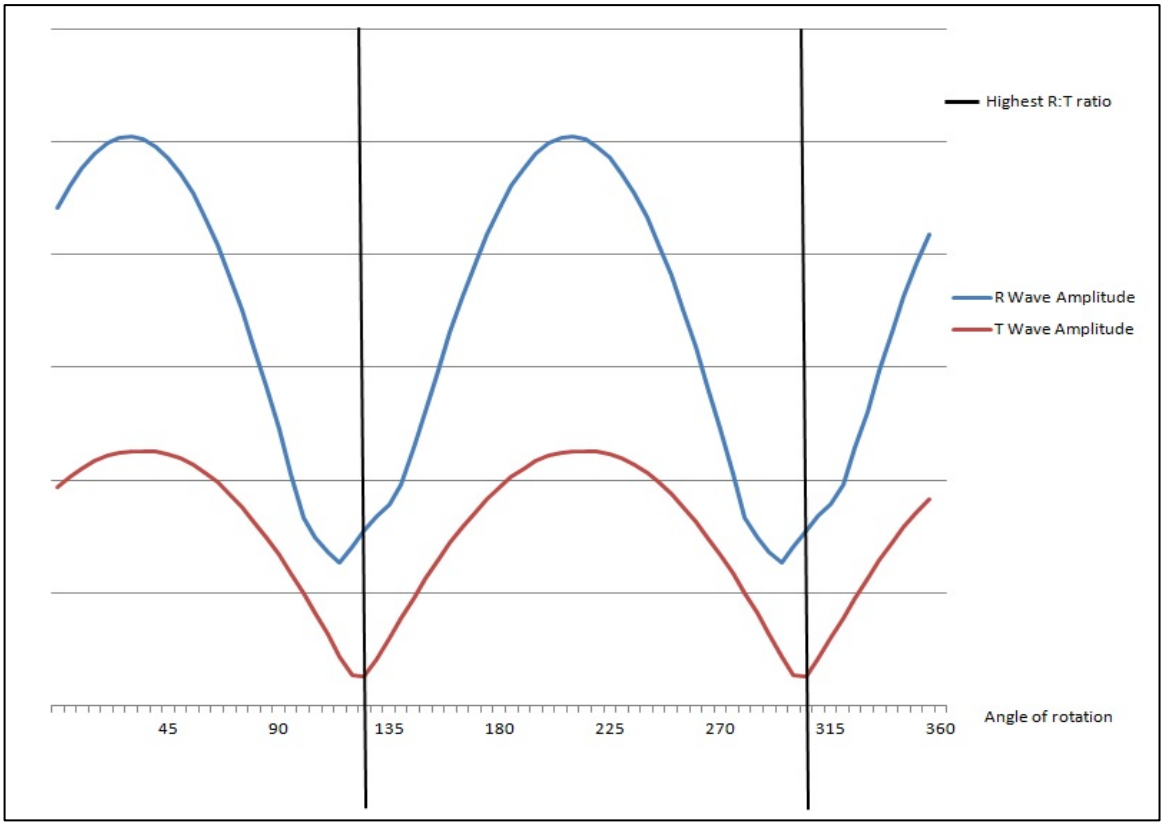

Figure 23: Absolute values of R and T versus angle of rotation

Amplitude (y axis) of the vector components R (blue), T (red) and R:T ratio (black) against angle of rotation (x-axis). The R wave and T wave amplitudes vary with a period of 180 degrees and the maximum R:T ratio is observed at two points exactly 180 degrees apart. A complete data set can therefore be achieved using 180 degrees of rotation. Note that in this example the highest ratio corresponds with a period of low overall signal amplitude.

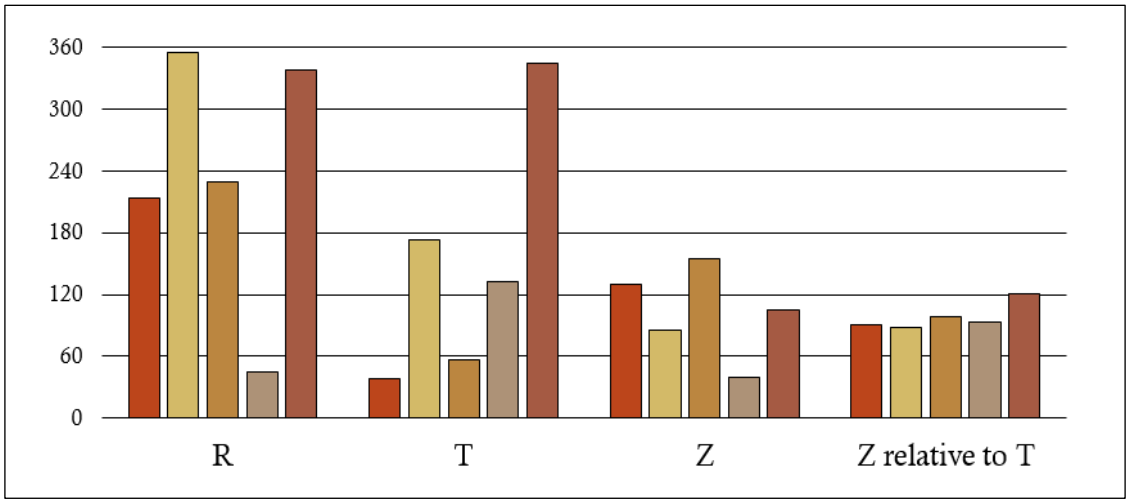

Figure 24: Personalised vector angle versus native axes

Bar chart showing the native R and T wave axes and the angle of rotation of the personalised vector in all five patients (each patient is denoted by a different colour). Right column: angle z relative to the intrinsic t wave angle. Note that the personalised vector angle seems to be found at approximately 90 degrees to the intrinsic T wave axes.

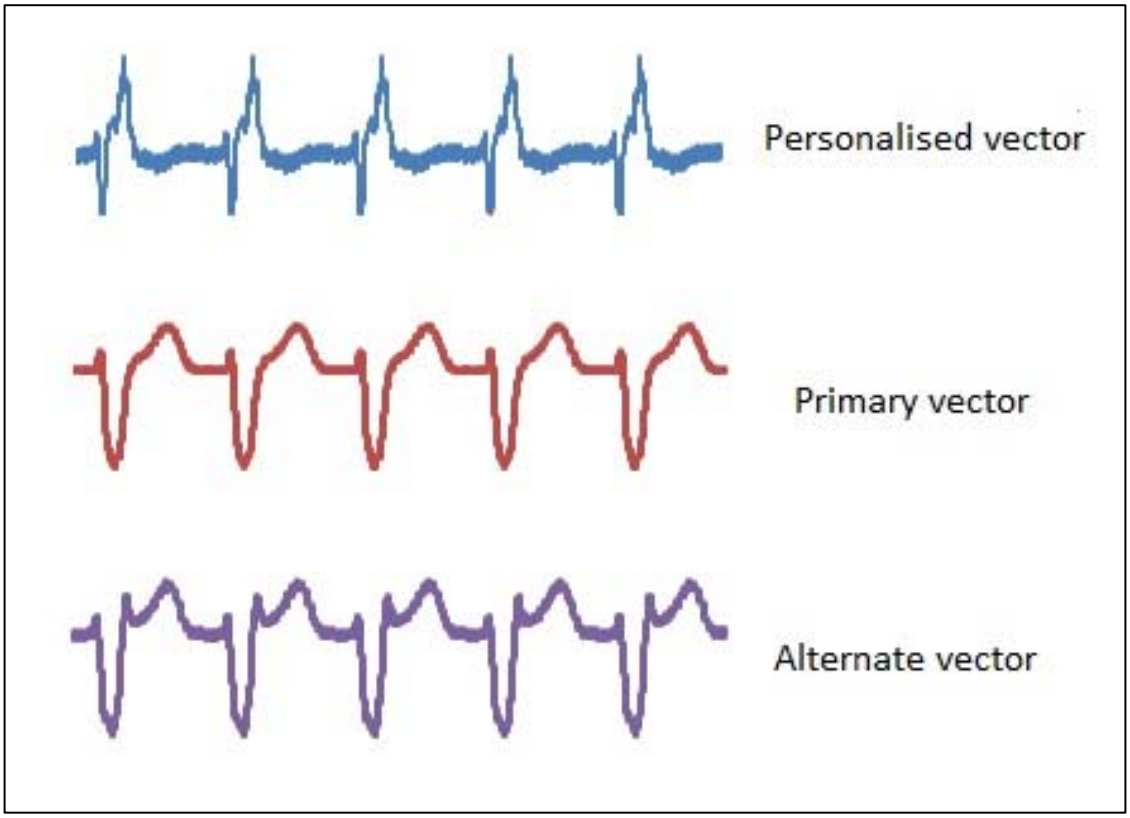

Figure 25: The personalised vector

Pictorial representation of the primary vector in comparison to the primary and alternate vectors in a given individual. The R:T ratio is considerably greater in the personalised vector which passes overlay screening.

3.5 Discussion

This study has successfully met each of its predefined objectives. I have demonstrated that in S-ICD ineligible patients, mathematical vector rotation significantly increases R:T ratio. I have also successfully increased S-ICD eligibility using this technique, with the personalised vectors achieving universal success in this regard.

This is a small study in which the rotation technique has only been applied to five individuals. As such, extrapolation to the wider ICD population must be done with caution. It is however the first experimental use of this technique and the results do appear to be potentially significant. They suggest that incorporation of this technique into future S-ICD programming, could both significantly increase eligibility and remove the need for pre-implant screening. The study does however have some limitations which should be considered.

Unfortunately, recruitment to this study pre-dated the routine use of automated S-ICD screening. Overlay screening was therefore used to assess personalised vector eligibility, with the personalised vectors printed prior to assessment. The limitation of this approach is that the impact of rotation on overall signal amplitude is ignored.

The angle at which the R:T ratio is maximal, may correspond to a vector with low signal amplitude. Even with an excellent ratio if the R wave is insufficient in amplitude then the vector will remain ineligible. A more robust technique would be to transfer the signal data to an S-ICD simulator. This would allow a vector score to be calculated which would represent a better evaluation of vector eligibility.

The use of an S-ICD simulator would also allow other features of S-ICD sensing to be incorporated into the assessment, such as the unique signal processing the S-ICD signal undergoes and also the device's blanking period. The blanking period is particularly relevant if the generated personalised vector has an RSR' type morphology, with a marked delay between the two signal peaks. In this study, where a manual assessment of R:T ratio was performed using a visual interpretation of what denotes T wave signal, the vector may have appeared acceptable. The S-ICD however will denote the R' peak as the T wave, if it falls outside of the blanking period. Consequently, the R:T ratio will be low when assessed by a simulator, resulting in a low vector score.

Further investigations into the role of personalised vectors must also consider the potential negative consequences of vector rotation. Accurate and timely identification of VF is a fundamental principle of S-ICD sensing. Given that we have demonstrated changes in R wave amplitude associated with rotation, we must consider whether rotation might therefore impact VF sensing. Might the device undersense VF that has been rotated, delaying or even preventing lifesaving therapy? This is a critical question that will be addressed in chapter 4.

All the patients had very different underlying ECG morphologies with wide variations in their intrinsic R and T wave axes. The personalised vector was therefore aptly named, with every angle of observation being unique to the individual. Some consistency was noted in that the personalised vector angles tended to occur at approximately 90 degrees to the T wave axis.

In many respects this was an expected finding given the electrocardiographic principles I have previously described. Angles of observation that are perpendicular to a wavefront minimise signal amplitude by creating a biphasic signal, whilst parallel angles of observation maximise signal amplitude. It is interesting to note that minimisation of the T wave by rotation, appears to have a greater impact on R:T ratio than maximisation of the R wave achieved by the same technique. The possibility is once again raised that rotation could be used to minimise the T wave in patients with acceptable vectors and that this could have a role in reducing T wave over-sensing. This will be addressed further in chapter 7.

3.6 Conclusions

In S-ICD ineligible patients, mathematical vector rotation can be used to generate a personalised vector, which has a significantly higher R:T ratio than their recorded S-ICD vectors. Use of the personalised vector, in an S-ICD ineligible cohort, increases device eligibility.

Chapter 4 Ventricular fibrillation detection

4.1 Introduction

All implantable defibrillators are programmed to treat episodes of VF with potentially life-saving high energy shock therapy. Effective therapy relies upon accurate and timely diagnosis as time to defibrillation is critical in survival from cardiac arrest. Delaying therapy by prolonging time to detection, or withholding therapy entirely, is associated with significantly poorer outcomes in both in-hospital and community cardiac arrests.[118-121]

In the preceding chapter, mathematical vector rotation was shown to cause variations in R wave amplitude by altering its angle of observation. The potentially beneficial effects of rotation (in optimising R:T ratio) were demonstrated, but the impact of vector rotation on dysrhythmia detection remains unknown.

VF is a life-threatening rhythm disturbance that is characterised by rapid and chaotic electrical activity. It is defined electrocardiographically by irregular QRS complexes of varying morphology. During VF there is no definable intrinsic axis as the direction of depolarisation varies rapidly. Signal amplitudes also vary significantly. Fortunately, a degree of under-sensing is accommodated by the probabilistic detection system, where a rolling '18 out of 24' interval system is used to diagnose tachycardia.

What will occur when VF is viewed from an alternative angle of observation? I believe that VF, at any angle of observation, will still look like VF, due the absence of a definable intrinsic axis. I would however expect the pattern of detection and under-sensing to change, as each individual R wave will be altered in amplitude, and the R waves which fall below the sensitivity level will vary.

However, I do not believe the device's overall ability to detect VF will be impaired. This assertion is based upon the extremely high rates of VF detection which have been consistently demonstrated in experimental trials and cohort studies. Furthermore, no difference has ever been identified in VF detection between the three pre-existing vectors, all of which record VF from a different angle. I would therefore expect the system to adequately accommodate VF from any newly generated angle. I hypothesise that

mechanical vector rotation will not prevent VF detection or significantly impair time to detection.

Experimental testing of VF detection using rotated vectors requires real life recordings of VF to be analysed by an S-ICD simulator. This can be achieved using surface ECG as a surrogate of vector morphology, in patients undergoing defibrillation threshold (DFT) testing. A DFT is a routine elective procedure that is used to assess the defibrillation efficacy of an implanted ICD system. VF is deliberately induced to allow ICD detection and treatment to be assessed. DFT testing is currently required in all S-ICD recipients and some TV-ICD recipients.

4.2 Objectives

- Compare the VF detection sensitivity of a series of rotated S-ICD vectors with the VF detection sensitivity of the three standard S-ICD vectors.
- Compare the time to VF detection in a series of rotated S-ICD vectors, with the time to VF detection sensitivity in the three standard S-ICD vectors.

4.3 Method

This was a prospective observational study performed between December 2017 and July 2018. Ethical approval (reference 17/LO/1952) was obtained from both the London (Bromley) REC and the HRA. The study was sponsored by the Department of Research and Development at UHS. Adult patients undergoing an elective VF induction in the EP laboratory at UHS were eligible for recruitment. There were no exclusion criteria aside from the inability to give informed written consent, which was required from all participants prior to enrolment.

Participants underwent continuous 3 lead ECG recording throughout their VF induction procedure, with ECG electrodes positioned to create surrogate recordings of all three S-ICD vectors. This was achieved using standard ECG limb leads placed according to the manufacturer's guidelines for S-ICD screening.[55] The ECG signal from all three vectors was recorded using the LABSYSTEM Pro EP system. The study was entirely observational, and the VF induction proceeded at the direction of the clinical team.

Post procedure, the ECG data from all three vectors was downloaded in ASCII format. For each vector, a 30 second template file was created using a period of stable intrinsic rhythm. Where VF induction had been achieved, further individual vector files were created for every discrete episode of VF. Signal artefact relating to the induction itself (50Hz burst) or to any shock therapies was removed. The VF recordings were also looped to effectively create infinitely long episodes for detection.

For every participant, mathematical vector rotation was performed. All the VF episodes, and all their corresponding templates, were rotated between 0 and 85 degrees at 5-degree intervals. For every VF episode this created 17 rotated vectors in addition to the 3 traditional recorded vectors.

The VF episodes were analysed using an S-ICD simulator. This is a computer-based software programme that accurately recreates the S-ICD sensing mechanism and has comparable programmable features to the S-ICD. Rotated and recorded VF episodes were analysed with dual zone programming at 170/250, (i.e. a conditional zone between 170 and 250bpm and a shock zone above 250bpm).

Simulator analysis was supported by the engineering department at Boston Scientific. Input from the manufacturer was required due to the proprietary information contained within the simulator programme. All the VF episodes were anonymised prior to analysis. Throughout the analysis I remained responsible for the production of the data sets, the clinical information pertaining to each recording, and the analysis of the simulator outputs.

VF detection was deemed to have occurred if the simulator reached ‘capacitor charging’. The proportion of episodes in which VF detection occurred (VF detection sensitivity) was calculated for both the recorded and rotated vector groups. These two proportions were displayed on a bivariate table and compared statistically. As they represented categorical data, a Chi squared test was used.

Where VF detection occurred, the time from rhythm onset to ‘capacitor charging’ was defined as the ‘time to VF detection’ and recorded in seconds. The mean time to VF detection in both the recorded and rotated vectors were compared statistically. An independent t-test was chosen to compare these values as they were continuous, nominal and expected to approximate normal distribution.

All the participants were also asked to provide some background medical information. With the patient's consent, hospital and device records were also used to record the device implant indication and the participant's EF (where this value had been assessed clinically in the preceding three years).

4.4 Results

A total of 13 patients were recruited with a mean age of 45.7 ± 8.4 years. VF was successfully recorded in 12 out of 13 patients and a total of 15 discrete VF episodes were captured, each from three different S-ICD vectors. These 45 recorded vectors were compared to 255 rotated vectors, after each VF episode had been rotated through 17 different angles. More detailed patient demographics are provided below. [*Table 8*]

Total Number of Participants (unless otherwise stated)		n = 13	
Demographics:	Mean age [years ± 95% CI]	45.7 [± 8.4]	
	Male	7	53.9%
Device:	Primary Prevention ICD	8	61.5%
	Secondary prevention ICD	5	38.5%
	S-ICD	10	76.9%
	TV-ICD	3	23.1%
Comorbidities:	Ischaemic heart disease	3	23.1%
	Severe LV impairment (EF<0.35)	3	23.1%
VF:	Patients in whom VF was recorded	12	92.3%
	Total number of VF episodes	15	
	Mean length [seconds ± 95% CI]	18.3 [± 6.8]	
	Total number of recorded VF vectors	45	
	Total number of rotated VF vectors	255	

Table 8: VF detection - patient demographics

In the recorded vectors (primary, alternate and secondary) VF detection sensitivity was found to be 97.78%, with capacitors charging in 44 out 45 episodes. In the rotated vectors, VF detection sensitivity was found to be 96.47% (246 out of 255 episodes). This was a non-significant reduction in sensitivity (p=0.65).

In the recorded vectors the mean time to VF detection was 6.14 seconds (± 0.29, n=44), whilst in the rotated vectors it was 6.34 seconds (± 0.30, n=246). This was a non-significant increase in VF detection time (p=0.65).

VF detection sensitivity and mean time to VF detection by individual vector and angle of rotation are shown below. [*Figure 26*, *Figure 27*]

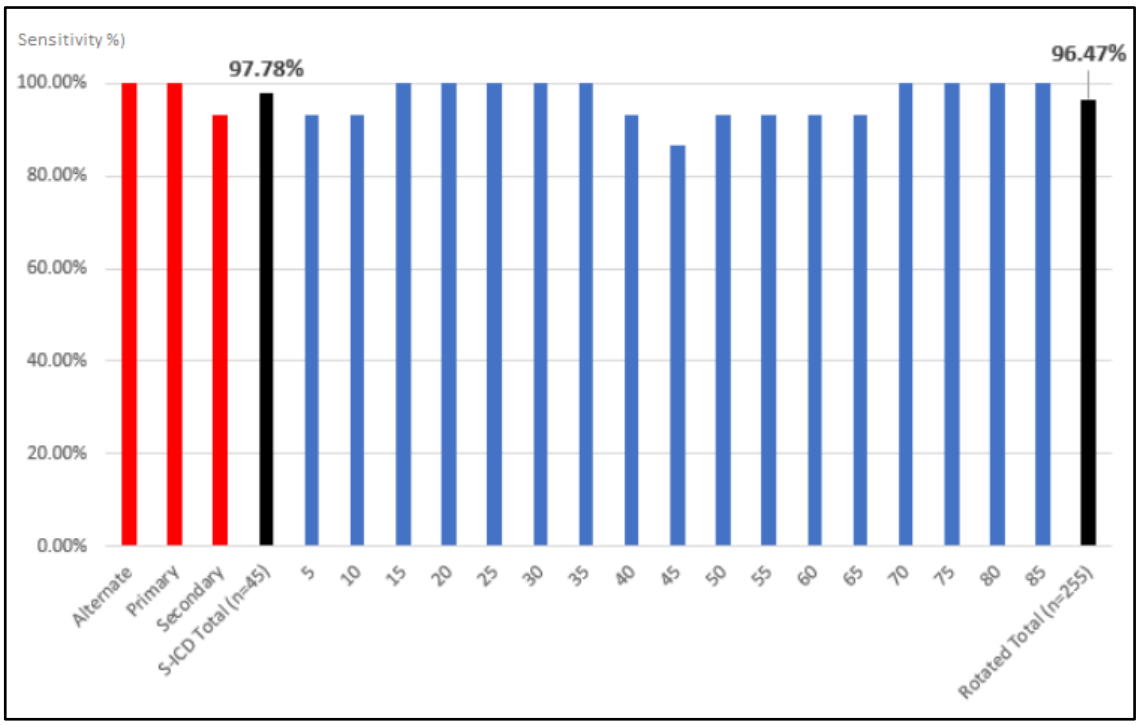

Figure 26: VF detection sensitivity - recorded versus rotated

VF detection sensitivity (%) is displayed for each vector. The red columns represent the three recorded vectors (primary, alternate, secondary). The blue columns represent the range of rotated vectors by angle of rotation. The black columns show the overall sensitivity for the red and blue groups.

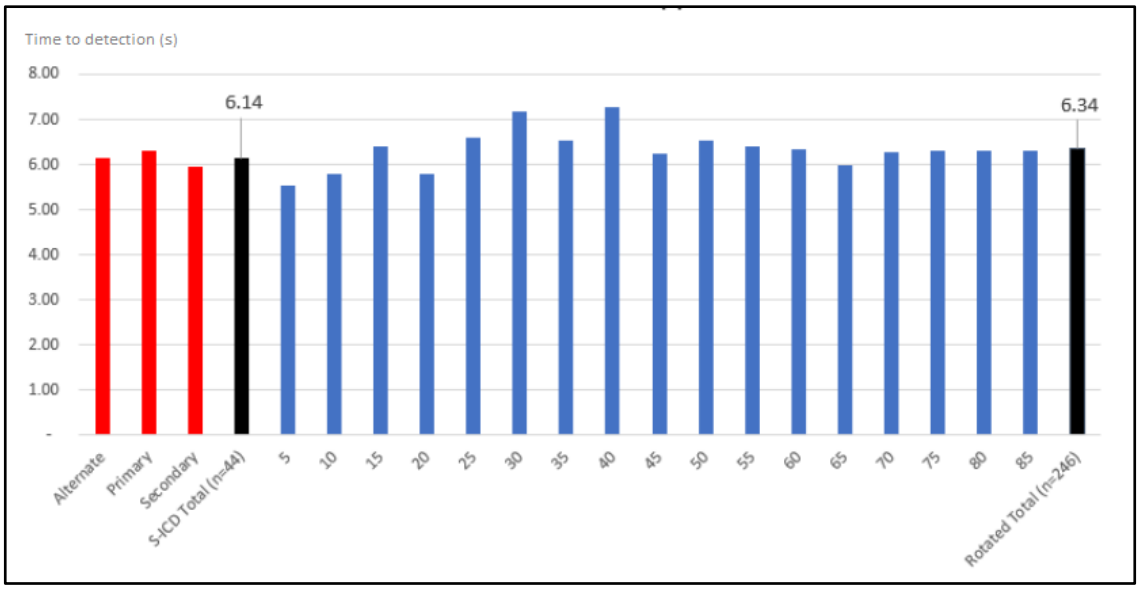

Figure 27: VF time to detection - recorded versus rotated

Mean time to VF detection (seconds) is displayed for each individual vector. The red columns represent the three recorded vectors (primary, alternate, secondary). The blue columns represent the range of rotated vectors by angle of rotation. The black columns show the mean times to detection for the red and blue groups.

4.5 Discussion

The objective of this study was to compare VF detection sensitivity, and time to VF detection, in recorded and rotated S-ICD vectors. The results strongly suggest that vector rotation does not impair VF detection. All the rotated vectors demonstrated high VF sensitivity levels and rotation was not associated with a significant increase in time to detection.

The episodes in which VF detection did not occur were all a result of under sensing. A possible explanation for this is the short duration of some of the episodes. Episodes were looped to create an infinitely long episode for analysis, but if under sensing occurred during a period of detection, this tended to occur on every subsequent loop of the data. Under these circumstances the probabilistic counter never reached VF detection. This may not have been the case with ongoing VF which would have continued to vary in amplitude and axis.

Eliminating short episodes of VF could have removed this potential problem and allowed for a more accurate calculation of sensitivity. However, the aim of the study was not to

determine the VF sensitivity of the S-ICD, but rather to compare recorded and rotated vectors. The same VF episodes were used in both groups and the under sensing in shorter episodes is therefore unlikely to have affected the overall findings.

Another possible limitation of this study is the use of 'capacitor charging' rather than 'shock delivered' as a marker of successful VF detection. 'Capacitor charging' was chosen as the time to detection on the simulator corresponds accurately to an implanted system. Whereas 'shock delivered' relies on an estimate of the time it would take to charge the capacitors. The use of 'capacitors charging' is unlikely to have impacted on the comparison between the two groups, although the influence of rotation on persistence analysis, which is performed immediately prior to shock delivery, cannot be assessed.

The relative rarity of DFT testing in clinical practice made recruitment for this study challenging and limited the overall number of VF episodes that were available for analysis. DFT testing is very rarely performed in TV-ICD systems, whilst S-ICD implants at our institution often have their DFT test performed at the time of device implantation. These S-ICD patients were not recruited to the study as accurate surface ECG positions could not be obtained without potentially interrupting the operator's sterile field. Recruitment was therefore limited to TV-ICD recipients and S-ICD patients undergoing a DFT outside of their device implant procedure.

4.6 Conclusion

The use of mathematical vector rotation does not affect the VF detection efficacy of the S-ICD system. High VF sensitivity levels are demonstrated across a wide range of rotated vectors, with no significant increase in time to detection compared to standard vectors. This is a reassuring finding with regards the possible future introduction of vector rotation as a mechanism for increasing S-ICD eligibility.

Chapter 5 SVT discrimination

5.1 Introduction

SVT are rapid abnormal heart rhythms that originate in the atria. Electrocardiographically they are usually characterised by narrow QRS complexes. Unlike ventricular arrhythmia, they are not associated with haemodynamic compromise or sudden death. Shock therapies delivered for SVT are considered inappropriate, whilst high energy treatment for broad complex tachycardia, presumed to be of ventricular origin, is considered appropriate.

The S-ICD offers dual zone programming, where two separate tachycardia zones are identified. In the 'conditional zone' discriminators are applied during tachycardia to assess the probable origin of the rhythm disturbance prior to treatment. Discriminators are based upon the morphological appearance of the QRS complex during tachycardia, with comparison made to a stored vector template. Conditional zone rhythms are treated by shock therapy if they have a combination of a poor QRS morphology match and either a variable beat to beat morphology, or an increased QRS width compared to the template.

Smart Pass is an additional programmable filter which can to be used to prevent inappropriate shock therapies and may be applied during tachycardia detection. Smart Pass is a high pass filter which reduces the amplitude of slow-moving signal (T waves) whilst preserving the amplitude of faster moving signal (R waves).

Patients who experience SVT are often investigated using an EPS, an elective procedure in which induction of SVT is attempted using a combination of pacing manoeuvres and pro-arrhythmic medication. Successful induction of an SVT in the EP lab allows the underlying aetiology to be identified, potentially facilitating a substrate-based ablation. Appropriately placed surface ECG leads, worn during an EPS, would allow surrogate S-ICD vector signal to be recorded during episodes of SVT. Offline analysis of rhythm discrimination could then be performed using an S-ICD programmer.

5.2 Objectives

- Compare the SVT discrimination sensitivity and specificity of recorded S-ICD vectors to a series of rotated S-ICD vectors.

- Determine whether vector rotation negatively impairs SVT discrimination.

5.3 Method

This was a prospective observational study performed between July 2016 and January 2017. Ethical approval (reference 16/WM/0182) was obtained from both the West Midlands (South Birmingham) REC and the HRA. The study was sponsored by the Department of Research and Development at UHS.

Adult patients undergoing an EPS involving an induction of SVT were eligible for recruitment. As paced ventricular complexes are inherently broad, patients with a permanent pacemaker or TV-ICD were excluded if they had a ventricular pacing percentage >1%. Informed written consent was provided by all participants prior to enrolment.

Throughout their EPS participants wore a five-lead two channel digital Holter recorder (Model AFT-1000, Holter Supplies, Paris) positioned to record surrogate signal of their primary and secondary sensing vectors. This was achieved using ECG electrodes positioned using the anatomical landmarks shown previously. [*Figure 18*]

The study was purely observational, and the EPS procedure was performed entirely at the discretion of the clinical team. Episodes of sustained tachycardia lasting ≥15 seconds were divided into narrow complex tachycardias (NCT) (QRS≤120ms) and broad complex tachycardias (BCT) (>120ms). The aetiology of each tachycardia was determined at the end of the EPS by the supervising Consultant.

The Holter data was downloaded in ASCII format at a frequency of 1000Hz. For every tachycardia episode, a data file containing up to 30 seconds of tachycardia was created, along with a corresponding template file containing 30 seconds of stable intrinsic rhythm. Mathematical vector rotation was performed on every data set, with rotated vectors generated from 0 to 85 degrees at 5-degree intervals.

The tachycardia episodes were analysed using an S-ICD simulator that was programmed with 170/250 dual zone programming (conditional zone from 170bpm, shock zone from 250bpm). The corresponding baseline rhythm files were used to build an accurate sensing template prior to tachycardia analysis. Vector scores for every template vector were

calculated during this assessment by the simulator, allowing ineligible vectors (score <100) to be excluded from later rhythm detection analysis. Tachycardia detection was performed with and without the addition of Smart Pass. As described in the previous chapter, the simulator analysis was supported by the engineering department at Boston Scientific.

Successful device identification of SVT was deemed to have occurred when, during the analysis of an NCT in an S-ICD eligible vector, 'capacitor charging' did not occur. SVT discrimination sensitivity was then the proportion of SVT episodes which were successfully identified. Overall sensitivities in the recorded and the rotated vectors, with and without the addition of Smart Pass, were calculated. The proportions were displayed on a bivariate table and compared statistically. As they represented categorical data, a Chi squared test was used.

A specificity analysis was also undertaken using episodes of BCT which occurred in S-ICD eligible vectors above the lower treatment zone of the simulator (170bpm). For these episodes 'capacitor charging' was used as a marker of successful SVT discrimination (i.e. the device correctly determined these episodes were not SVT). The proportion of episodes corrected identified as not SVT defined specificity. The results from recorded and rotated vectors were again compared statistically using a Chi squared test.

All the participants were asked to provide some background medical information. With the patient's consent, hospital and device records were also used to record the device implant indication and the participant's EF (where this value had been assessed clinically in the preceding three years).

5.4 Results

A total of fifty-seven patients (age 49.5 ± 4.5 years, 35.1% male) were recruited. None of the recruited patients had an ICD, 3.8% had severe LV systolic dysfunction and 1.8% had a history of coronary artery disease.

More detailed patient demographics are provided below. [*Table 9*]

Total Number of Participants (unless otherwise stated)		n = 57	
Demographics:	Male	20	35.1%
	Mean age [years ± 95% CI]	49.5 [± 4.5]	
	Mean body mass index (BMI) [kilograms / metres^2]	28.4 [± 1.5]	
Co-morbidities:	Hypertension	13	22.8%
	History of atrial fibrillation	9	15.8%
	History of atrial flutter	7	12.3%
	Valve disease (>mild) or previous valve surgery (n=53)	4	7.5%
	Diabetes	4	7.0%
	Severe left ventricular (LV) systolic dysfunction (n=53)	2	3.8%
	Haemoglobin < 120 g/dL	2	3.5%
	Ischaemic heart disease	1	1.8%
	eGFR < 60 ml/min/1.73m^2	1	1.8%
	QRS prolongation at baseline	0	0.0%

Table 9: Participant demographics - SVT discrimination study

Not all participants had undergone echocardiograms within the pre-determined time period for inclusion. Where these results were unavailable adjusted values of 'n' are provided.

34 episodes of NCT were recorded in 102 different vectors, of which 68 (66.7%) were S-ICD eligible. The commonest aetiologies were AVNRT (61.8%) and orthodromic AVRT (20.6%). Vector rotation created 578 new vectors, of which 350 (60.6%) were S-ICD eligible.

There were 6 episodes of BCT above 170bpm, all of which were supraventricular in origin. QRS broadening in each case was due to either antidromic accessory pathway conduction or acute rate related BBB. BCT episodes occurred in 8 eligible recorded vectors and 49 eligible rotated vectors.

The recorded and the rotated vectors both showed high sensitivity in SVT discrimination, with no significant difference identified between the two groups. The baseline sensitivity in the recorded vectors was 96% versus 95% in the rotated vectors (p=0.73). After the addition of Smart Pass programming the sensitivity values were 91% and 95% respectively (p=0.19).

There was no significant difference in SVT specificity between the two groups. Specificity levels in the recorded vectors were 88% (75% with Smart Pass) compared to 86% (78% with Smart Pass) in the rotated vectors, p=0.88 (p=0.85 with Smart Pass).

Overall the addition of Smart Pass programming did not significantly alter the sensitivity (95% versus 94%, p=0.52) or the specificity (86% versus 77%, p=0.22).

Full results are displayed below. [*Table 11-14*]

Episodes of induced narrow complex tachycardia (NCT)	34
- AVNRT	21 (61.8%)
- Orthodromic AVRT	7 (20.6%)
- Focal atrial tachycardia	4 (11.8%)
- Atrial fibrillation	1 (2.9%)
- Atrial flutter	1 (2.9%)
Mean NCT heart rate (bpm, ± 95% CI)	181 ± 9.7
Induced NCT episodes in recorded S-ICD vectors (total episodes x 3)	102
Induced NCT episodes in recorded S-ICD eligible vectors	68 (66.7%)
Rotated NCT episodes (total episodes x 17)	578
Rotated NCT episodes in S-ICD eligible vectors	350 (60.6%)
Episodes of induced broad complex tachycardia (BCT) at greater than 170bpm	6
- Antidromic AVRT	3 (50.0%)
- AVNRT with rate related bundle branch block	2 (33.3%)
- Orthodromic AVRT with rate related bundle branch block	1 (16.7%)
Mean BCT heart rate (bpm, ± 95% CI)	207 ± 21.5
Induced BCT episodes in recorded S-ICD vectors (total episodes x 3)	18
Induced BCT episodes in recorded S-ICD eligible vectors	8 (44.4%)
Rotated BCT episodes (total episodes x 17)	102
Rotated BCT episodes in S-ICD eligible vectors	49 (48.0%)

Table 10: Tachycardia episodes

Smart Pass off	Recorded vectors		Rotated vectors		p value
	NCT	BCT	NCT	BCT	
No charge	65	1	332	7	
Capacitors charged	3	7	18	42	
Sensitivity	96%		95%		0.73
Specificity	88%		86%		0.88

Table 11: Recorded versus rotated (Smart Pass off)

Smart Pass on	Recorded vectors		Rotated vectors		p value
	NCT	BCT	NCT	BCT	
No charge	62	2	333	11	
Capacitors charged	6	6	17	38	
Sensitivity	91%		95%		0.19
Specificity	75%		78%		0.85

Table 12: Recorded versus rotated (Smart Pass on)

	Smart Pass on		Smart Pass off		p value
	NCT	BCT	NCT	BCT	
No charge	395	13	397	8	
Capacitors charged	23	44	21	49	
Sensitivity	94%		95%		0.52
Specificity	77%		86%		0.22

Table 13: All vectors (Smart Pass on versus off)

5.5 Discussion

Vector rotation does not impair the sensitivity or specificity of SVT discrimination by the S-ICD. This study has therefore met its primary objective. However, the followings limitation should be considered.

Firstly, the cohort who have been studied are not an ICD population, but a typical SVT population. Caution must therefore be displayed when extrapolating these findings to real world recipients of an S-ICD. In the study cohort the mean age was under 50, the vast majority had normal LV systolic function, and there was a very low prevalence of coronary disease. The commonest rhythm disturbances were AVNRT and orthodromic AVRT, and no recruits had a prolonged QRS duration at baseline. By comparison, a typical ICD population would be older, with a high prevalence of LV impairment, coronary artery disease and QRS prolongation. The commonest dysrhythmia in an ICD population would almost certainly be atrial fibrillation.

Secondly, in calculating the sensitivity percentages in this study, I defined a 'true positive' as a patient with an NCT that did not lead to capacitors charging. This assumes that the device was able to diagnose tachycardia, but also to determine a supraventricular origin and withhold therapy.

However, some of the tachycardia episodes had a heart rate under the lower end of the treatment zone (<170bpm). In these cases, we cannot be certain that tachycardia was diagnosed at all. They were included in the analysis as one potential risk of vector rotation is an increase in T wave size, which could have led to over sensing. It would therefore have been possible for vector rotation to lead to a false negative, even at a heart rate below 170bpm.

Conversely, only BCT episodes greater than 170bpm were included. This is because any rhythm below that threshold should be ignored by the device, regardless of rhythm origin. Episodes below 170bpm could therefore not be used to determine device specificity. The specificity results were limited by the BCT cohort size. This was felt to be acceptable given the results of the previous chapter, in which identification of ventricular dysrhythmia was addressed separately.

The findings relating to Smart Pass are worthy of discussion. In this study the addition of Smart Pass programming made no statistical difference to device performance. I would hypothesise that this is because the analysis was only performed in passing S-ICD vectors, and that Smart Pass is more likely to have a clinical role in patients who experience fluctuations in T wave amplitude and vector score.

In all the rhythm disturbances in this study the vector score immediately prior to rhythm onset was, by study design, greater than 100. In the real world, S-ICDs are implanted after ECG screening is performed, but the vector score at the moment of screening, may not reflect the vector score during subsequent tachycardia detection.

5.6 Conclusion

The use of mathematical vector rotation does not affect SVT discrimination. High SVT sensitivity levels are demonstrated across a wide range of rotated vectors, with no significant difference when compared to standard vectors. This is a reassuring finding with regards the possible future introduction of vector rotation as a mechanism for increasing S-ICD eligibility.

Chapter 6 Alternating angle of observation

6.1 Introduction

In Chapter 3, I applied the principles of mathematical vector rotation to a cohort of S-ICD ineligible patients. Rotation was used to identify the single angle of observation associated with the greatest R:T ratio for each individual. This personalised vector was then tested for S-ICD eligibility using an overlay technique. The results were promising with S-ICD eligibility demonstrated throughout the cohort.

The method used in chapter 3 was unable to assess whether the overall amplitude of the personalised vector was adequate for sensing. It also relied upon a visual determination of R and T wave amplitude. This does not accurately reflect how a signal is processed by an S-ICD. Vector score, a numerical value which combines an assessment of R:T ratio with a measure of overall amplitude, is a more robust assessment of eligibility. It can be calculated using an S-ICD simulator, with eligible vectors always scoring >100.

In this chapter, I shall revisit the ineligible cohort of patients from Chapter 3, moving the focus of assessment from R:T ratio to vector score. I shall also introduce the idea of 'alternating angle of observation'. Thus far mathematical rotation has been used to generate vectors from a single angle of observation. The truly personalised vector however need not be limited to a single angle.

The introduction of the Smart Pass algorithm [*Section 1.7.4*] has demonstrated that R wave and T wave periods can be successfully differentiated using signal processing techniques, and that this information can be used to optimise vector morphology. In the case of Smart Pass, differentiation is achieved using a high pass filter, exploiting the intrinsic difference in frequency between T wave signal and R wave signal. Importantly, vector manipulation, performed prior to rhythm assessment, allows the underlying principles of tachycardia detection to be retained.

Could vector rotation be combined with R and T wave differentiation? This would be an attractive prospect. It would allow a different angle of observation to be employed during R and T wave periods. A vector which combined both a maximal R wave and a minimal T wave, as determined by vector score, would be a truly optimal vector for that individual.

The generation of personalised vectors, as described in chapter 3, involved a simple mathematical algorithm. The inputs to the algorithm were the current primary and alternate vectors, and the output was the personalised vector. The algorithm used a mathematical formula for which the only additional information required was an angle of observation. In chapter 3 one angle was chosen, selected based upon the results of additional analysis of the individual's ECG morphology.

In this chapter, the process will be modified such that the output of the system can vary between two different angles. This requires an additional filter, which is designed to separate R and T wave periods. At any given point in time the algorithm will combine the primary and alternative vectors using angles associated with either optimal R, or optimal T wave amplitudes. These two optimal angles will once again be calculated from additional analysis of the individual's baseline ECG morphology.

Two novel techniques for differentiating R and T wave periods will be explored; a gradient filter and a morphological screen. Both systems have been self-designed, the latter with the support of the University of Southampton Department of Electronics and Computer Science.

The gradient filter is similar in mechanism to the Smart Pass algorithm, differentiating the rapidly changing vector amplitudes which occur during an R wave, from the slowly changing amplitudes of a T wave. Unfortunately, using Smart Pass itself was not possible due to the proprietary nature of the algorithm.

The morphological screen uses a template R wave morphology to differentiate the R wave signal from all background noise. For publication and presentation purposes I have named the combined use of a morphological screen with vector rotation as IMPROVE (integrated morphology filter with personalised rotation of vectors).

6.2 Objectives

- Quantify the impact of using alternating angles of vector rotation on the R:T ratio, vector score and vector eligibility, of individuals who are currently S-ICD ineligible.

6.3 Method

This study was performed using the same electronic data obtained in Chapter 3. The methods employed in collecting this data have been comprehensively described and will therefore not be repeated here. In brief, the data compromised simultaneous primary and alternate vectors, recorded using surrogate surface ECG. It was obtained from S-ICD ineligible individuals who were identified after overlay screening was performed on a cohort of ICD recipients. Unlike the previous study, where individual QRST complexes were spliced for analysis, in this study sixty second recordings for each vector were utilised.

Mathematical vector rotation was performed on all the data sets, with rotation applied at 5-degree intervals between 5 and 175 degrees, generating 35 new vectors for each patient. The angles of observation associated with the smallest absolute amplitude T wave (T_{MIN}) and the largest absolute amplitude R wave (R_{MAX}) were identified. Although vectors with an R wave amplitude >3.25mV were not selected as this is above the maximum amplitude the S-ICD system can accommodate.

6.3.1 Gradient vector

The gradient filter was created after a detailed gradient analysis was performed using single template QRS complexes from each primary vector. Gradient graphs, displaying 'change in signal amplitude' against time, were created for each individual patient. These confirmed that higher gradient signals were observed during R wave periods than during T wave periods. A combined gradient graph for the entire cohort was also created and a wide variation in individual signal amplitude was noted. Consequently, a numerical gradient value (measured in mV/ms) differentiating between R and T wave periods, could not be identified.

The gradients were reassessed, measuring change in amplitude as a percentage of peak R wave amplitude, rather than an absolute measure in mV. A change of greater than 50%, across a time interval of 100ms, was found to accurately differentiate R waves from T waves. Signals meeting this criterion were considered 'high gradient', with all remaining signal classified as 'low gradient'.

During 'high gradient' signal the primary and alternate vectors were combined using the mathematical formula associated with the angle $R_{MAX.}$ During 'low gradient' signal the vectors were combined using the formula associated with the angle T_{MIN}. Mean R:T ratios and vector scores of the resulting 'gradient vectors' were calculated using an S-ICD simulator. These were compared statistically to the corresponding values from the recorded vectors. Statistical analysis was performed using an independent t test. Vector scores >100 were defined as eligible and overall S-ICD eligibility in the cohort was calculated.

6.3.2 IMPROVE vector

A template QRS complex was chosen from the primary vector to represent standard QRS morphology. Hierarchical clustering was then undertaken to identify all the R wave signals in the data set. Hierarchical clustering is a common machine learning algorithm that seeks to determine the hierarchy of all clusters by analysing similarity or dissimilarity between pairs of points. It can be performed using software in the MATTLAB platform.

Specifically, a range of 2-4 clusters were used with a blanking period of 250ms to prevent the detection of bifid R waves as separate peaks. The application of hierarchical clustering to the data sets was performed with the support of the Department of Electronics and Engineering at University of Southampton.

During R wave signal the primary and alternate vectors were combined using the mathematical formula associated with the angle $R_{MAX.}$ At all other times, the vectors were combined using the formula associated with the angle T_{MIN}.

The mean R:T ratio and vector scores of the resulting 'IMPROVE vectors' were calculated using an S-ICD simulator and compared to the corresponding values in the recorded vectors as described above. Vector scores >100 were defined as eligible and overall S-ICD eligibility in the cohort was calculated

6.4 Results

Full patient demographics and the results from the initial screening process for this study are provided in Chapter 3. In brief, a total of 92 participants were recruited with a mean age of 64.9 (±2.7) years. Overlay S-ICD screening revealed that 94.6% of patients had at least one passing vector. The remaining 5.4% (n=5) had no passing vector and were therefore S-ICD ineligible by virtue of their vector morphology.

6.4.1 Gradient vector

Mean R:T ratios increased significantly from 2.62 ± 0.14 in the recorded vectors, to 6.93 ± 1.9 in the generated vectors ($p<0.001$). Mean vector scores also increased significantly from 23.52 ± 1.94 in the recorded vectors to 374.86 ± 186.25 in the gradient vectors ($p<0.001$). All the gradient vectors had scores >100. Overall S-ICD eligibility was therefore 100%. A visual representation of this process is provided below. [*Figure 28*]

6.4.2 IMPROVE vector

Significant increases in R:T ratio and vector score were observed with the IMPROVE vector. The mean increase in R:T was 4.78 ± 1.82 ($p<0.01$), whilst the mean increase in vector score was 451.2 ± 310.7 ($p=0.08$). All the IMPROVE vectors had vector scores >100 and overall S-ICD eligibility was therefore 100%. R:T ratio and vector score results for each patient in the IMPROVE group are shown below. [*Figure 29, Figure 30*]

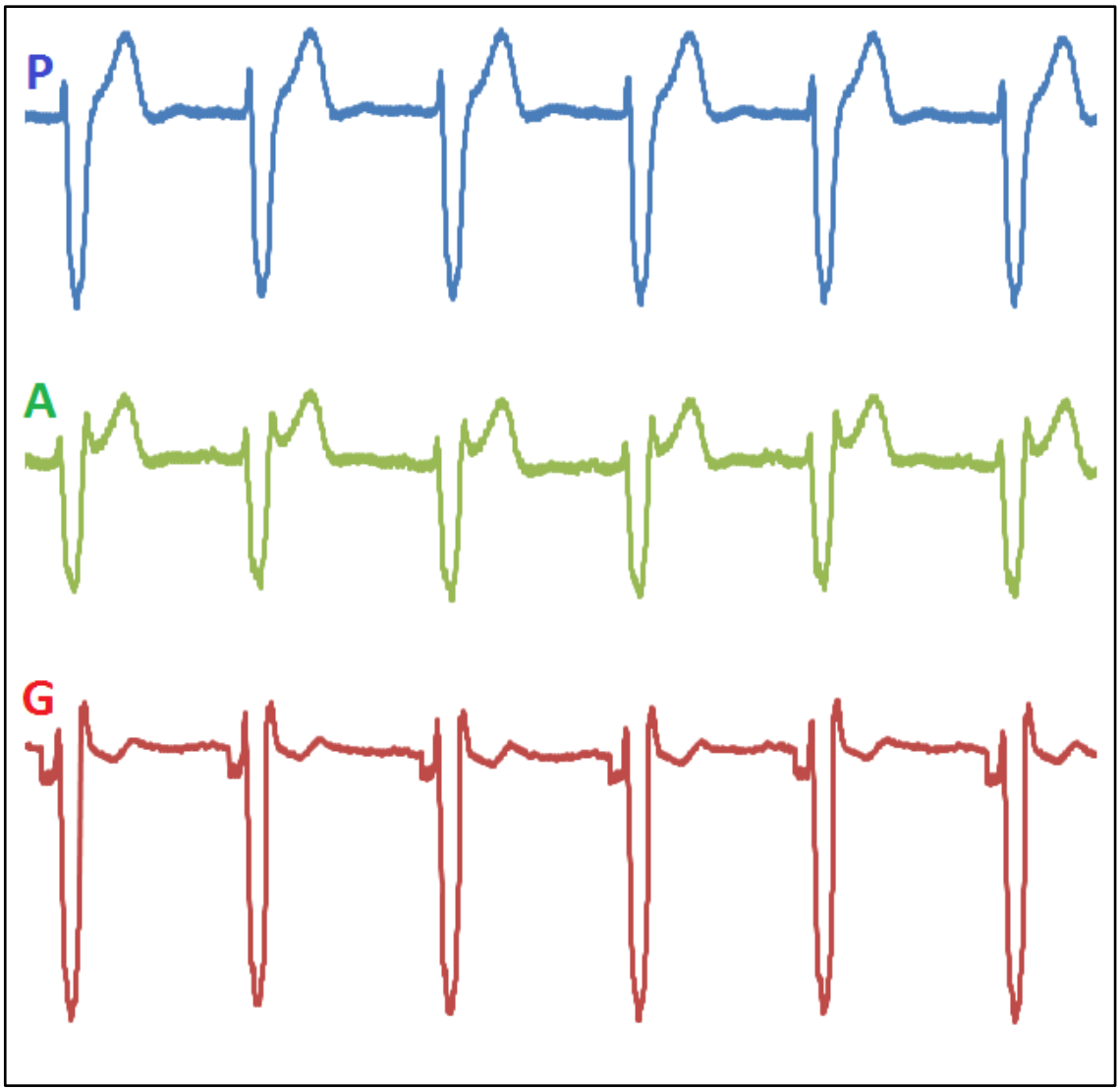

Figure 28: Gradient vector

Top (blue): an individual patient's primary vector (P). Middle (green): the alternate vector (A) of the same individual. Bottom (red): the gradient vector (G) which has a significantly larger R wave amplitude and smaller T wave amplitude than the recorded vectors. The T wave in G is biphasic, with equal amplitudes above and below the isoelectric line, suggesting the angle of observation is perpendicular to the intrinsic T wave axis.

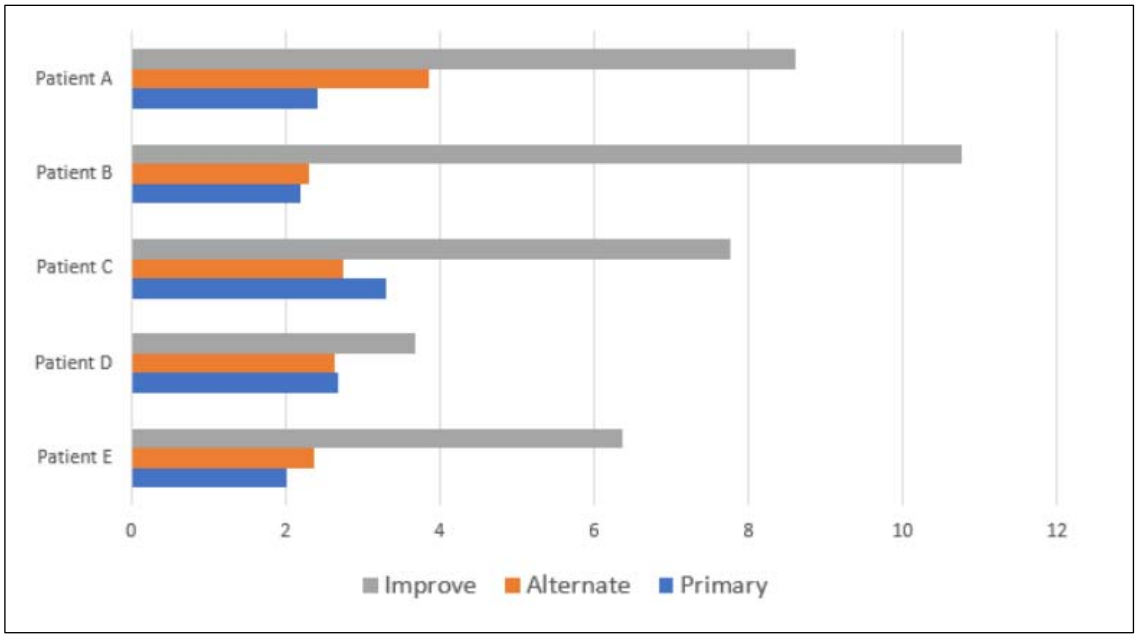

Figure 29: IMPROVE results - R:T ratio

X-axis: R:T ratio. Y-axis: for each patient (A-E) the top bar (grey) represents the IMPROVE vector. The middle bar (orange) is the recorded alternate vector, and the bottom bar (blue) is the recorded primary vector.

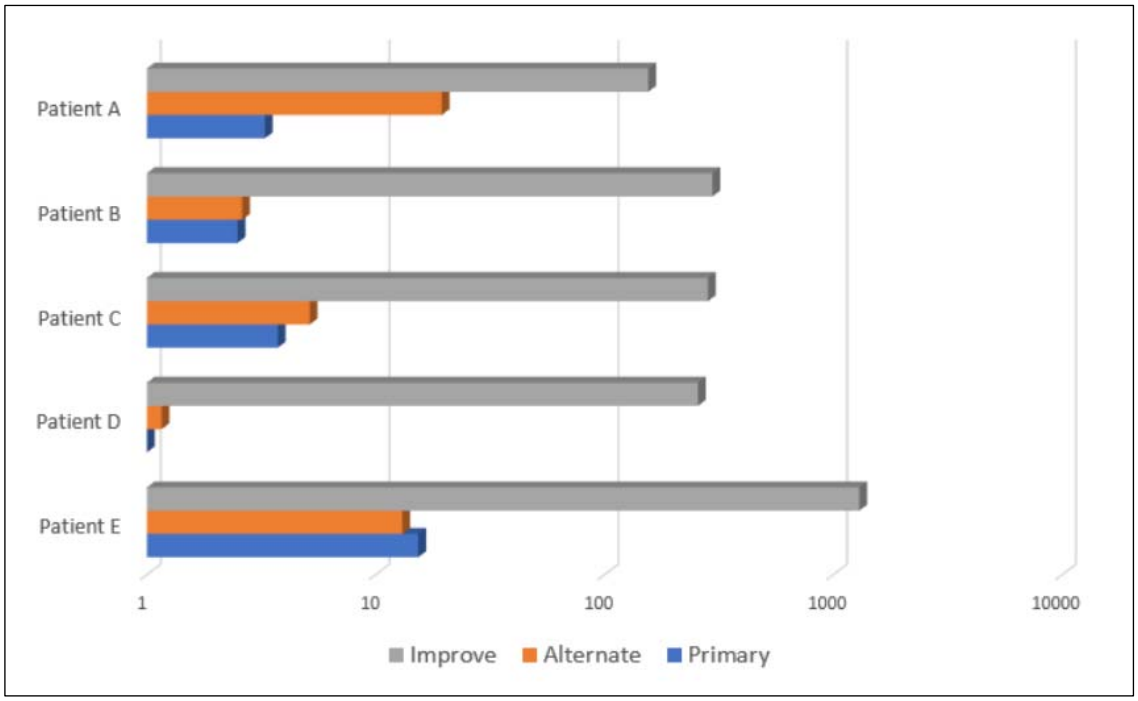

Figure 30: IMPROVE results - vector score

X-axis: vector score displayed on a logarithmic scale, with every vertical line representing a 10-fold increase. Y-axis: for each patient, the top bar (grey) represents the IMPROVE vector, whilst the middle bar (orange) is the recorded alternate vector, and the bottom bar (blue) is the recorded primary vector.

6.5 Discussion

The objective of this study was to quantify the impact of using alternating angles of vector rotation on R:T ratio, vector score and S-ICD eligibility. The study focussed on a cohort of individuals who are currently S-ICD ineligible. The objectives were met using two different filtering techniques. Significant increases in R:T ratio and vector score were observed, with universal S-ICD eligibility also demonstrated.

This study represents a significant progression from the previously described work. Firstly, the newly created vectors have been successfully analysed using an S-ICD simulator. The simulator accurately recreates the S-ICD's filtering and detection process and vector score represents a higher threshold than R:T ratio in terms of vector eligibility. Sixty seconds of new vector signal have also been assessed, rather than the signal isolated QRST complexes that were used previously. It is reassuring to know that small variations in QRS morphology and amplitudes which occur with respiration for example, have not negatively impacted on the performance of the algorithm.

This work has a number of limitations. The cohort size was small, so more testing would be required before these results could be safely extrapolated to the wider ICD population. The novel filtering systems would also require significantly more testing and development prior to clinical use. The sensitivity and specificity of both filtering techniques remains largely unknown and has never been tested in the presence of dysrhythmia or even in multiple postures.

The gradient filter would require further testing to ensure that distinguishing between high gradient and low gradient accurately separates R and T wave periods. In this study the gradient level was determined from the same data set in which the technique was subsequently evaluated. This is clearly a limited approach which may not be reproducible in other patient groups.

In the longer term combining the theory of vector rotation with a pre-existing filter might be more productive than further evaluations of the novel gradient system described. The Smart Pass algorithm for example has been extensively tested and approved for clinical use but was unavailable for this research due to concerns regarding proprietary information.

The main limitation of the IMPROVE technique is that accurate identification of the R wave period relies on the patient having a consistent ECG morphology. This is concerning as in chapter one I discussed many different factors which can alter an individual's ECG morphology. Although morphological matching to a stored template is currently successfully used by several different ICD systems. Many manufacturers have already trademarked morphology matching algorithms which help to differentiate between rhythms of ventricular and supraventricular origin. These systems operate within a margin of error, which might suggest that subtle changes in morphology could be overcome by future iterations of IMPROVE.

Given the results presented in earlier chapters, we can be confident that VF detection and SVT discrimination are likely to be equally effective at any angle of observation, for example R_{Max} or T_{Min}. The findings of the previous two chapters do not however address the possible problem of fused vectors. A fused vector, one in which the QRST morphology from two angles are inappropriately amalgamated, might introduce unexpected challenges to the sensing mechanism. Consideration should therefore be given to repeating the previously performed rhythm assessments using the IMPROVE system.

Despite the limitations of this study, I believe that the ideas presented in this chapter could have a significant impact on future S-ICD sensing. In this study, the vector rotation algorithm rapidly alternated between two chosen angles with the hope of eliminating ineligibility. This is just one possible application of the technology.

In the future, variations in angle of observation could be driven by any number of parameters which are already routinely recorded by ICD systems. For example, in patients who experience inappropriate shock therapies due to TWOS during exercise. Could the detected heart rate be used to alter the angle of observation? Perhaps a certain vector angle is beneficial at rest, but during peak exertion, T wave amplitude changes demand an alternative angle be utilised? Changes of this sort could be automated within the S-ICD system.

Alternative angles of observation could also potentially also be used in rhythm detection. Presently, in the device's conditional zone, a number of criteria are assessed to determine arrhythmia origin. It is conceivable that assessment from an alternative angle, might provide supplementary information to improve rhythm detection. I have demonstrated

already that VF, which has no clearly defined axis, looks like VF from any angle. This is not the case in normal rhythm and this distinction could potentially be explored in preventing over-sensing.

The battery life of an S-ICD is approximately 10 years, during which time morphological ECG changes can occur due to progression of the underlying cardiovascular disease. In these scenarios, patients must hope that their new ECG morphology remains compatible with at least one S-ICD vector, or an alternative ICD system will be required. They must also hope that the change is recognised before inappropriate shock therapies occur. Hypothetically, if the angle of observation of the vector could simply be changed, either at a routine follow up assessment then this problem could be averted.

A fully automated S-ICD system, using truly personalised vectors, is also a future possibility. The S-ICD programmer's automated screening tool already has the ability to detect and evaluate S-ICD vectors, calculating vector score using a series of algorithms. This software could be integrated into the S-ICD device.

ICD systems are already programmed to performed regular automated testing. For example, many TV-ICD systems can conduct daily checks of pacing threshold, allowing the device output to be automatically altered to sit just above the threshold level, conserving battery longevity whilst providing reliable pacing.

Future S-ICD systems could therefore be programmed to performed automated vector assessments, at every possible angle of observation, to continuously update the personalised vector, depending on the underlying R and T morphology at that time. This could be repeated every day, hour, or even after every detected beat. A vector with optimal morphology would always be presented for rhythm assessment. The challenges which variations in morphology present could then be eliminated, and the device recipient would benefit from a truly personalised S-ICD.

6.6 Conclusions

In S-ICD ineligible individuals, mathematical vector rotation can be used to identify the angles of observation that are associated with vectors displaying a maximal R wave amplitude and a minimal T wave amplitude. These contrasting signals can be combined

using an alternating angle of observation, driven by a filter which separates R wave and T wave signal. The resulting vectors have significantly greater R:T ratios and significantly greater vector scores. In a small cohort this has been demonstrated to result in universal device eligibility, but further testing and development would be required before clinical application.

Chapter 7 Eligible vector time

7.1 Introduction

In the preceding chapters mathematical vector rotation has been applied in S-ICD ineligible individuals, with vector manipulation resulting in increased S-ICD eligibility. This could be a significant clinical finding for the 5% of potential S-ICD recipients who are currently ineligible to receive the device. The role of mathematical vector rotation in the remaining 95% is less clear.

One might expect that the principles of vector rotation could be used to 'improve' any individual's vector morphology. Hypothetically, converting a passing vector with a score of 120 into a passing vector with a score of 1200. But would this 'better' vector, with its greater R:T ratio, result in less incidents of TWOS or less inappropriate shock therapies? Does the S-ICD function more effectively or with greater safety, in patients with higher vector scores?

Answering these questions is difficult. TWOS often occurs at random, in recipients with normally functioning devices and no previous sensing concerns. The relationship between vector score and clinical outcomes have also never been addressed. To date, the only clinical application of vector scores has been in S-ICD screening. Morphological vector assessments have retained a binary outcome and the score has not routinely been reported to the patient or clinician. The vector score, at a single point in time, has been used to determine eligibility alone.

In chapter one, I described at length how variations in R and T wave amplitude occur in all individuals. The impact this has on vector morphology, from the perspective of an S-ICD, is unclear. It is generally accepted that all vectors will display variations in morphology but are these variations important? Do 'passing vectors' for example, ever become 'failing' vectors? Post implantation, if there are time periods during which vectors are ineligible, do these relate chronologically to episodes of TWOS or shock therapies?

In this chapter, I will begin to investigate these questions. If vector eligibility is not binary but shows significant variability, then perhaps the degree to which the vectors vary will be associated with known risk factors for TWOS. Demonstrating significant variability in vector

score might be the first step towards proving that optimisation of vector morphology can reduce adverse event rates. This could significantly increase the potential clinical benefits of vector rotation.

For the purposes of this study I shall define a new concept; 'eligible vector time' (EVT). A series of vector scores will be calculated at regular intervals across a pre-determined time period and EVT will be the percentage of vector scores that are greater than 100. An EVT of 100% would equate to a vector that remains eligible, whilst an EVT of 0% would equate to a vector that is ineligible throughout the recording period. A correlation between risk factors for TWOS and EVT would also suggest a possible relationship between EVT and TWOS. Mean vector score across the recording period will also be calculated , which may or may not relate to EVT.

7.2 Objectives

- Describe a reproducible method for calculating EVT and mean vector score using ambulatory ECG recordings.
- Calculate the correlations between EVT and QRS duration, and between EVT and pTc, in a cohort of ICD patients who pass standard S-ICD screening in at least one vector.
- Calculate the overall correlation between mean vector score and EVT.

7.3 Method

A prospective observational study was performed between July 2016 and March 2017 for which ethical approval (reference 16/LO/0534) was obtained from the London (Brent) REC and the HRA. The study was sponsored by the Department of Research and Development at UHS. All study participants gave informed written consent prior to study enrolment.

Adult patients with implanted ICD systems (either TV-ICD or S-ICD) were recruited at the time of a routine device follow up. Patients were excluded if device interrogation revealed a ventricular pacing percentage of >1% as intermittent ventricular pacing would result in variable vector morphology during the ambulatory recordings.

All study participants underwent standardised S-ICD screening in line with the pre-implant S-ICD screening guidelines provided by the manufacturer.[55] ECG recordings were undertaken in both standing and supine positions at amplitudes of 5mm/mV, 10mm/mV and 20mm/mV. The resulting ECG morphologies were assessed against the manufacturer's screening tool by a cardiologist or cardiac physiologist trained in S-ICD template screening. Individual vectors were suitable if the vector passed screening in both postures.

All participants also underwent a 12 lead ECG as per the British Cardiovascular Society (BCS) Clinical Guideline for performing a standard 12 lead ECG.[122] The ECGs were electronically scanned and magnified to 500%, with digital callipers used to calculate the QRS interval, RR interval and the pT, from three consecutive complexes. Mean values for each of these parameters were then calculated with heart rate correction performed where necessary.

Patients with no eligible vector were excluded from further involvement in the study. The remaining participants were placed into quartiles based upon their QRS duration and pTc. Sample patients from each of the following three groups were then invited to undergo a 24-hour ambulatory ECG.

- Group 1: Patients in the top quartile for QRS duration.
- Group 2: Patients in the top quartile for pTc.
- Group 3: Patients in the third or fourth quartile for both QRS duration and pTc (control group).

24-hour ambulatory ECGs were performed using a five-lead two channel digital Holter recorder (Model AFT-1000, Holter Supplies, Paris) which was positioned to simultaneously capture the patient's primary and alternate vectors. [*Figure 21]*

The recordings were downloaded in ISHNE (International Society for Holter and Non-invasive Electrocardiology) format and the secondary vector generated from the recorded primary and alternate vector data. All three vectors were analysed using an S-ICD simulator with vector score calculations performed every minute, using 6 automatically identified QRST complexes in each minute period. In passing vectors, the mean vector score and EVT were calculated. The following relationships were then compared statistically; QRS duration and EVT, pTc and EVT, mean vector score and EVT.

All the participants were asked to provide some background medical information. With the patient's consent, hospital and device records were used to record the device implant indication, the participant's EF (where this value had been assessed clinically in the preceding three years) and the haemoglobin and renal function (where this had been assessed clinically in the preceding twelve months).

7.4 Results

A total of 100 patients were recruited. The mean age was 63.8 ± 2.8 years, 78% were male, 92% had TV-ICD systems and 36% had primary prevention devices. Comorbidities included ischaemic heart disease (48%), atrial dysrhythmia (37%), severe LV systolic dysfunction (30.2%) and hypertension (29%).

After S-ICD screening had been performed 5 patients were found to be S-ICD ineligible and were excluded from further involvement. From the remaining 95 patients a total of 14 underwent a 24-hour ambulatory ECG, on average 7.5 [± 1.4] months after initial screening. In total 42, 24-hour vector recordings, were presented to the S-ICD simulator for analysis. In total 21 of these 42 vectors (50%) had passed the original S-ICD screening process.

Unfortunately, two passing vectors had to be eliminated from further analysis. One patient had developed left bundle branch block between the ECG screening and the ambulatory ECG, a significant QRS change that had resulted in all his S-ICD vectors becoming ineligible. Another patient had coarse atrial fibrillation with large fibrillatory waves that significantly impaired the vector score assessment effectively rendering the patient S-ICD ineligible. This left 19 passing vectors, from 12 different patients, that were suitable for further assessment.

Detailed patient demographics for both the overall screened cohort (n=100) and the Holter group (n=14) along with a summary of results is provided below. [*Table 14, Table 15*]

As described previously, the S-ICD simulator analysis was undertaken with the support of the engineering department at Boston Scientific.

		Overall n=100		Holter group n=14	
Demographics:	Mean age [years ± 95% CI]	63.8 [± 2.8]		63.7 [± 5.2]	
	Mean time: screening to Holter [months ± 95% CI]	n/a		7.5 [± 1.4]	
	Male	78	78.0%	10	71.4%
Device:	Mean time since implant [months ± 95% CI]	73.6 [± 9.9]		75.1 [± 20.7]	
	Primary Prevention	36	36.0%	4	14.0%
	Secondary prevention	64	64.0%	10	71.4%
	Transvenous ICD	92	92.0%	13	92.9%
	Subcutaneous ICD	8	8.0%	1	7.1%
Co-morbidities:	Ischaemic heart disease	48	48.0%	6	42.9%
	Previous atrial fibrillation or atrial flutter	37	37.0%	3	23.1%
	Severe LV systolic dysfunction (n=96, n=14)	29	30.2%	4	28.6%
	Hypertension	29	29.0%	3	23.1%
	eGFR < 60 ml/min/1.73m^2 (n=80, n=10)	19	23.8%	1	10.0%
	Diabetes	14	14.0%	2	14.3%
	Valve disease (>mild) or valve surgery (n=96, n=14)	13	13.5%	2	14.3%
	Airways disease	13	13.0%	3	23.1%
	Previous coronary artery bypass graft (CABG)	12	12.0%	2	14.3%
	Haemoglobin < 120 g/dL (n=79, n=11)	5	6.3%	1	9.1%
	Cerebrovascular disease	6	6.0%	1	7.1%
	Peripheral vascular disease	6	6.0%	1	7.1%
	eGFR < 30 ml/min/1.73m^2 (n=80, n=10)	3	3.8%	1	10.0%

Table 14: Eligible vector time demographics

Where haematology or biochemistry results were unavailable, or where an assessment of EF had not been performed during the required time period an alternative value is given for 'n' is given.

Patient	QRS (ms)	pTc (ms)	Vector	Mean vector score (± 95% CI)	EVT (%)
6	107	304	Primary	385.0 (± 4.0)	99.7
			Secondary	306.5 (± 5.4)	96.9
22	100	419	Secondary	358.7 (± 6.7)	96.2
33	103	275	Primary	807.5 (± 27.4)	80.6
			Secondary	930.3 (± 23.7)	84.3
37	185	403	Primary	120.0 (± 9.5)	47.2
			Secondary	208.5 (± 11.6)	69.9
45	97	369	Primary	536.6 (± 14.9)	100.0
49	119	371	Primary	201.0 (± 15.4)	42.7
68	127	376	Primary	386.1 (± 11.5)	73.0
			Secondary	571.1 (± 9.6)	94.8
70	100	252	Primary	1046.8 (± 13.8)	99.4
74	88	324	Alternate	989.1 (± 12.0)	100.0
			Primary	453.7 (± 12.3)	97.0
81	151	483	Primary	314.1 (± 13.8)	69.7
			Secondary	137.2 (± 6.8)	55.7
85	144	281	Primary	1161.9 (± 11.2)	99.9
			Secondary	366.0 (± 10.5)	84.0
96	160	433	Primary	247.3 (± 15.2)	60.7

Table 15: STEP summary of results

In all of the vectors the lower 95% confidence interval of the calculated mean vector score was found to be greater than the S-ICD eligibility threshold of 100. A significant variation in EVT was however observed. Only 2/19 vectors (10.5%) had an EVT of 100%, whilst 6/19 (31.6%) had an EVT >95%. Remarkably, in 2 vectors (10.5%) the EVT was <50%, meaning that during the recording period these vectors were ineligible for a greater time period than they were eligible.

A pictorial representation of the variation in vector score is provided below. [*Figure 31*]

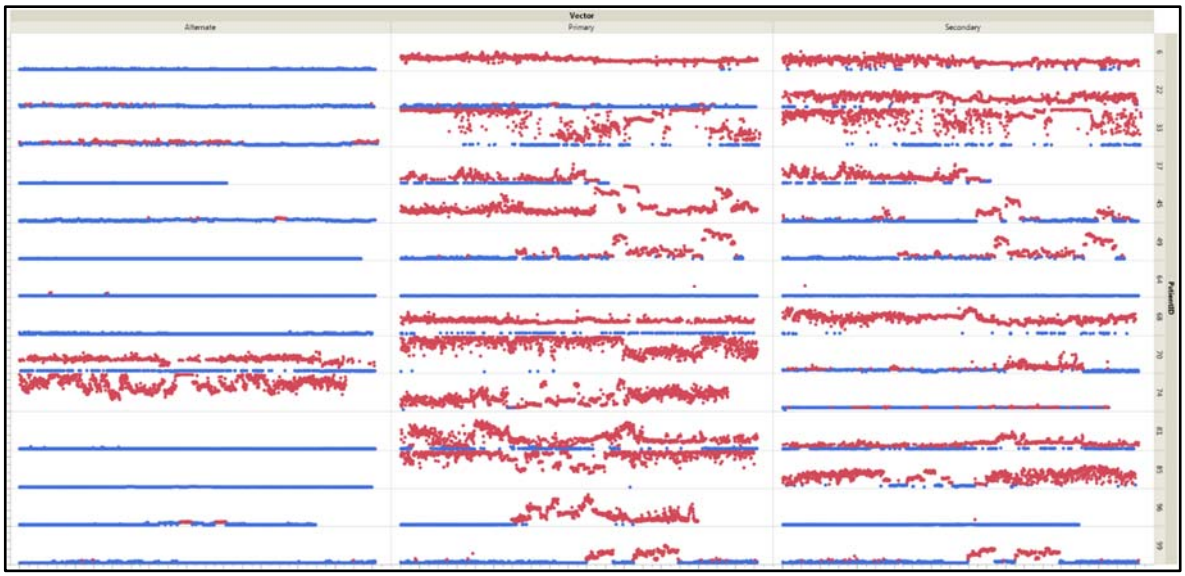

Figure 31: Minute by minute vector score

Vector score results across the entire recording period are shown for all patients and in all vectors (left column = alternate vector, middle column = primary vector, right column = secondary vector). Each cell contains a graph of vector score (y axis, scale 0-1200) against time (x axis, scale 0-24 hours). Red dots indicate a vector score > 100 (eligible) and blue dots represent a vector score <100 (ineligible). Variations in vector eligibility are observed throughout the recording periods. Vector eligibility appears to be lower overall in the alternate vector. In some patients (i.e. 49) there is an obvious visual correlation between the variations in vector score in the primary and secondary vectors, but this is not universally evident. Vectors which passed the initial screening process are not distinguished from those which failed in this figure.

In vectors with a high EVT, there are intermittent recordings of low vector score which appear to occur throughout the day, with no obvious pattern to these events. In vectors with a low overall EVT, rapid changes in vector score can be observed, with large minute to minute variations observed.

A statistically significant negative correlation was identified between QRS duration and EVT, with longer QRS durations associated with lower EVT percentages (Pearson correlation -0.60, p=0.007). [*Figure 32*] A trend towards negative correlation between pTc and EVT was also observed, but this did not reach statistical significance using the pre-determined alpha value of 0.05 (Pearson correlation -0.44, p=0.062). [*Figure 32*]

A trend towards positive correlation between mean vector score and EVT was observed, but this also failed to reach statistical significance (Pearson correlation 0.58, p=0.09). [*Figure 33*] In these statistical calculations EVT, which has not previously been described, was assumed to approximate normal distribution.

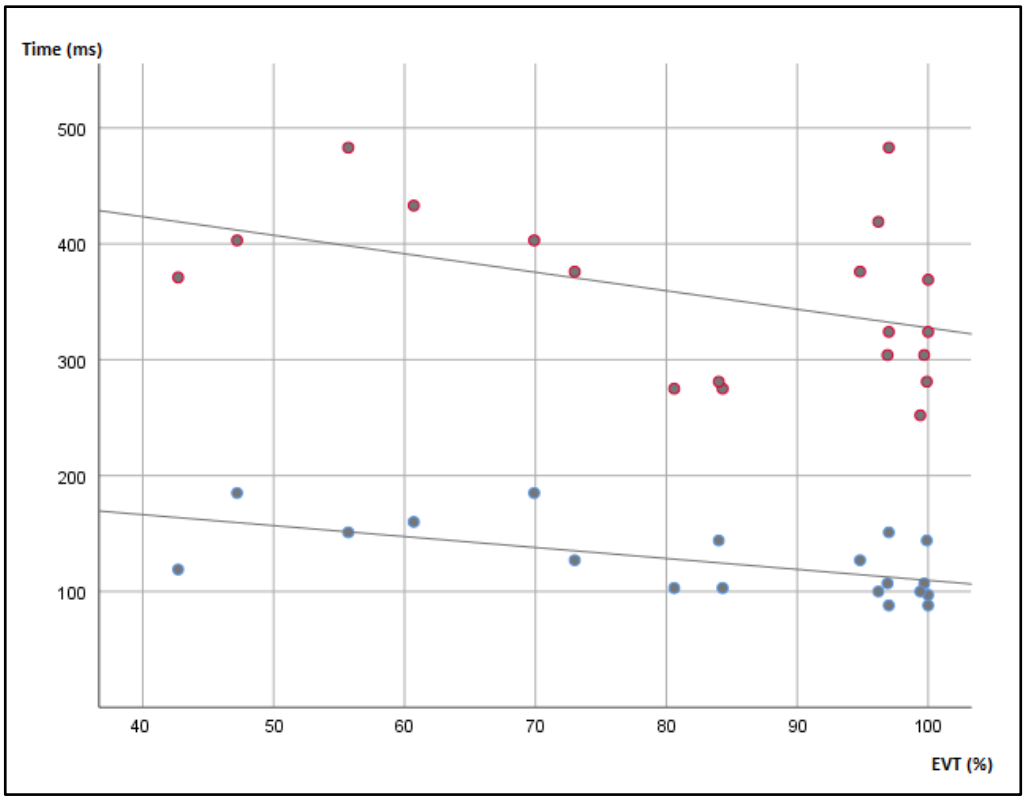

Figure 32: EVT versus QRS and pTc

Red dots (top line) = pTc versus EVT, Pearson correlation -0.44 (p=0.062)

Blue dots (bottom line) = QRS versus EVT, Pearson correlation -0.60 (p=0.007)

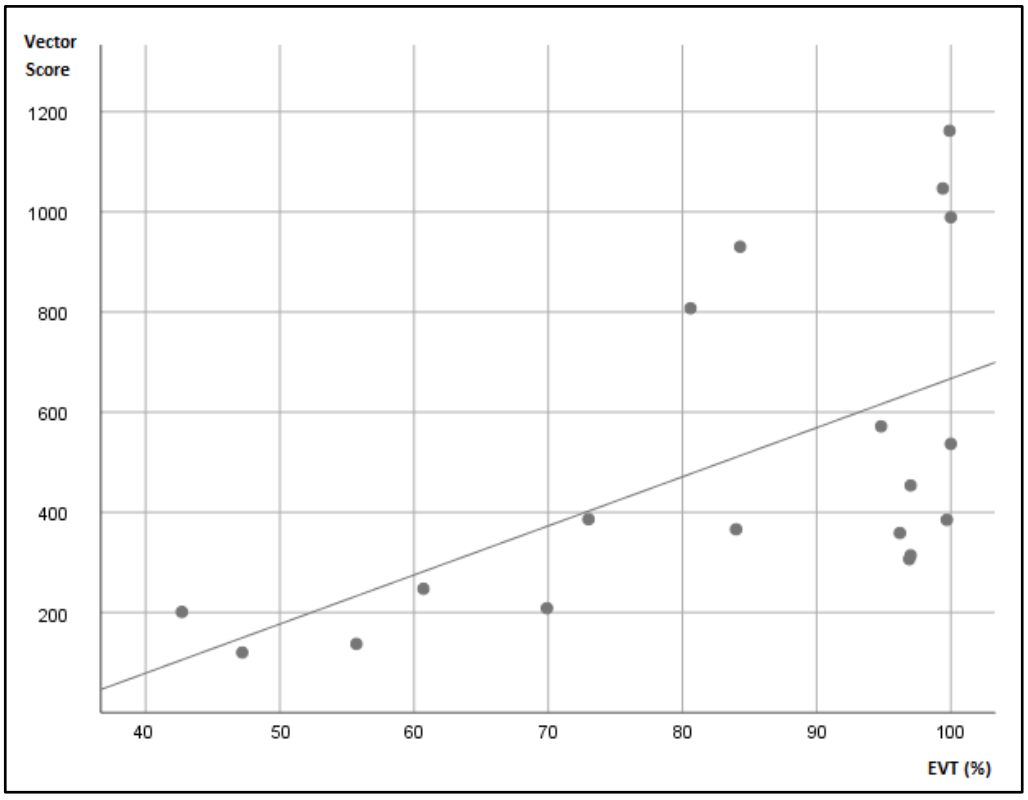

Figure 33: EVT versus vector score

Pearson correlation = 0.58 (p=0.09)

7.5 Discussion

In these studies, I have demonstrated for the first time, that vector scores are not consistent. They vary significantly, even over relatively short periods of ambulatory recording. The consequence is that many vectors fluctuate between 'passing' and 'failing', with variations in vector score frequently crossing the eligibility threshold of 100. This is highly significantly when one considers the role of S-ICD screening, which is performed at a single point in time.

The observed variations in vector score were negatively correlated with QRS duration, a baseline ECG parameter that has previously been identified as conveying risk of TWOS. This finding should therefore justify further research into the relationship between vector score and TWOS events. The potential clinical benefits of optimising a vector score, for example by mathematical vector rotation, also warrant investigation.

This study was conducted as a pilot study, to determine the feasibility of assessing EVT using an S-ICD simulator. Study numbers were therefore small. A significant relationship between pTc and EVT was not identified, although a trend to negative causation was identified. This should be investigated further in a larger cohort study, along with other baseline ECG parameter and clinical features which have been shown to predict inappropriate shock therapies.

A limitation of this study is that both ECG parameters were calculated from a single screening visit, with Holter monitoring then undertaken approximately seven months later. The ECG parameters were also measured using the longest QRS and pTc observed on a single 12 lead ECG, rather than measured in each unique vector. I am aware that both of these ECG parameters can display variations and that this method might therefore introduce inaccuracy. However, in the earlier studies that identified these parameters as risk factors for TWOS, the same technique was used. ECG parameters were identified from a single pre-implant ECG, with episodes of inappropriate shock therapy due to TWOS occurring many months later.

A further limitation of this study is that the influence of signal artefact on the Holter recordings is unclear. The ambulatory nature of recordings, taken over a 24-hour period, means that a degree of signal artefact is inevitable. The S-ICD simulator does integrate a

series of filters that endeavour to remove possible artefact prior to analysis. However, in the future a visual analysis of some of the low vector score events might be useful in developing a greater understanding of what mechanism is driving the low score. This additional analysis would also provide an understanding of whether the low scores are cause primarily by low overall amplitude, variations in R:T ratio or dysrhythmic events such as ventricular bigeminy or frequent ventricular ectopics.

Due to the volume of data analysed (approximately one billion data points) automated vector analysis using the S-ICD simulator had to be employed in this study. A visual assessment of every recorded vector score was felt to be unfeasible. This was also a pilot study, in which EVT was assessed and calculated for the first time. In future work a visual analysis of a subset of low vector scores will be considered to support he overall findings.

The results of this study have wide ranging implications for the S-ICD. Firstly, they question the current role of vector screening at a single point in time. Justifying implantation decisions on the basis of a single assessment of morphology seems arbitrary when the overall degree of variation in eligibility is considered. Secondly it challenges our understanding of TWOS events, which may well be a consequence of sudden falls in vector score, given their newly discovered prevalence and their possible correlation to ECG parameters which predict TWOS.

7.6 Conclusion

In an ICD population, vector scores can vary significantly over a 24-hour period, impacting S-ICD eligibility. The degree of variability can be assessed using EVT, a measure of percentage time with an eligible vector.

EVT is negatively correlated with QRS duration, an ECG parameter previously identified as a risk factors for TWOS. Low EVT values may therefore be associated with TWOS which would suggest a clinical benefit to vector score optimisation in patients with eligible S-ICD vectors. Further research in this area is justified.

Chapter 8 Haemodialysis

8.1 Introduction

In chapter 1, the concept of 'special patient groups' were introduced. These are cohorts of patients who challenge the sensing mechanism of the S-ICD by virtue of their dynamically changing ECG morphologies. One example was patients undergoing haemodialysis, in whom both the potential benefits and challenges of S-ICD therapy were discussed in detail. [*Section 1.9.4*]

In chapter 7, the concept of EVT was explored for the first time. Significant changes in vector score were found to be common in the general ICD population, with the majority of passing vectors become failing vectors for short periods during a 24-hour period.

An assessment of EVT has never been undertaken in a group of patients undergoing haemodialysis. Understanding how vector eligibility varies for patients on haemodialysis might support the future role of vector modification, for example by mathematical rotation, in this unique cohort. It may also provide further insight into how haemodialysis patients should be screened for S-ICD suitability.

8.2 Objectives

- Compare the vector eligibility status of haemodialysis patients at the start of a haemodialysis session with their vector eligibility at the end of a session.
- Calculate EVT across a single session of haemodialysis in a cohort of patients undergoing dialysis therapy and compare this to EVT values of the ICD patients from Chapter 7.
- Calculate the overall correlation between mean vector score and EVT for haemodialysis patients.
- Determine whether dialysis volume is correlated to EVT.

8.3 Method

Haemodialysis Associated Changes in R:T Ratio and T Wave Morphology (Heart-Two study) was a prospective multi-site observational study performed between April 2018 and June 2018. Ethical approval (reference 17/SC/0623) was obtained from the South Central (Oxford A) REC and the HRA. The study was sponsored by the Department of Research and Development at UHS. Patients from both UHS and Portsmouth Hospitals NHS Foundation Trust were eligible for recruitment, although all the patients were ultimately recruited from the latter institution.

All study participants gave informed written consent prior to study enrolment. Adult patients undergoing haemodialysis were approached for involvement in the study. Patients were excluded if they had a permanent pacemaker or a TV-ICD with a ventricular pacing percentage of >1%, to avoid the problem of intermittent ventricular pacing affecting QRS morphology.

All the participants were asked to provide some background medical information. With the patient's consent, hospital records were used to record the participant's EF (where this value had been assessed clinically in the preceding three years). All participants were asked to wear a five-lead two channel digital Holter recorder (Model AFT-1000, Holter Supplies, Paris) throughout a single dialysis session. The study was purely observational and did not impact the dialysis in any way. The Holter was positioned as previously described to simultaneously capture the patient's primary and alternate vectors.

The recordings were downloaded in ASCII format and the secondary vector generated from the recorded primary and alternate vectors. Recordings were then spliced to correspond to the precise start and end times of dialysis. All three vectors were analysed using an S-ICD simulator with vector score calculations performed every minute, as described in chapter 7.

Vector eligibility at the start and end of dialysis was determined using the vector score. In vectors with a passing score at the start of dialysis mean vector score and EVT were calculated. The correlation between mean vector score and EVT was determined, as was the correlation between dialysis volume and EVT. EVT values across the cohort were compared to the EVT values described in the previous chapter.

8.4 Results

In total 25 dialysis patients were recruited with a mean age of 64.3 [± 5.5] years, 68% of whom were male. In comparison to the previous EVT study cohort, there was a lower prevalence of both ischaemic heart disease (16%), LV systolic dysfunction (8%) and previous atrial dysrhythmia (8%). The patients had a variety of different underlying renal aetiologies. Mean dialysis volume was 1.63 [± 0.35] litres. More detailed patient demographics are shown below. [*Table 16*]

Total Number of Participants (unless otherwise stated)		n = 25	
Demographics:	Mean age [years ± 95% CI]	64.3 [± 5.5]	
	Male	17	68.0%
	Mean dialysis volume [litres ± 95% CI]	1.63 [± 0.35]	
Co-morbidities:	Hypertension	11	44.0%
	Diabetes	5	20.0%
	Cerebrovascular disease	4	16.0%
	Ischaemic heart disease	4	16.0%
	LV systolic dysfunction	2	8.0%
	Previous atrial fibrillation or atrial flutter	2	8.0%
	Previous cardiac surgery	1	4.0%
	Adult polycystic kidney disease	4	16.0%
	Glomerulonephritis	3	12.0%
	Bilateral small kidneys	3	12.0%
	Hypertensive nephropathy	2	8.0%
	Diabetic nephropathy	2	8.0%
	Alport's syndrome	2	8.0%

Table 16: Dialysis group demographics

Vector recordings were successfully made in 24 patients, as one withdrew from the study prior to having the Holter device fitted. This generated 72 different vectors for analysis.

At the start of the dialysis session 47 vectors were S-ICD eligible (65.2%). By the end of dialysis, eligibility status had changed in six vectors, with 53 vectors now eligible (73.6%). All the passing vectors at the start of dialysis retained their eligibility to the end of the session.

Mean vector score was found to have a strong positive correlation with EVT (Pearson correlation 0.727, p<0.001, n=72.) [*Figure 34*] No correlation was found between dialysis volume and EVT (Pearson correlation -0.022, p=0.86)

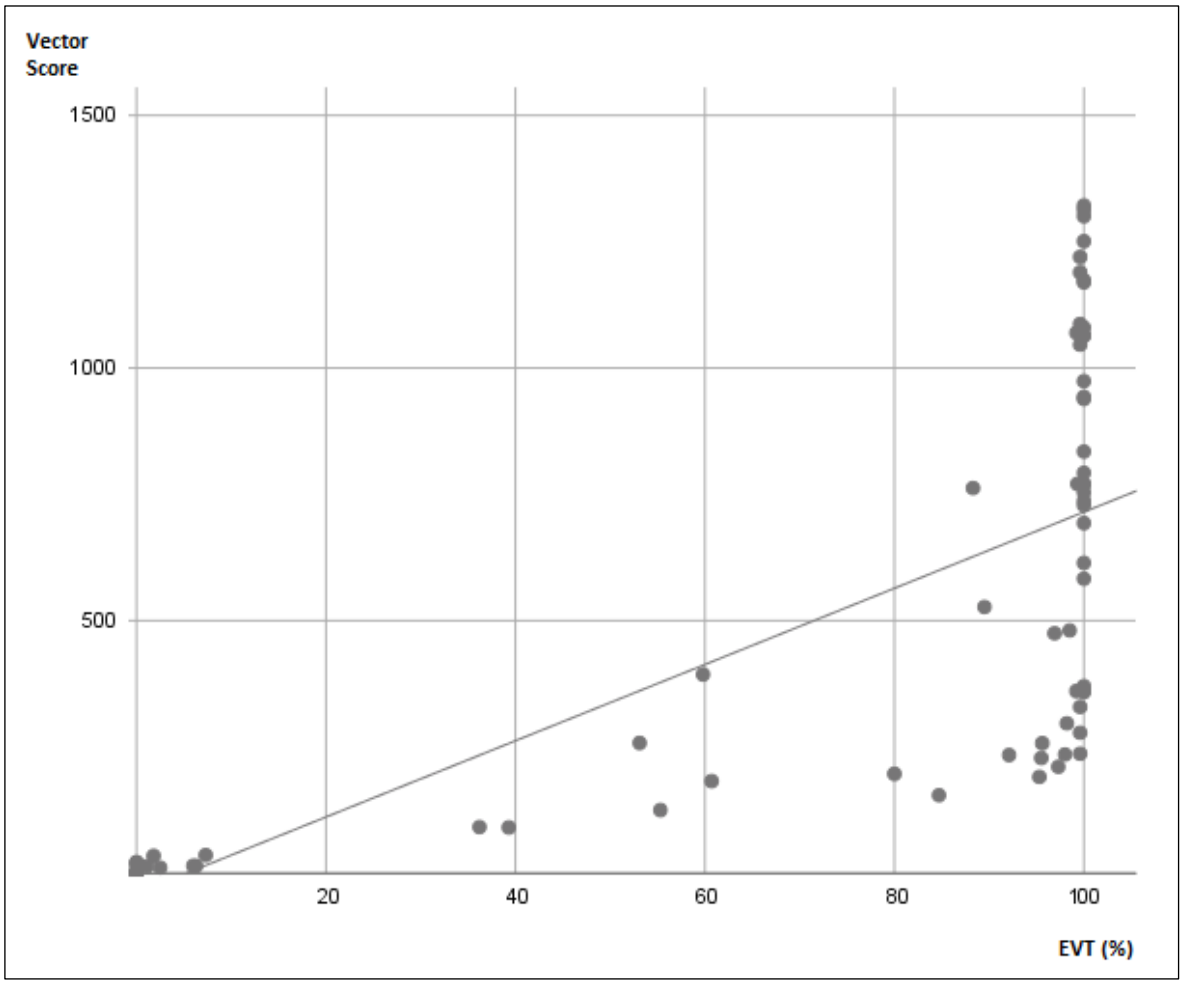

Figure 34: Haemodialysis - vector score versus EVT

In the cohort of passing vectors, 42/47 (89.3%) had an EVT >95%. This is significantly higher than the 31.6% of vectors which achieved this threshold in the previous study (p<0.0001, Chi-squared test). No passing vectors had an EVT<50%.

8.5 Discussion

The variation in vector score observed in this haemodialysis population was significantly less than in the previous ICD population. There are several factors which may explain this.

Firstly, the period of measurement was much shorter in the dialysis cohort, where the patients also remained very still throughout. By comparison in the ICD group, the patients underwent a full 24-hours of activity, which included both day and night time recordings. The vectors in the ICD group would therefore have been more exposed to greater variations in posture, heart rate, respiratory rate and autonomic activity.

The impact of haemodialysis itself may also have been missed by recording only the duration of a single session. For example, it can take several hours for dialysis to impact intracellular electrolyte levels and the resulting ECG changes may have been observed between dialysis sessions.

The underlying patient characteristics are also very likely to have impacted the EVT values in the two corresponding groups. Nobody within the haemodialysis group had an ICD and the vast majority had normal LV function. It would have been preferable to have only enrolled dialysis patients who met primary or secondary prevention guidelines for an ICD as the results could then have been more easily extrapolated to the question of S-ICD safety in dialysis. Unfortunately, the limited available of these unique patients prevented this work from being feasible.

8.6 Conclusion

Patients undergoing haemodialysis, who themselves are not ICD candidates, appear to have higher EVT values than ICD recipients. Less variation in vector eligibility is observed in this cohort and S-ICD screening prior to dialysis appears to be a more reliable indicator of overall eligibility than screening at the end of dialysis.

Chapter 9 Conclusions

9.1 Summary of findings

ECG obtained from surface locations that overlie the anatomical position of the S-ICD sensing components is highly correlated to the corresponding vectors of an implanted S-ICD. Surface ECG is therefore an appropriate surrogate of vector morphology in research and device screening. Additionally, modelling the S-ICD vectors as a right-angled triangle in the two-dimensional frontal plane is a reliable research technique. [*Chapter 2*]

Mathematical vector rotation is a novel technique whereby the angle of observation of an S-ICD vector is manipulated mathematically, using data recorded by the pre-existing S-ICD sensing mechanism. In S-ICD ineligible patients, who make up approximately 5% of all potential ICD recipients, mathematical vector rotation can be used to generate a personalised vector, with a significantly higher R:T ratios than their recorded S-ICD vectors. [*Chapter 3*]

The use of mathematical vector rotation does not affect the VF detection efficacy of the S-ICD system. High VF sensitivity levels are demonstrated across a wide range of rotated vectors. Rotation is also not associated with a significant increase in time to detection compared to standard vectors. [*Chapter 4*]

Mathematical vector rotation does not affect the SVT discrimination properties of the S-ICD system. The sensitivity of SVT detection is high across a wide range of rotated vectors, with no significant difference when compared to standard vectors. [*Chapter 5*]

In S-ICD ineligible individuals, mathematical vector rotation can be used to identify the angles of observation that are associated with vectors displaying a maximal R wave amplitude and a minimal T wave amplitude. These contrasting signals can be combined using an alternating angle of observation technique, driven by either a gradient filter or a morphological filter. The resulting vector has a significantly greater R:T ratio and a significantly greater vector score than the recorded vectors in that individual. This has been demonstrated to result in universal device eligibility in a small cohort. [*Chapter 6*]

In an ICD population, vector scores vary significantly over a 24-hour period, impacting an individual's S-ICD eligibility status. The degree of variability can be assessed using EVT, which is negatively correlated to QRS duration. Low EVT values may be associated with T wave over-sensing which would suggest a clinical benefit to vector score optimisation in eligible vectors as well as ineligible vectors. [*Chapter 7*]

Patients undergoing haemodialysis, who themselves are not ICD candidates, appear to have higher EVT values than ICD recipients. S-ICD screening prior to dialysis appears to be a more reliable indicator of overall eligibility than screening performed at the end of dialysis. [*Chapter 8*]

9.2 Overall limitations

In each of the preceding chapters, the limitations that are relevant to each individual study have been described. However, with regards to the overall project, two further limitations are worthy of discussion.

Firstly, one must concede that converting this mathematical theory into programming would be a significant undertaking. The application of a new sensing mechanism would undoubtedly require numerous bedside tests, conducted in collaboration with the device manufacturer. Post implementation a large clinical trial would also be required to ensure the safety and efficacy of the new sensing mechanism.

Secondly, it is important to recognise that the current S-ICD system is only able to record a single vector at any one time. Mathematical vector rotation, whereby two simultaneous vectors are combined would therefore require significant modification to the current S-ICD hardware. This would potentially impact the size, memory and battery capabilities of the current system.

The benefits of mathematical rotation that have been demonstrated, might be outweighed, if they mandate a significant reduction in battery life. Patients, clinicians and commissioners would be unlikely to accept an S-ICD which required significantly more frequent pulse generator changes, even with the benefits of increased eligibility or decreased inappropriate therapies.

9.3 Proposed further work

9.3.1 S-ICD ineligible vectors

The principles of personalised vector formation clearly needs to be tested in a significantly larger cohort of patients. This would likely require a multisite study, due to relatively low prevalence of ineligibility in the ICD population. Fortunately, the introduction of the automated screening process into routine clinical process, would make this eminently achievable. All patients who fail screening now have an electronic record of their vector morphology created during the screening process. Obtaining this data, with patient consent, would allow the creation of a large cohort of S-ICD ineligible patients in a short period of time, each of whom could undergo personalised vector rotation and a further assessment of eligibility.

The sensitivity and specificities of both the gradient filter and the morphological filter also need to be explored in a larger cohort and tested in the presence of dysrhythmia. This would not necessarily require vector surrogate ECG, as the principles of defining R and T wave period could be tested on any ECG signal. It should therefore be possible to test both filters against a large cohort of both dysrhythmia and normal rhythm. Alternatively, permission could be sought to combine the pre-existing Smart Pass algorithm with the concept of vector rotation.

The impact of rotation on VF detection and SVT discrimination have been adequately assessed, where a single angle of rotation is used. For completeness, these rhythm episodes should also be tested against an alternating angle vector such as that generated by the IMPROVE algorithm. Monomorphic ventricular tachycardia should also be assessed in the future. To achieve this the methods described in this thesis could be easily applied to patients undergoing VT ablation procedures, where VT is routinely induced in the electrophysiology laboratory.

9.3.2 S-ICD eligible vectors

Within this thesis I have demonstrated that some eligible vectors do in fact exhibit variable eligibility, with significant fluctuations in their vector score over short periods of time.

Further research in this area is warranted, specifically with regards the possible link between vector score variability and inappropriate shock therapy.

The challenge, from a practical perspective, would be the low frequency of inappropriate shock events that occur per year in a cohort of S-ICD recipients. A prospective study would therefore require a large cohort and a follow up period of several years. A retrospective study may however be achievable, in which the EVT of patients who have experienced inappropriate shock therapy due to over sensing are compared to a control group.

Investigating the possible link between vector score and inappropriate shock therapy would certainly be achievable given the introduction of routine automated screening. This ensures that all S-ICD recipients have their vector score recorded prior to implant, with electronic recordings of their three vectors also stored during the screening process.

The ultimate research goal would be a direct comparison between the incidence of inappropriate shock therapies in recorded vectors and personalised vectors. I firmly believe that mathematical vector rotation can improve an S-ICD recipient's vector morphology, increase both their vector score and their EVT, and that this should result in fewer inappropriate shock therapies. However, until this theory is transcribed into programming, it is difficult to obtain the necessary data to prove this hypothesis and future work is therefore required.

9.4 Summary

Mathematical vector rotation can be used to generate a truly personalised sensing vector, with an optimal R:T ratio and maximal vector score for that individual. This can be achieved using data recorded from the current S-ICD configuration.

The introduction of mathematical vector rotation into S-ICD sensing could significantly increase S-ICD eligibility, allowing a new cohort of patients access to the potential benefits of an extravascular defibrillator system. Importantly, this could be achieved without disrupting the system's excellent VF detection and SVT discrimination efficacy.

In the future, mathematical vector rotation and personalised sensing vectors may also have a role in the reduction of TWOS and inappropriate shock therapies, a common complication

of S-ICD therapy that is associated with psychological and physical morbidity and an increase in overall mortality.

The principles explored in this thesis go beyond the relatively narrow world of S-ICD sensing. The wider utility of ECG manipulation, using the concepts described, could have wide-ranging future applications in clinical diagnostics, therapeutics and monitoring.

Appendix

A.1 Publications arising from work in this thesis

- Wiles BM, Roberts PR, Allavatum V, Maharatna K, Acharyya A, Chen H, et al. The future of S-ICD sensing: 'IMPROVE' significantly increases R:T ratio and generates universal device eligibility without impairing VF detection. EP Europace 2018:20(s4):iv1

- Wiles BM, Roberts PR, Acharyya A, Allavatum V, Wilson DG, Vemishetty N, et al. Universal S-ICD eligibility: eliminating the need for pre-implant screening using mathematical vector rotation and a gradient filter. EP Europace 2018;20(s1):i175-176

- Wiles BM, Roberts PR, Acharyya A, Vemishetty N, Morgan JM. The end of pre-implant subcutaneous ICD screening? Using mathematical vector rotation to generate a personalised sensing vector resulting in universal device eligibility. EP Europace 2017;19(s1):i2

- Wiles BM, Wilson DG, Roberts PR, Allavatam V, Acharyya A, Vemishetty N, et al. Assessing the accuracy of surface ECG as a surrogate for the sensing vectors of the subcutaneous ICD. EP Europace 2017;19(s3):iii83

- Wiles BM, Wilson DG, Roberts PR, Allavatam V, Acharyya A, Vemishetty N, et al. Understanding the triangular relationship between subcutaneous ICD sensing vectors: can we accurately generate the secondary vector using just trigonometry? EP Europace 2017;19(s3):iii82

- Wiles BM, Roberts PR. Lead or be led: an update on leadless cardiac devices for general physicians. Clinical Medicine (London) 2017;17:33-36

A.2 Prizes arising from work in this thesis

- Winner, Young Investigators' Award, Heart Rhythm Congress 2018
    - The future of S-ICD sensing: 'IMPROVE' significantly increases R:T ratio and generates universal device eligibility without impairing VF detection.

- Finalist, Young Investigators' Award, Heart Rhythm Congress 2017
    - The end of pre-implant subcutaneous ICD screening? Using mathematical vector rotation to generate a personalised sensing vector resulting in universal device eligibility.

References

1. Mehra R. Global public health problem of sudden cardiac death. *J Electrocardiol* 2007;40(6 Suppl):S118-22.

2. Sharma S, Whyte G, McKenna WJ. Sudden death from cardiovascular disease in young athletes: fact or fiction? *Br J Sports Med* 1997;31(4):269-76.

3. Papadakis M, Sharma S, Cox S, et al. The magnitude of sudden cardiac death in the young: a death certificate-based review in England and Wales. *Europace* 2009;11(10):1353-8.

4. Robertus JL SM. The CRY Sudden Cardiac Death Database. 18 years of Referral for Expert Opinion. *Heart* 2015;101:A42-A43.

5. Berdowski J, Berg RA, Tijssen JG, et al. Global incidences of out-of-hospital cardiac arrest and survival rates: Systematic review of 67 prospective studies. *Resuscitation* 2010;81(11):1479-87.

6. London Ambulance Service Cardiac Arrest Annual Report 2012/13. www.londonambulance.nhs.uk, 2013. [Accessed online January 2017]

7. Perkins GD, Cooke MW. Variability in cardiac arrest survival: the NHS Ambulance Service Quality Indicators. *Emerg Med J* 2012;29(1):3-5.

8. Holmberg M, Holmberg S, Herlitz J. Incidence, duration and survival of ventricular fibrillation in out-of-hospital cardiac arrest patients in sweden. *Resuscitation* 2000;44(1):7-17.

9. Larsen MP, Eisenberg MS, Cummins RO, et al. Predicting survival from out-of-hospital cardiac arrest: a graphic model. *Ann Emerg Med* 1993;22(11):1652-8.

10. Valenzuela TD, Roe DJ, Cretin S, et al. Estimating effectiveness of cardiac arrest interventions: a logistic regression survival model. *Circulation* 1997;96(10):3308-13.

11. Mirowski M, Mower MM, Gott VL, et al. Feasibility and effectiveness of low-energy catheter defibrillation in man. *Circulation* 1973;47(1):79-85.

12. Wiles BM, Roberts PR. Lead or be led: an update on leadless cardiac devices for general physicians. *Clin Med (Lond)* 2017;17(1):33-36.

13. McAlister FA, Ezekowitz J, Hooton N, et al. Cardiac resynchronization therapy for patients with left ventricular systolic dysfunction: a systematic review. *JAMA* 2007;297(22):2502-14.

14. Antiarrhythmics versus Implantable Defibrillators I. A comparison of antiarrhythmic-drug therapy with implantable defibrillators in patients resuscitated from near-fatal ventricular arrhythmias. *N Engl J Med* 1997;337(22):1576-83.

15. Connolly SJ, Gent M, Roberts RS, et al. Canadian implantable defibrillator study (CIDS) : a randomized trial of the implantable cardioverter defibrillator against amiodarone. *Circulation* 2000;101(11):1297-302.

16. Sheldon R, Connolly S, Krahn A, et al. Identification of patients most likely to benefit from implantable cardioverter-defibrillator therapy: the Canadian Implantable Defibrillator Study. *Circulation* 2000;101(14):1660-4.

17. Kuck KH, Cappato R, Siebels J, et al. Randomized comparison of antiarrhythmic drug therapy with implantable defibrillators in patients resuscitated from cardiac arrest : the Cardiac Arrest Study Hamburg (CASH). *Circulation* 2000;102(7):748-54.

18. Connolly SJ, Hallstrom AP, Cappato R, et al. Meta-analysis of the implantable cardioverter defibrillator secondary prevention trials. AVID, CASH and CIDS studies. Antiarrhythmics vs Implantable Defibrillator study. Cardiac Arrest Study Hamburg . Canadian Implantable Defibrillator Study. *Eur Heart J* 2000;21(24):2071-8.

19. Moss AJ, Hall WJ, Cannom DS, et al. Improved survival with an implanted defibrillator in patients with coronary disease at high risk for ventricular arrhythmia. Multicenter Automatic Defibrillator Implantation Trial Investigators. *N Engl J Med* 1996;335(26):1933-40.

20. Buxton AE, Lee KL, Fisher JD, et al. A randomized study of the prevention of sudden death in patients with coronary artery disease. Multicenter Unsustained Tachycardia Trial Investigators. *N Engl J Med* 1999;341(25):1882-90.

21. Gold MR, Nisam S, Multicenter Automatic Defibrillator Implantation Trial. Multicenter Unsustained Tachycardia T. Primary prevention of sudden cardiac death with implantable cardioverter defibrillators: lessons learned from MADIT and MUSTT. *Pacing Clin Electrophysiol* 2000;23(11 Pt 2):1981-5.

22. Moss AJ, Zareba W, Hall WJ, et al. Prophylactic implantation of a defibrillator in patients with myocardial infarction and reduced ejection fraction. *N Engl J Med* 2002;346(12):877-83.

23. Bardy GH, Lee KL, Mark DB, et al. Amiodarone or an implantable cardioverter-defibrillator for congestive heart failure. *N Engl J Med* 2005;352(3):225-37.

24. Kober L, Thune JJ, Nielsen JC, et al. Defibrillator Implantation in Patients with Nonischemic Systolic Heart Failure. *N Engl J Med* 2016;375(13):1221-30.

25. Luni FK, Singh H, Khan AR, et al. Mortality Effect of ICD in Primary Prevention of Nonischemic Cardiomyopathy: A Meta-Analysis of Randomized Controlled Trials. *J Cardiovasc Electrophysiol* 2017;28(5):538-43.

26. Priori SG, Blomstrom-Lundqvist C, Mazzanti A, et al. 2015 ESC Guidelines for the management of patients with ventricular arrhythmias and the prevention of sudden cardiac death: The Task Force for the Management of Patients with Ventricular Arrhythmias and the Prevention of Sudden Cardiac Death of the European Society of Cardiology (ESC)Endorsed by: Association for European Paediatric and Congenital Cardiology (AEPC). *Europace* 2015;17(11):1601-87.

27. Sabbag A, Suleiman M, Laish-Farkash A, et al. Contemporary rates of appropriate shock therapy in patients who receive implantable device therapy in a real-world setting: From the Israeli ICD Registry. *Heart Rhythm* 2015;12(12):2426-33.

28. Kirkfeldt RE, Johansen JB, Nohr EA, et al. Complications after cardiac implantable electronic device implantations: an analysis of a complete, nationwide cohort in Denmark. *Eur Heart J* 2014;35(18):1186-94.

29. Maisel WH. Transvenous implantable cardioverter-defibrillator leads: the weakest link. *Circulation* 2007;115(19):2461-3.

30. Kleemann T, Becker T, Doenges K, et al. Annual rate of transvenous defibrillation lead defects in implantable cardioverter-defibrillators over a period of >10 years. *Circulation* 2007;115(19):2474-80.

31. van der Heijden AC, Borleffs CJ, Buiten MS, et al. The clinical course of patients with implantable cardioverter-defibrillators: Extended experience on clinical outcome, device replacements, and device-related complications. *Heart Rhythm* 2015;12(6):1169-76.

32. Kusumoto FM, Schoenfeld MH, Wilkoff BL, et al. 2017 HRS expert consensus statement on cardiovascular implantable electronic device lead management and extraction. *Heart Rhythm* 2017;14(12):e503-51.

33. Bongiorni MG, Kennergren C, Butter C, et al. The European Lead Extraction ConTRolled (ELECTRa) study: a European Heart Rhythm Association (EHRA) Registry of Transvenous Lead Extraction Outcomes. *Eur Heart J* 2017;38(40):2995-3005.

34. Sears SF, Jr., Todaro JF, Lewis TS, et al. Examining the psychosocial impact of implantable cardioverter defibrillators: a literature review. *Clin Cardiol* 1999;22(7):481-9.

35. Sears SF, Jr., Conti JB. Quality of life and psychological functioning of icd patients. *Heart* 2002;87(5):488-93.

36. Herrmann C, von zur Muhen F, Schaumann A, et al. Standardized assessment of psychological well-being and quality-of-life in patients with implanted defibrillators. *Pacing Clin Electrophysiol* 1997;20(1 Pt 1):95-103.

37. Suzuki T, Shiga T, Kuwahara K, et al. Prevalence and persistence of depression in patients with implantable cardioverter defibrillator: a 2-year longitudinal study. *Pacing Clin Electrophysiol* 2010;33(12):1455-61.

38. Van den Broek KC, Nyklicek I, Van der Voort PH, et al. Shocks, personality, and anxiety in patients with an implantable defibrillator. *Pacing Clin Electrophysiol* 2008;31(7):850-7.

39. Ladwig KH, Schoefinius A, Dammann G, et al. Long-acting psychotraumatic properties of a cardiac arrest experience. *Am J Psychiatry* 1999;156(6):912-9.

40. von Kanel R, Baumert J, Kolb C, et al. Chronic posttraumatic stress and its predictors in patients living with an implantable cardioverter defibrillator. *J Affect Disord* 2011;131(1-3):344-52.

41. *Assessing fitness to drive - a guide for medical professionals*. www.gov.uk/dvla/fitnesstodrive: Crown copyright; 2019. [Accessed online August 2017]

42. Weiss R, Knight BP, Gold MR, et al. Safety and efficacy of a totally subcutaneous implantable-cardioverter defibrillator. *Circulation* 2013;128(9):944-53.

43. Pedersen SS, Lambiase P, Boersma LV, et al. Evaluation oF FactORs ImpacTing CLinical Outcome and Cost EffectiveneSS of the S-ICD: design and rationale of the EFFORTLESS S-ICD Registry. *Pacing Clin Electrophysiol* 2012;35(5):574-9.

44. Lambiase PD, Barr C, Theuns DA, et al. Worldwide experience with a totally subcutaneous implantable defibrillator: early results from the EFFORTLESS S-ICD Registry. *Eur Heart J* 2014;35(25):1657-65.

45. Burke MC, Gold MR, Knight BP, et al. Safety and Efficacy of the Totally Subcutaneous Implantable Defibrillator: 2-Year Results From a Pooled Analysis of the IDE Study and EFFORTLESS Registry. *J Am Coll Cardiol* 2015;65(16):1605-15.

46. Boersma L, Barr C, Knops R, et al. Implant and Midterm Outcomes of the Subcutaneous Implantable Cardioverter-Defibrillator Registry: The EFFORTLESS Study. *J Am Coll Cardiol* 2017;70(7):830-41.

47. Olde Nordkamp LR, Brouwer TF, Barr C, et al. Inappropriate shocks in the subcutaneous ICD: Incidence, predictors and management. *Int J Cardiol* 2015;195:126-33.

48. Olde Nordkamp LR, Knops RE, Bardy GH, et al. Rationale and design of the PRAETORIAN trial: a Prospective, RAndomizEd comparison of subcuTaneOus and tRansvenous ImplANtable cardioverter-defibrillator therapy. *Am Heart J* 2012;163(5):753-60 e2.

49. Migliore F, Allocca G, Calzolari V, et al. Intermuscular Two-Incision Technique for Subcutaneous Implantable Cardioverter Defibrillator Implantation: Results from a Multicenter Registry. *Pacing Clin Electrophysiol* 2017;40(3):278-85.

50. Winter J, Siekiera M, Shin DI, et al. Intermuscular technique for implantation of the subcutaneous implantable cardioverter defibrillator: long-term performance and complications. *Europace* 2017;19(12):2036-41.

51. Quast ABE, Baalman SWE, Brouwer TF, et al. A novel tool to evaluate the implant position and predict defibrillation success of the subcutaneous implantable cardioverter-defibrillator: The PRAETORIAN score. *Heart Rhythm* 2018.

52. Ellenbogen KA, Kaszala K. *Cardiac pacing and ICDs*. 6th edition. ed. Chichester: Wiley Blackwell; 2014.

53. Wiles BM, Fitzsimmons SJ, Roberts PR. Postmortem therapy from a subcutaneous ICD: What is the mechanism? *Pacing Clin Electrophysiol* 2017;40(6):735-7.

54. Wilson D, Yue A, Roberts PR, et al. Oversensing and Shock Delivery in the S-ICD: Five Shocks Two Mechanisms. *Pacing Clin Electrophysiol* 2015;38(8):1009-13.

55. *User's Manual Emblem S-ICD, Emblem MRI S-ICD. Subcutaneous implantable cardioverter defibrillator Ref A209, A219*. http://www.bostonscientific.com/content/dam/Manuals/eu/current-rev-en/359481-001%20EMBLEM%20S-ICD_UM_en-GBR_S.pdf [Accessed online April 2017].

56. Gold MR, Theuns DA, Knight BP, et al. Head-to-head comparison of arrhythmia discrimination performance of subcutaneous and transvenous ICD arrhythmia detection algorithms: the START study. *J Cardiovasc Electrophysiol* 2012;23(4):359-66.

57. Datino T, Almendral J, Gonzalez-Torrecilla E, et al. Rate-related changes in QRS morphology in patients with fixed bundle branch block: implications for differential diagnosis of wide QRS complex tachycardia. *Eur Heart J* 2008;29(19):2351-8.

58. Guo H, Hecker S, Levy S, et al. Ventricular tachycardia with QRS configuration similar to that in sinus rhythm and a myocardial origin: differential diagnosis with bundle branch reentry. *Europace* 2001;3(2):115-23.

59. Wathen MS, DeGroot PJ, Sweeney MO, et al. Prospective randomized multicenter trial of empirical antitachycardia pacing versus shocks for spontaneous rapid ventricular tachycardia in patients with implantable cardioverter-defibrillators: Pacing Fast Ventricular Tachycardia Reduces Shock Therapies (PainFREE Rx II) trial results. *Circulation* 2004;110(17):2591-6.

60. Bellardine Black CL, Stromberg K, van Balen GP, et al. Is surface ECG a useful surrogate for subcutaneous ECG? *Pacing Clin Electrophysiol* 2010;33(2):135-45.

61. Olde Nordkamp LR, Warnaars JL, Kooiman KM, et al. Which patients are not suitable for a subcutaneous ICD: incidence and predictors of failed QRS-T-wave morphology screening. *J Cardiovasc Electrophysiol* 2014;25(5):494-9.

62. Randles DA, Hawkins NM, Shaw M, et al. How many patients fulfil the surface electrocardiogram criteria for subcutaneous implantable cardioverter-defibrillator implantation? *Europace* 2014;16(7):1015-21.

63. Zeb M, Curzen N, Veldtman G, et al. Potential eligibility of congenital heart disease patients for subcutaneous implantable cardioverter-defibrillator based on surface electrocardiogram mapping. *Europace* 2015;17(7):1059-67.

64. Garside H, Leyva F, Hudsmith L, et al. Eligibility for subcutaneous implantable cardioverter defibrillators in the adult congenital heart disease population. *Pacing Clin Electrophysiol* 2019;42(1):65-70.

65. Afzal MR, Lastinger L, Weiss R. Subcutaneous defibrillators in the adult congenital heart disease population: One size does not fit all: Comment on "Eligibility for subcutaneous implantable cardioverter defibrillators in the adult congenital heart disease population". *Pacing Clin Electrophysiol* 2019;42(1):71-2.

66. Maurizi N, Olivotto I, Olde Nordkamp LR, et al. Prevalence of subcutaneous implantable cardioverter-defibrillator candidacy based on template ECG screening in patients with hypertrophic cardiomyopathy. *Heart Rhythm* 2016;13(2):457-63.

67. Authors/Task Force m, Elliott PM, Anastasakis A, et al. 2014 ESC Guidelines on diagnosis and management of hypertrophic cardiomyopathy: the Task Force for the Diagnosis and Management of Hypertrophic Cardiomyopathy of the European Society of Cardiology (ESC). *Eur Heart J* 2014;35(39):2733-79.

68. Persson R, Earley A, Garlitski AC, et al. Adverse events following implantable cardioverter defibrillator implantation: a systematic review. *J Interv Card Electrophysiol* 2014;40(2):191-205.

69. Proietti R, Labos C, Davis M, et al. A systematic review and meta-analysis of the association between implantable cardioverter-defibrillator shocks and long-term mortality. *Can J Cardiol* 2015;31(3):270-7.

70. Poole JE, Johnson GW, Hellkamp AS, et al. Prognostic importance of defibrillator shocks in patients with heart failure. *N Engl J Med* 2008;359(10):1009-17.

71. Daubert JP, Zareba W, Cannom DS, et al. Inappropriate implantable cardioverter-defibrillator shocks in MADIT II: frequency, mechanisms, predictors, and survival impact. *J Am Coll Cardiol* 2008;51(14):1357-65.

72. van Rees JB, Borleffs CJ, de Bie MK, et al. Inappropriate implantable cardioverter-defibrillator shocks: incidence, predictors, and impact on mortality. *J Am Coll Cardiol* 2011;57(5):556-62.

73. Moss AJ, Schuger C, Beck CA, et al. Reduction in inappropriate therapy and mortality through ICD programming. *N Engl J Med* 2012;367(24):2275-83.

74. Tan VH, Wilton SB, Kuriachan V, et al. Impact of programming strategies aimed at reducing nonessential implantable cardioverter defibrillator therapies on mortality: a systematic review and meta-analysis. *Circ Arrhythm Electrophysiol* 2014;7(1):164-70.

75. Gasparini M, Proclemer A, Klersy C, et al. Effect of long-detection interval vs standard-detection interval for implantable cardioverter-defibrillators on antitachycardia pacing and shock delivery: the ADVANCE III randomized clinical trial. *JAMA* 2013;309(18):1903-11.

76. Sharma D, Sharma PS, Miller MA, et al. Position and sensing vector-related triple counting and inappropriate shocks in the subcutaneous implantable cardioverter-defibrillator system. *Heart Rhythm* 2015;12(12):2458-60.

77. Jimenez-Candil J, Hernandez J, Perdiguero P, et al. Prognostic Significance of Nonsustained Ventricular Tachycardia Episodes Occurring Early After Implantable Cardioverter-Defibrillator Implantation Among Patients With Left Ventricular Dysfunction. *Am J Cardiol* 2016;118(10):1503-10.

78. Wilson DG, Leventigiannis G, Barr C, et al. ECG predictors of T wave oversensing in subcutaneous implantable cardioverter defibrillators. *Int J Cardiol* 2016;220:27-31.

79. El-Chami MF, Harbieh B, Levy M, et al. Clinical and electrocardiographic predictors of T wave oversensing in patients with subcutaneous ICD. *J Arrhythm* 2016;32(3):181-5.

80. Emblem MRI S-ICD In Service SMART Pass Module. CRM-384027-AA: Boston Scientific Corporation or its affiliates, 2016.

81. Theuns D, Brouwer TF, Jones PW, et al. Prospective blinded evaluation of a novel sensing methodology designed to reduce inappropriate shocks by the subcutaneous implantable cardioverter-defibrillator. *Heart Rhythm* 2018;15(10):1515-22.

82. Fogoros RN. *Electrophysiologic Testing*: Blackwell Publishing Ltd.; 2006.

83. Landstrom AP, Dobrev D, Wehrens XHT. Calcium Signaling and Cardiac Arrhythmias. *Circ Res* 2017;120(12):1969-93.

84. Zipes DP, Jalife J. *Cardiac Electrophyiology: from cell to bedside*. 6th ed: Elsevier Saunders; 2014.

85. Madias JE, Bazaz R, Agarwal H, et al. Anasarca-mediated attenuation of the amplitude of electrocardiogram complexes: a description of a heretofore unrecognized phenomenon. *J Am Coll Cardiol* 2001;38(3):756-64.

86. Madias JE. QTc interval in patients with changing edematous states: implications on interpreting repeat QTc interval measurements in patients with anasarca of varying etiology and those undergoing hemodialysis. *Pacing Clin Electrophysiol* 2005;28(1):54-61.

87. Fosbol EL, Seibaek M, Brendorp B, et al. Prognostic importance of change in QRS duration over time associated with left ventricular dysfunction in patients with congestive heart failure: the DIAMOND study. *J Card Fail* 2008;14(10):850-5.

88. Al-Zaiti SS, Runco KN, Carey MG. Increased T wave complexity can indicate subclinical myocardial ischemia in asymptomatic adults. *J Electrocardiol* 2011;44(6):684-8.

89. Assanelli D, Di Castelnuovo A, Rago L, et al. T-wave axis deviation and left ventricular hypertrophy interaction in diabetes and hypertension. *J Electrocardiol* 2013;46(6):487-91.

90. Hasan MA, Abbott D, Baumert M. Relation between beat-to-beat QT interval variability and T-wave amplitude in healthy subjects. *Ann Noninvasive Electrocardiol* 2012;17(3):195-203.

91. Walker BD, Krahn AD, Klein GJ, et al. Drug induced QT prolongation: lessons from congenital and acquired long QT syndromes. *Curr Drug Targets Cardiovasc Haematol Disord* 2003;3(4):327-35.

92. Arbel Y, Birati EY, Shapira I, et al. T-wave amplitude is related to physical fitness status. *Ann Noninvasive Electrocardiol* 2012;17(3):214-8.

93. Deckers JW, Vinke RV, Vos JR, et al. Changes in the electrocardiographic response to exercise in healthy women. *Br Heart J* 1990;64(6):376-80.

94. Afzal MR, Evenson C, Badin A, et al. Role of exercise electrocardiogram to screen for T-wave oversensing after implantation of subcutaneous implantable cardioverter-defibrillator. *Heart Rhythm* 2017;14(10):1436-9.

95. Ziacchi M, Corzani A, Diemberger I, et al. Electrocardiographic Eligibility for Subcutaneous Implantable Cardioverter Defibrillator: Evaluation during Bicycle Exercise. *Heart Lung Circ* 2016;25(5):476-83.

96. Conte G, Kawabata M, de Asmundis C, et al. High rate of subcutaneous implantable cardioverter-defibrillator sensing screening failure in patients with Brugada syndrome: a comparison with other inherited primary arrhythmia syndromes. *Europace* 2018;20(7):1188-93.

97. Tachibana M, Nishii N, Morita H, et al. Exercise stress test reveals ineligibility for subcutaneous implantable cardioverter defibrillator in patients with Brugada syndrome. *J Cardiovasc Electrophysiol* 2017;28(12):1454-9.

98. Francia P, Adduci C, Palano F, et al. Eligibility for the Subcutaneous Implantable Cardioverter-Defibrillator in Patients With Hypertrophic Cardiomyopathy. *J Cardiovasc Electrophysiol* 2015;26(8):893-9.

99. United Stated Renal Data System annual data report 2013: Epidemiology of kidney disease in the United States. 2013 ed: National Institutes of Health, National Institute of Diabetes and Digestive and Kidney Disease, Bethesda, MD, USA, 2013.

100. Saravanan P, Freeman G, Davidson NC. Risk assessment for sudden cardiac death in dialysis patients: how relevant are conventional cardiac risk factors? *Int J Cardiol* 2010;144(3):431-2.

101. Pun PH, Hellkamp AS, Sanders GD, et al. Primary prevention implantable cardioverter defibrillators in end-stage kidney disease patients on dialysis: a matched cohort study. *Nephrol Dial Transplant* 2015;30(5):829-35.

102. Epstein AE, DiMarco JP, Ellenbogen KA, et al. 2012 ACCF/AHA/HRS focused update incorporated into the ACCF/AHA/HRS 2008 guidelines for device-based therapy of cardiac rhythm abnormalities: a report of the American College of Cardiology Foundation/American Heart Association Task Force on Practice Guidelines and the Heart Rhythm Society. *Circulation* 2013;127(3):e283-352.

103. Bogdan S, Nof E, Eisen A, et al. Clinical Outcomes in Patients with Severe Renal Dysfunction Including Dialysis Following Defibrillator Implantation. *Am J Nephrol* 2015;42(4):295-304.

104. Guha A, Maddox WR, Colombo R, et al. Cardiac implantable electronic device infection in patients with end-stage renal disease. *Heart Rhythm* 2015;12(12):2395-401.

105. Greenspon AJ, Patel JD, Lau E, et al. 16-year trends in the infection burden for pacemakers and implantable cardioverter-defibrillators in the United States 1993 to 2008. *J Am Coll Cardiol* 2011;58(10):1001-6.

106. Tompkins C, McLean R, Cheng A, et al. End-stage renal disease predicts complications in pacemaker and ICD implants. *J Cardiovasc Electrophysiol* 2011;22(10):1099-104.

107. Gold MR, Aasbo JD, El-Chami MF, et al. Subcutaneous implantable cardioverter-defibrillator Post-Approval Study: Clinical characteristics and perioperative results. *Heart Rhythm* 2017;14(10):1456-63.

108. Mondesert B, Bashir J, Philippon F, et al. Rationale and design of the randomized prospective ATLAS study: Avoid Transvenous Leads in Appropriate Subjects. *Am Heart J* 2019;207:1-9.

109. Koman E, Gupta A, Subzposh F, et al. Outcomes of subcutaneous implantable cardioverter-defibrillator implantation in patients on hemodialysis. *J Interv Card Electrophysiol* 2016;45(2):219-23.

110. El-Chami MF, Levy M, Kelli HM, et al. Outcome of Subcutaneous Implantable Cardioverter Defibrillator Implantation in Patients with End-Stage Renal Disease on Dialysis. *J Cardiovasc Electrophysiol* 2015;26(8):900-04.

111. Covic A, Diaconita M, Gusbeth-Tatomir P, et al. Haemodialysis increases QT(c) interval but not QT(c) dispersion in ESRD patients without manifest cardiac disease. *Nephrol Dial Transplant* 2002;17(12):2170-7.

112. Malhis M, Al-Bitar S, Farhood S, et al. Changes in QT intervals in patients with end-stage renal disease before and after hemodialysis. *Saudi J Kidney Dis Transpl* 2010;21(3):460-5.

113. Nemati E, Taheri S. Electrocardiographic manifestations of hyperkalemia in hemodialysis patients. *Saudi J Kidney Dis Transpl* 2010;21(3):471-7.

114. Cobo Sanchez JL, Alconero Camarero AR, Casaus Perez M, et al. Hyperkalaemia and haemodialysis patients: eletrocardiographic changes. *J Ren Care* 2007;33(3):124-9.

115. Poulikakos D, Banerjee D, Malik M. T wave morphology changes during hemodialysis. *J Electrocardiol* 2013;46(6):492-6.

116. You C, Sharma S, Bavishi A, et al. Dialytic interval and the timing of electrocardiographic screening for subcutaneous cardioverter-defibrillator placement in chronic hemodialysis patients. *J Interv Card Electrophysiol* 2018;52(2):179-84.

117. Hinkle DE, Wiersman W, Jurs S. *Applied statistics for the behavioural sciences*: Houghton Mifflin Boston; 1988.

118. Aschieri D, Penela D, Pelizzoni V, et al. Outcomes after sudden cardiac arrest in sports centres with and without on-site external defibrillators. *Heart* 2018;104(16):1344-9.

119. Krittayaphong R, Saengsung P, Chawaruechai T, et al. Early defibrillation: a key for successful outcome of in-hospital cardiac arrest. *J Med Assoc Thai* 2009;92 Suppl 2:S1-5.

120. Chan PS, Krumholz HM, Nichol G, et al. Delayed time to defibrillation after in-hospital cardiac arrest. *N Engl J Med* 2008;358(1):9-17.

121. Murakami Y, Iwami T, Kitamura T, et al. Outcomes of out-of-hospital cardiac arrest by public location in the public-access defibrillation era. *J Am Heart Assoc* 2014;3(2):e000533.

122. . *Clinical Guidelines by Consensus (Recording a standar 12-lead electrocardiogram) An Approved Methodology*. https://www.bcs.com/documents/consensus_guidelines.pdf [Accessed online 26/01/2016].